

Learning 3D geometry

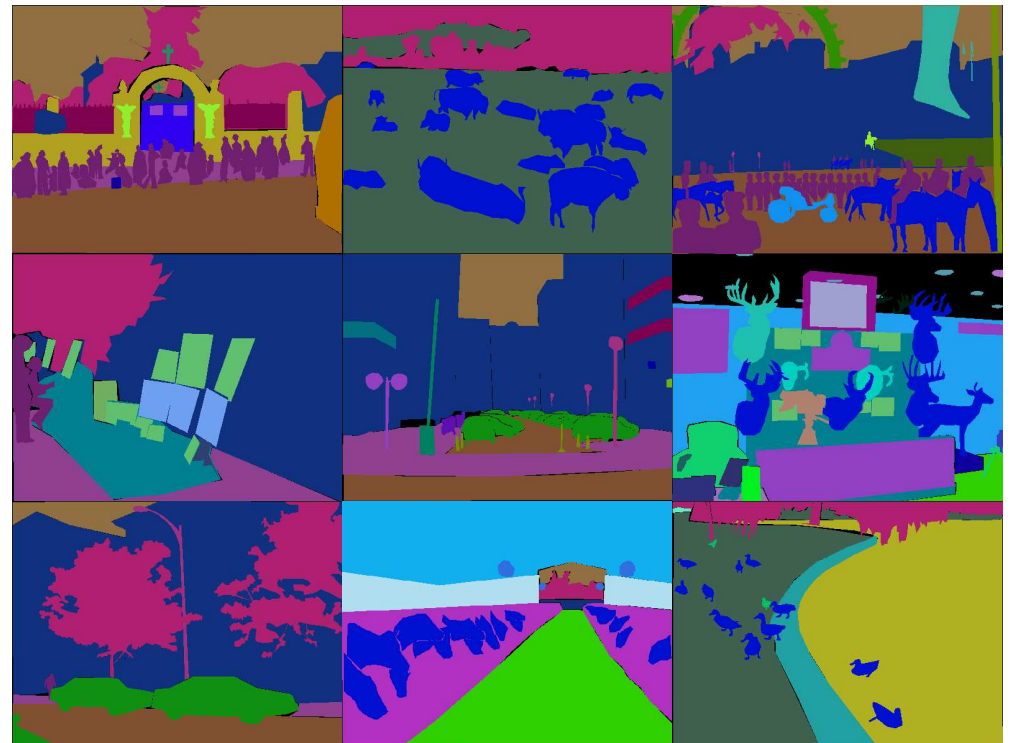
Andrea Vedaldi

Supervised learning

Images



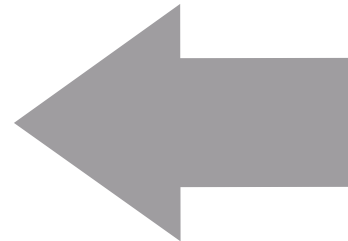
Labelled concepts



Scene parsing through ADE20K dataset. Zhou, Zhao, Puig, Fidler, Barriuso, Torralba. CVPR, 2017.

Learning without supervision

Images



Unsupervised learning

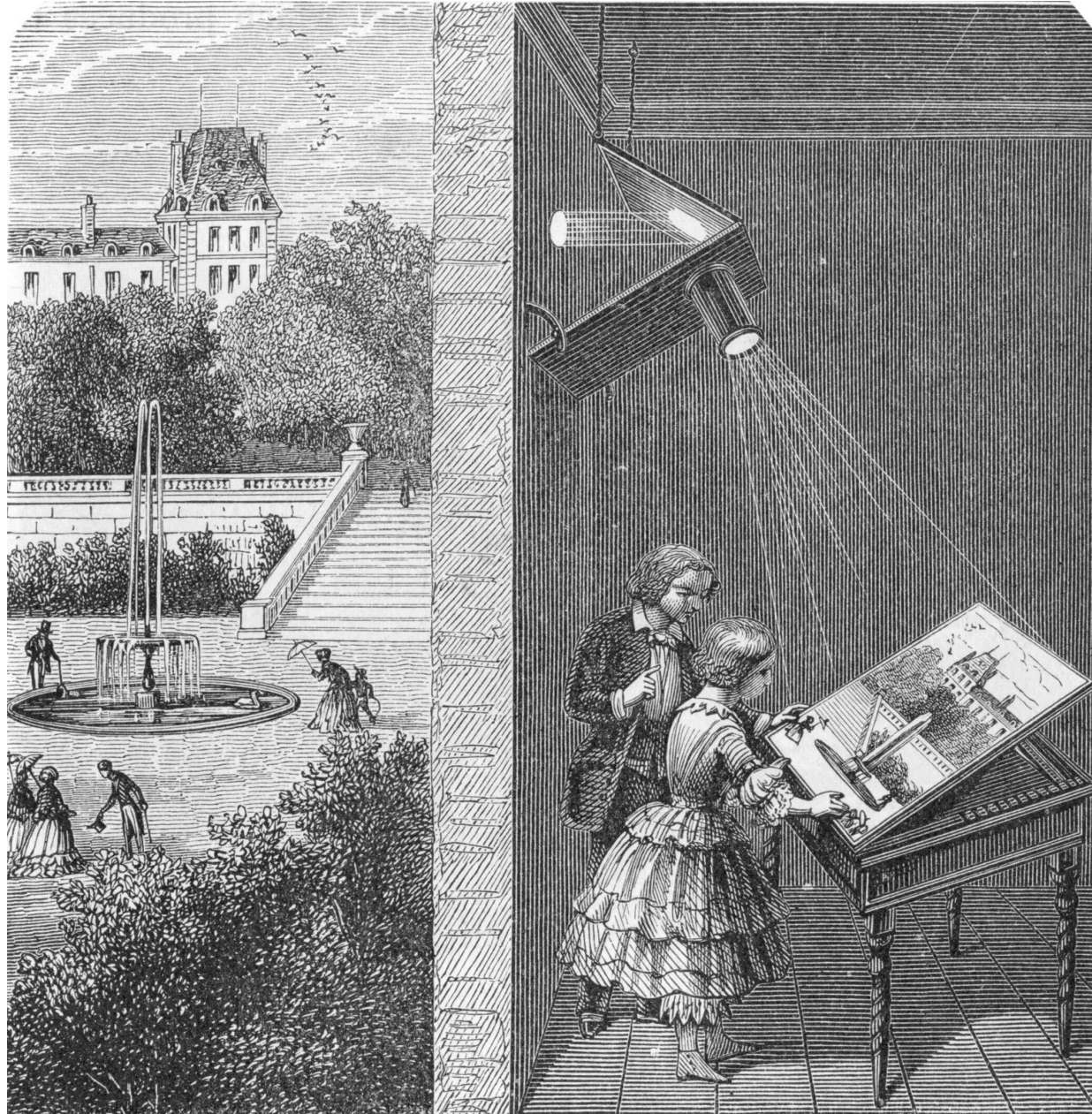
Scene parsing through ADE20K dataset. Zhou, Zhao, Puig, Fidler, Barriuso, Torralba. CVPR, 2017.

World models

The real challenge of vision is not modelling images, but **modelling their content** (i.e., the world)

Tasks such as classification, detection, segmentation provide very limited characterisations of the world

Excessive simplification leads to lack of generality and misses learning opportunities

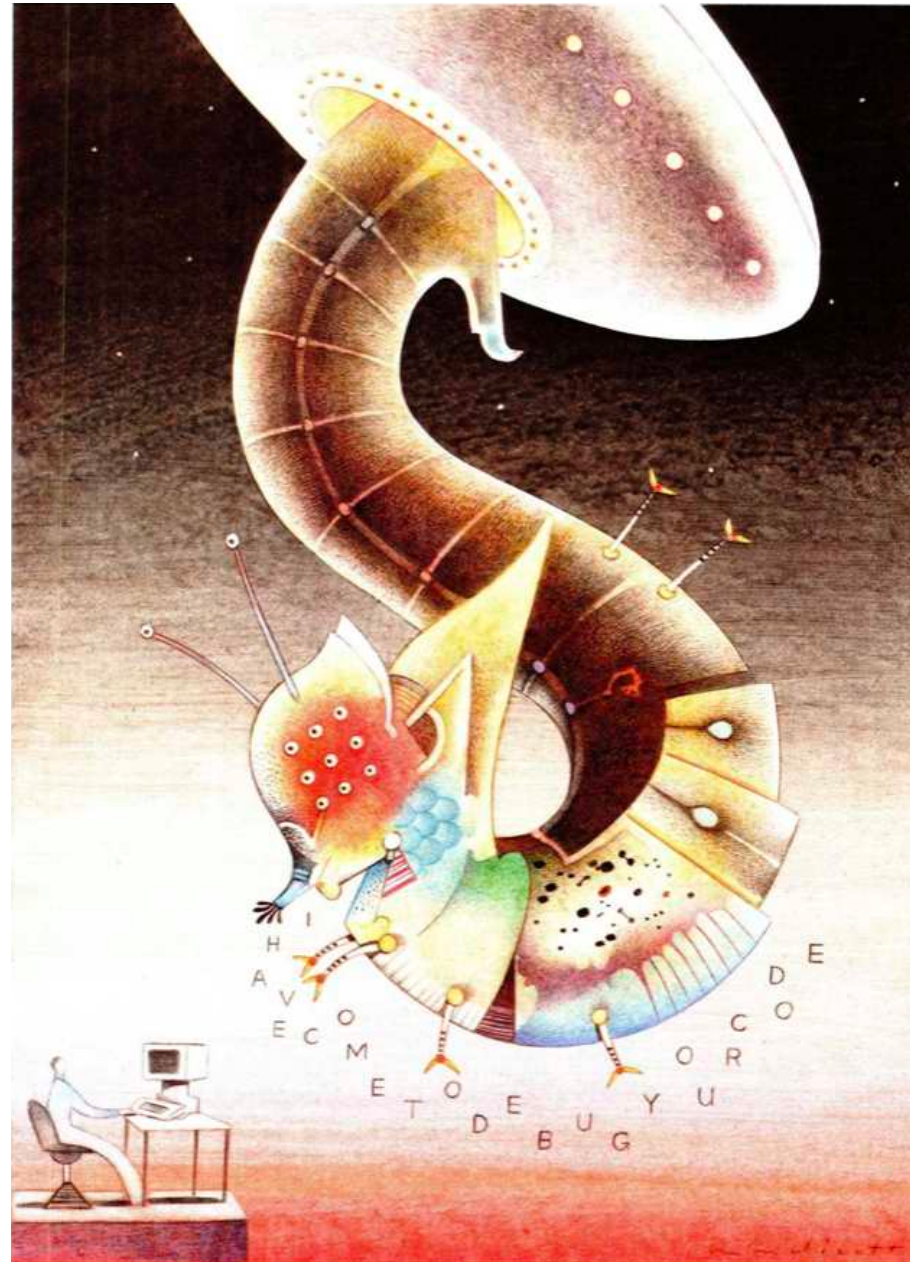


Talking to aliens

“All problem-solvers, intelligent or not, are subject to the same ultimate constraints-limitations on **space, time, and materials** [...]”

“They must have ways to represent the situations they face, and they must have processes for manipulating those representations

Communication with Alien Intelligence. Minsky, Byte, 1985



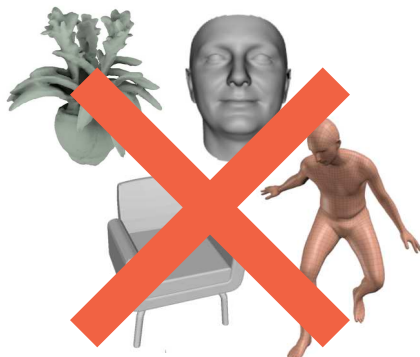
Learning geometry

We can expect most intelligences to develop an understanding of geometry

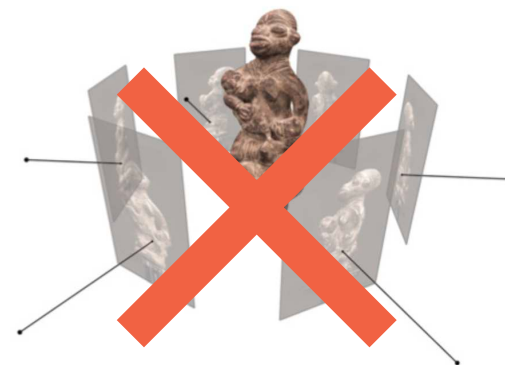
Such an understanding is likely to be roughly equivalent



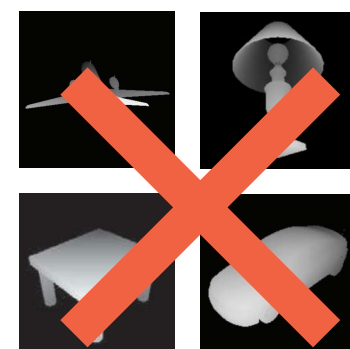
Supervision for 3D Reconstruction



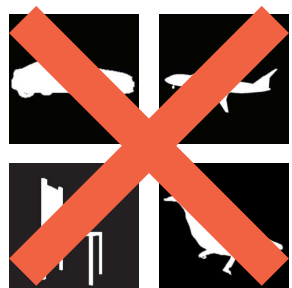
3D ground truth or
shape models



multi-views



depth maps



silhouettes

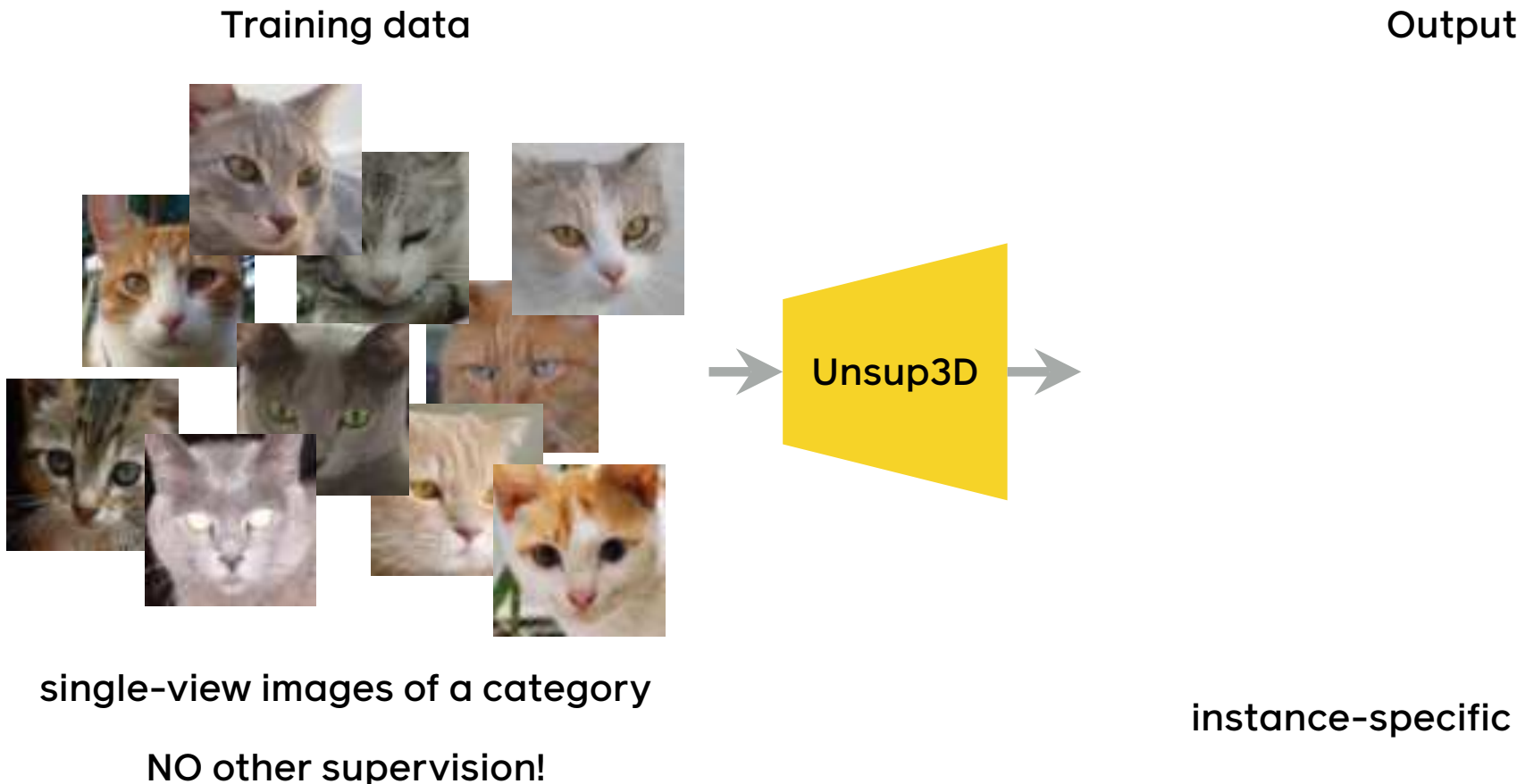


keypoints



camera viewpoint

Unsupervised Learning of 3D Objects

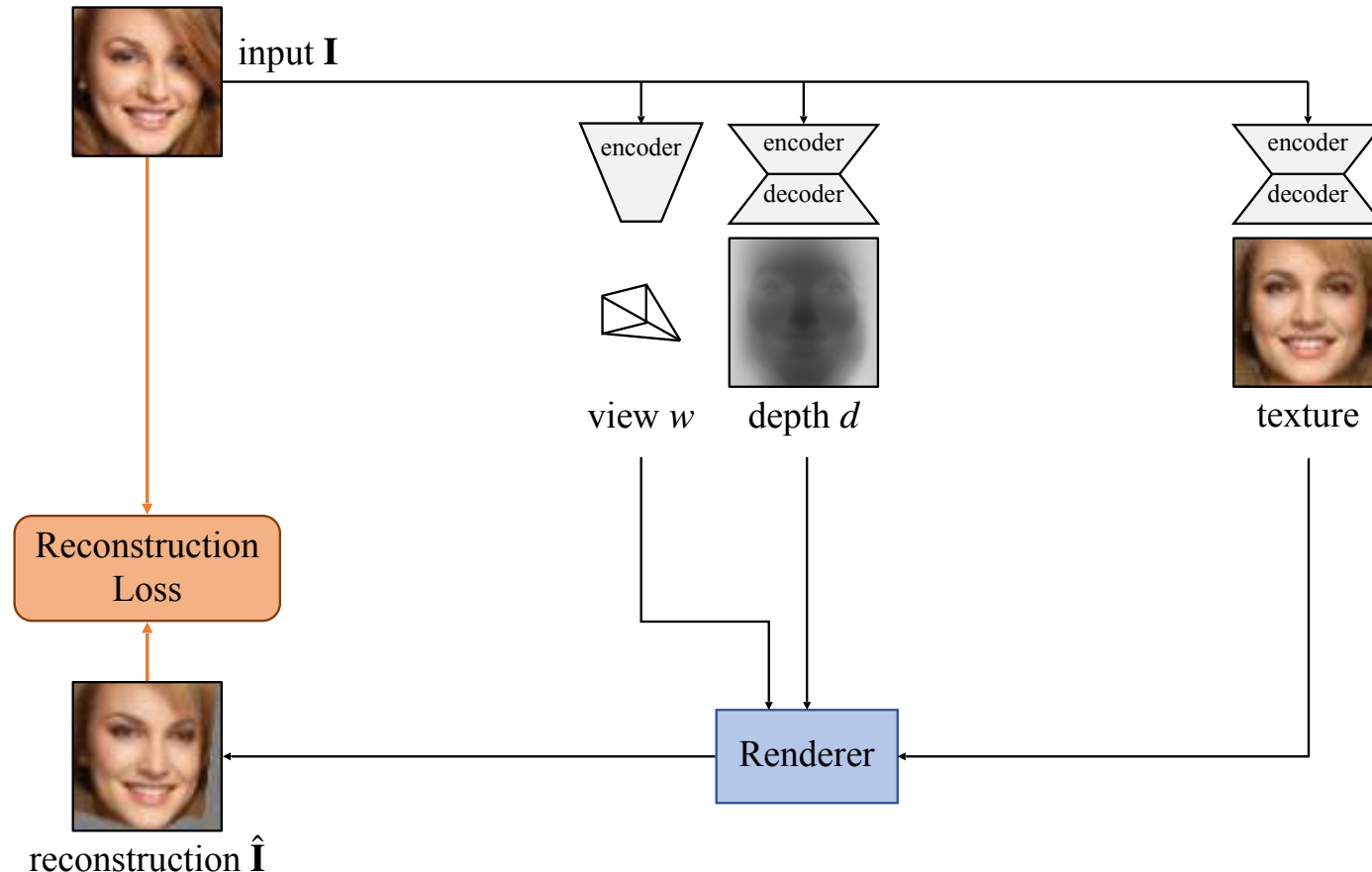


Symmetries in the world

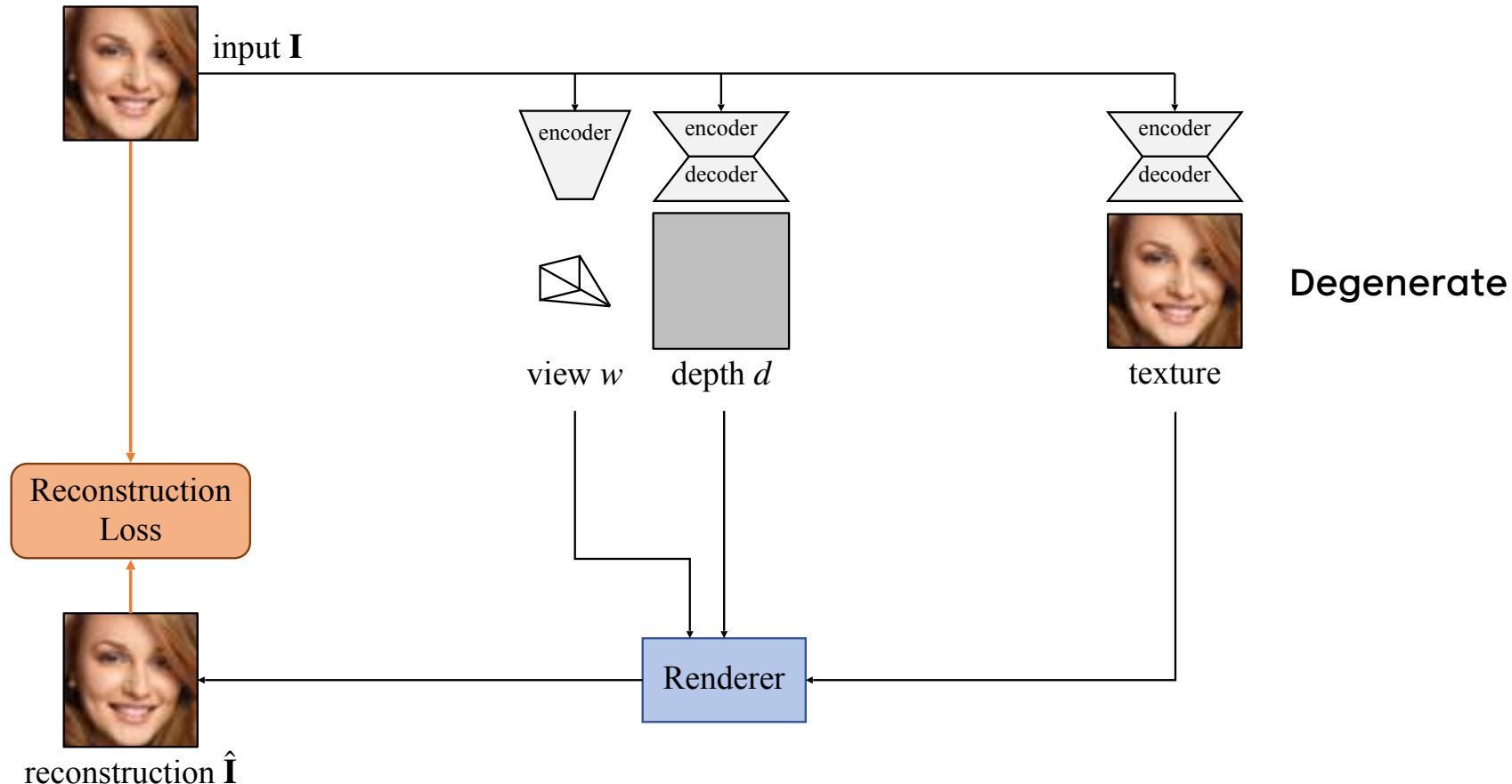


Unsupervised learning of probably symmetric deformable 3D objects from images in the wild. Wu, Rupprecht, Vedaldi. CVPR, 2020

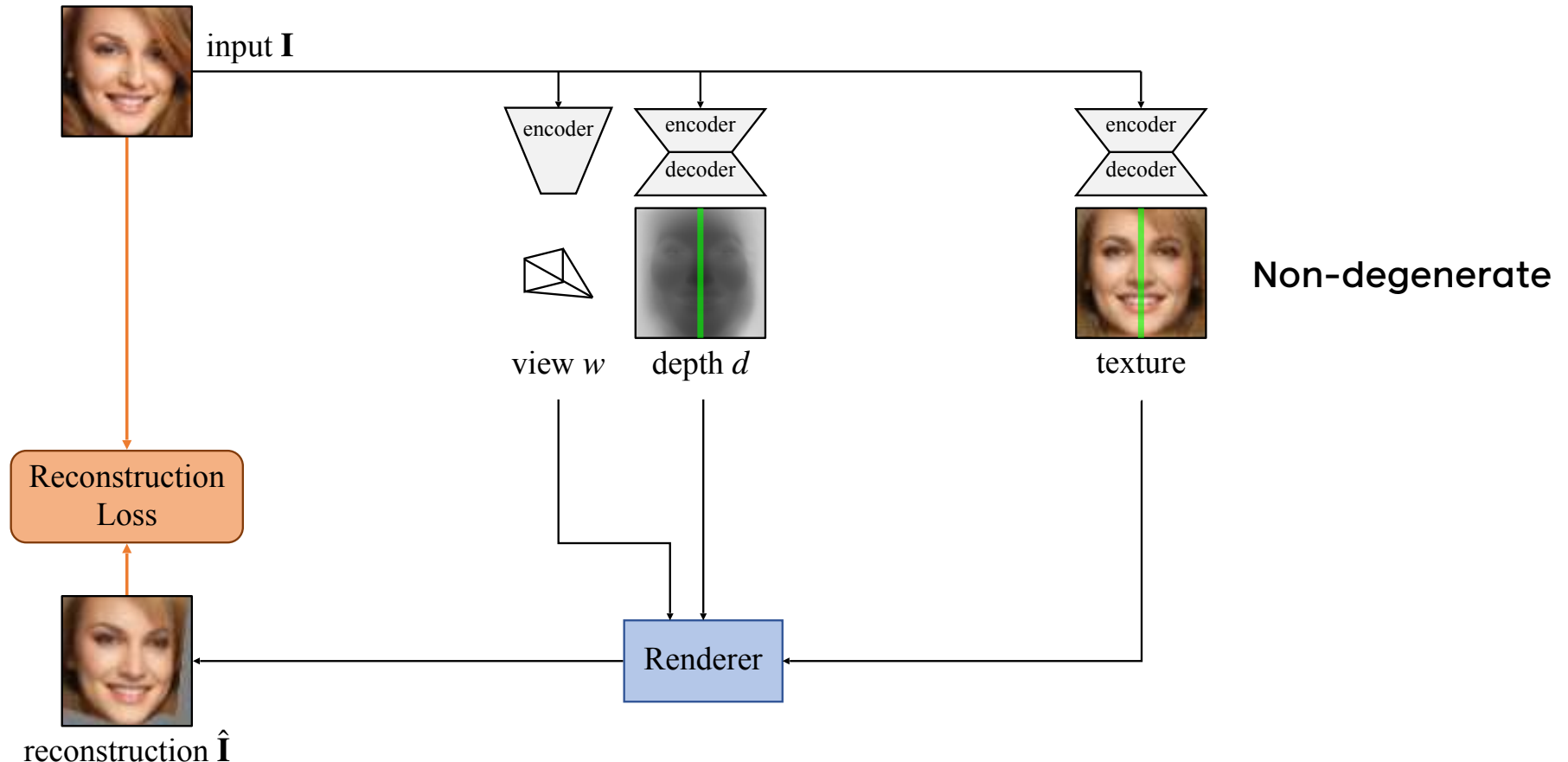
Photo-geometric autoencoding



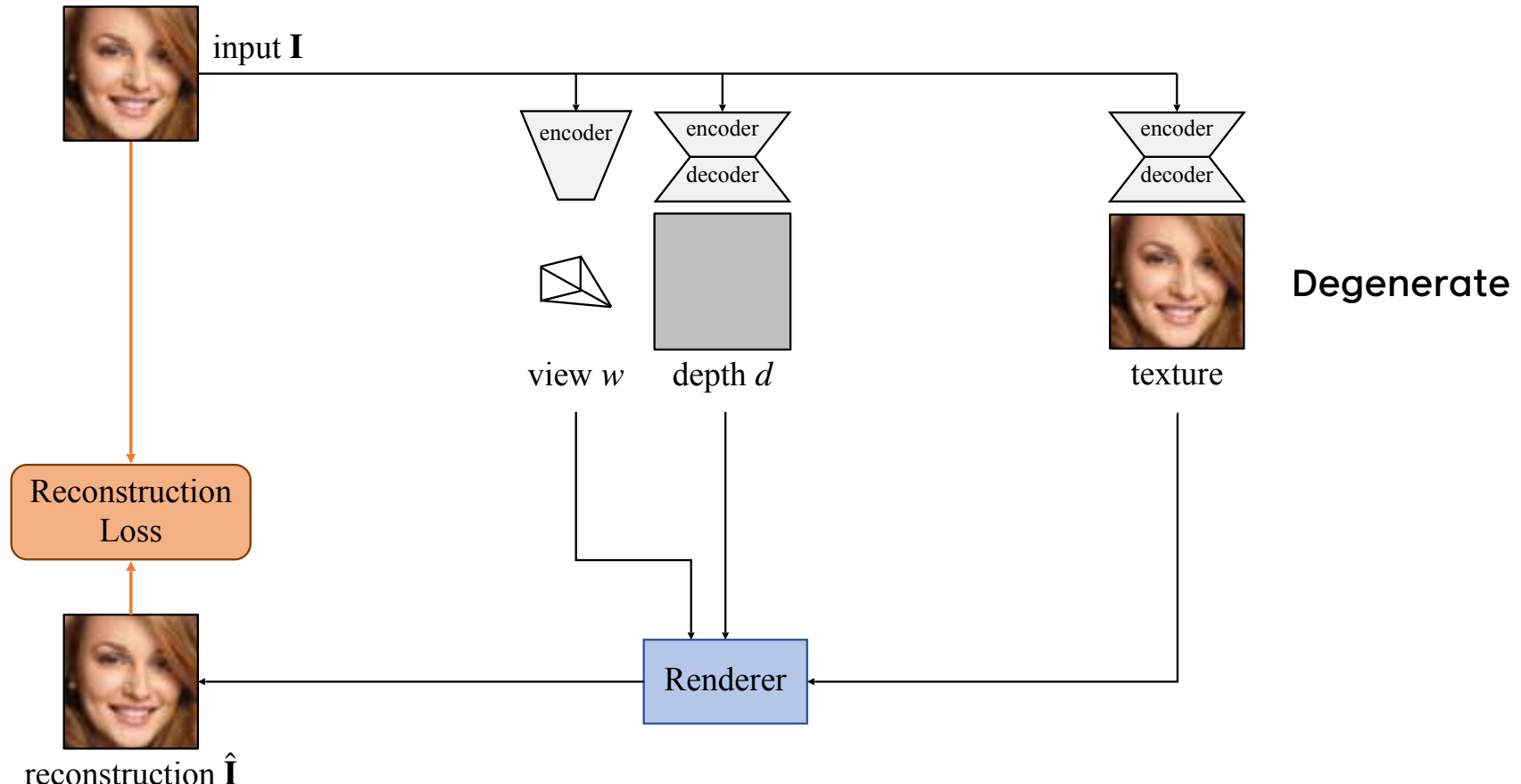
How to avoid degenerate solutions?



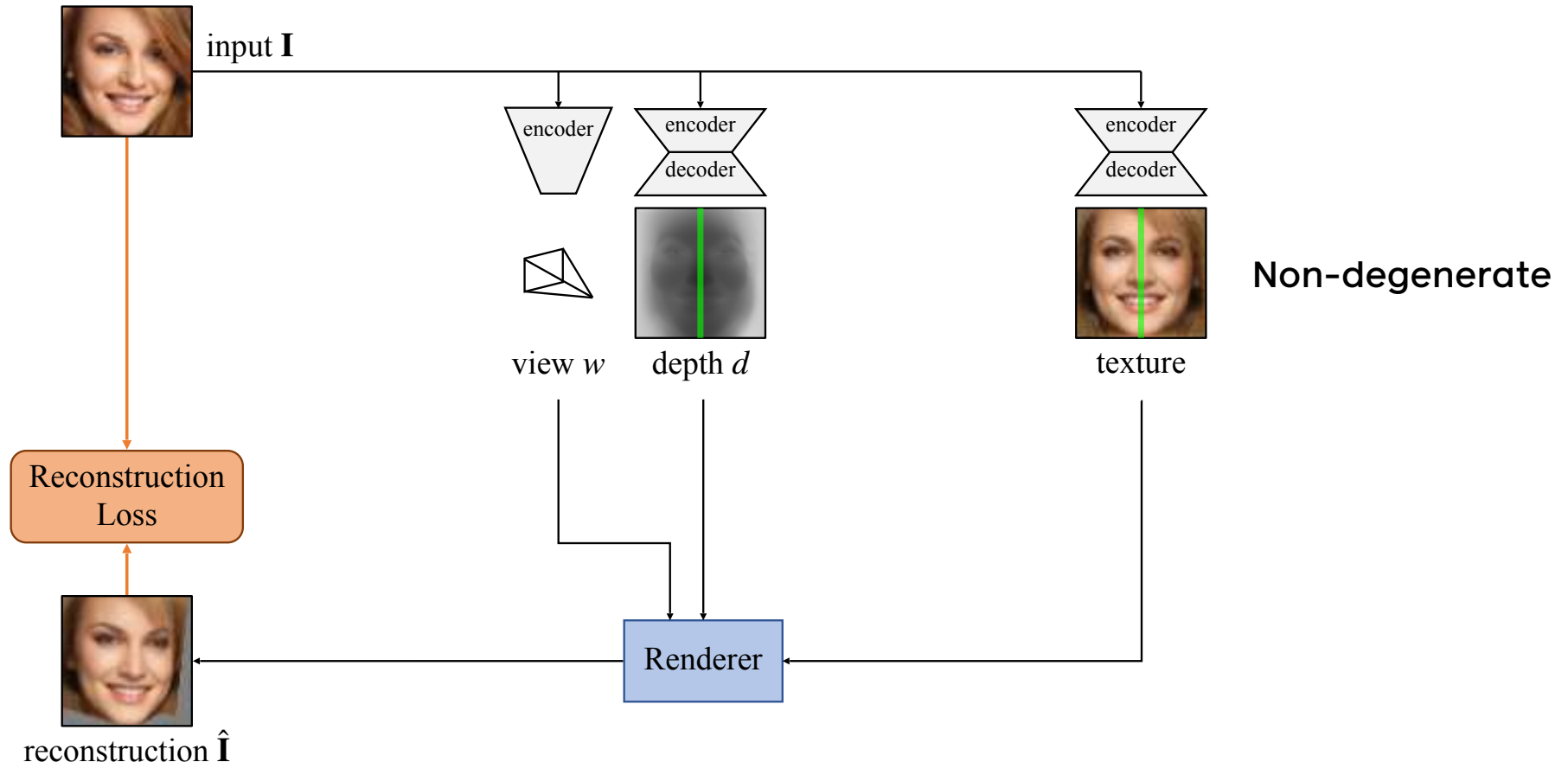
How to avoid degenerate solutions? Enforce symmetry



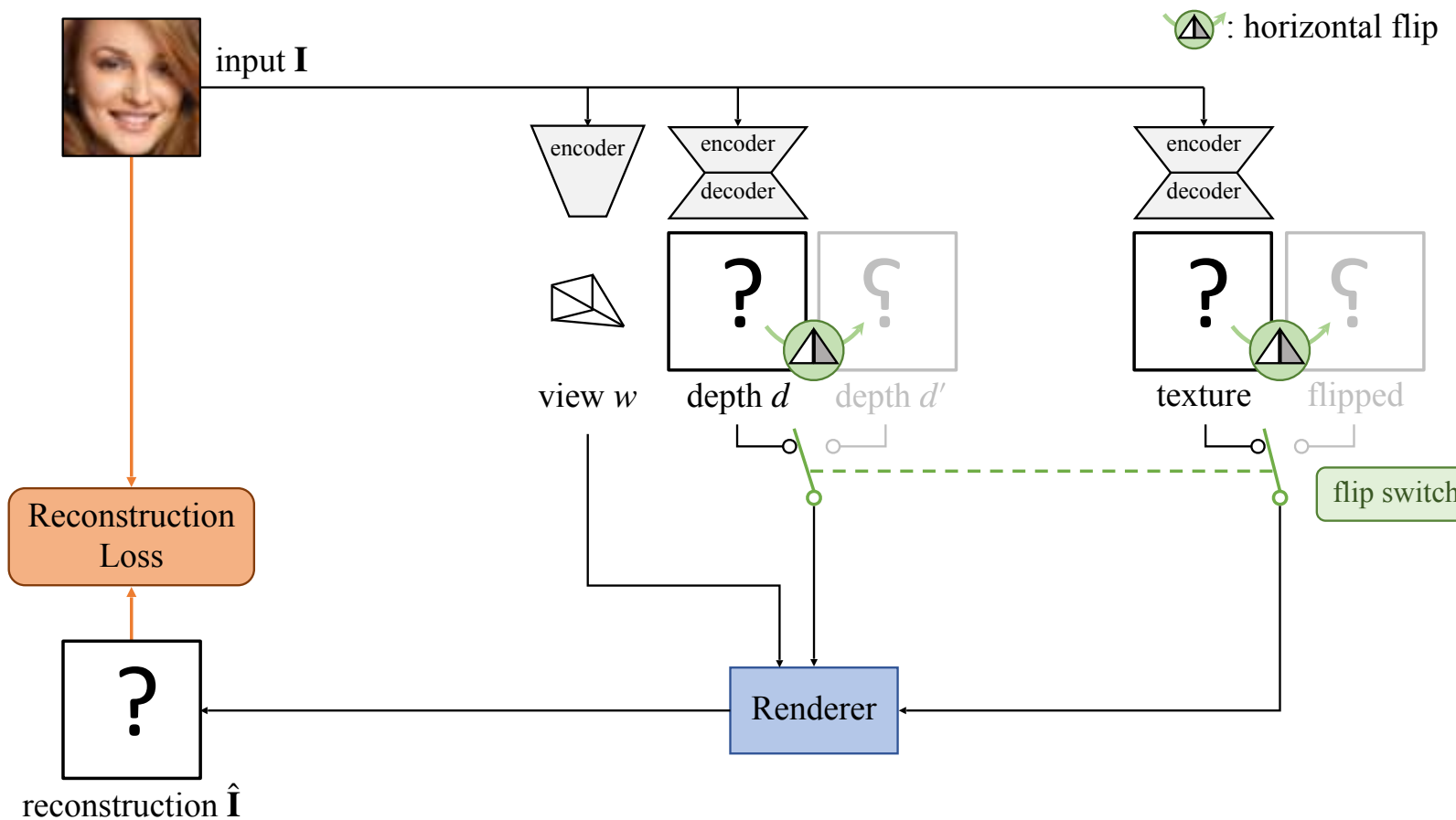
How to avoid degenerate solutions? Enforce symmetry



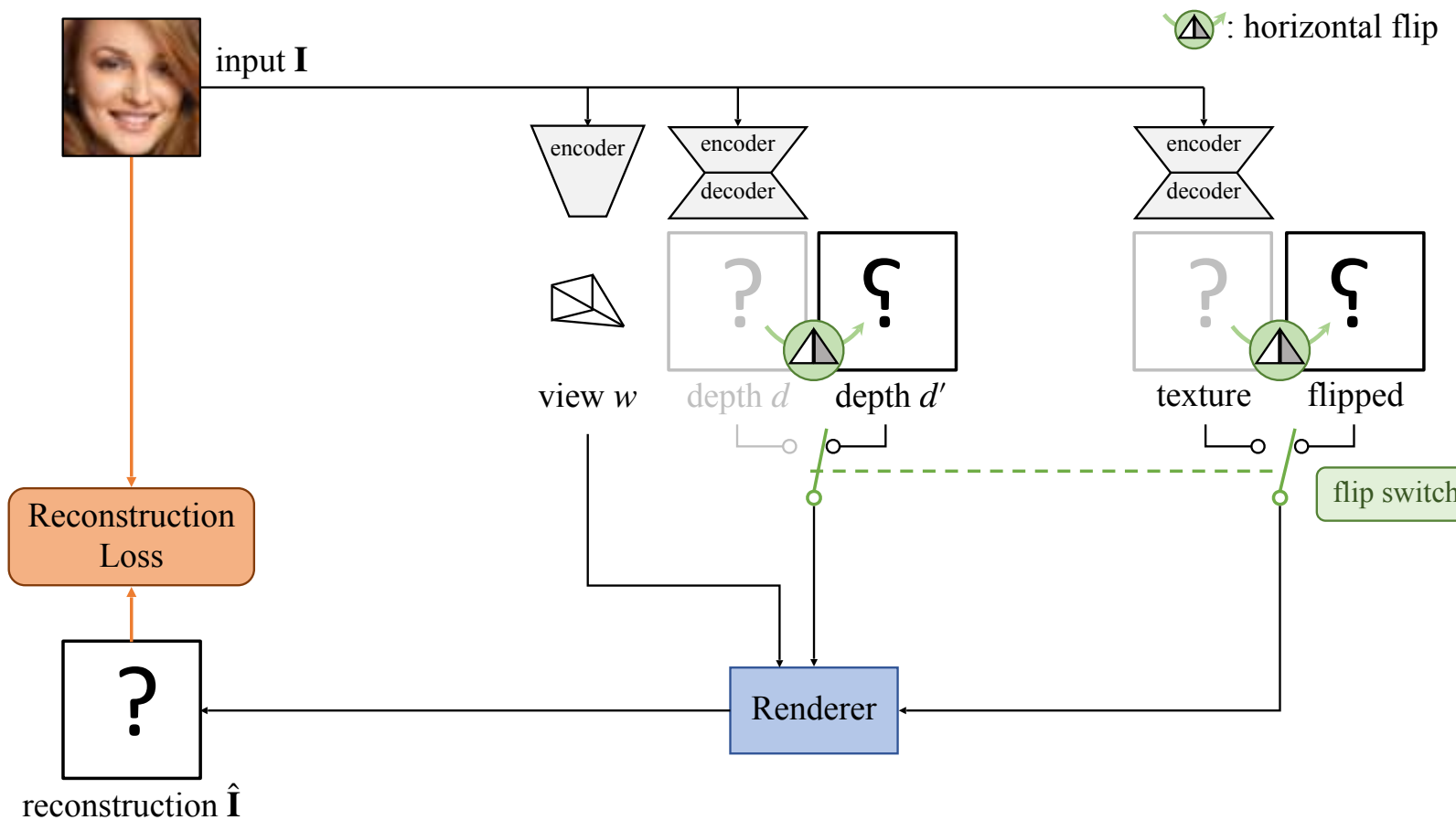
How to avoid degenerate solutions? Enforce symmetry



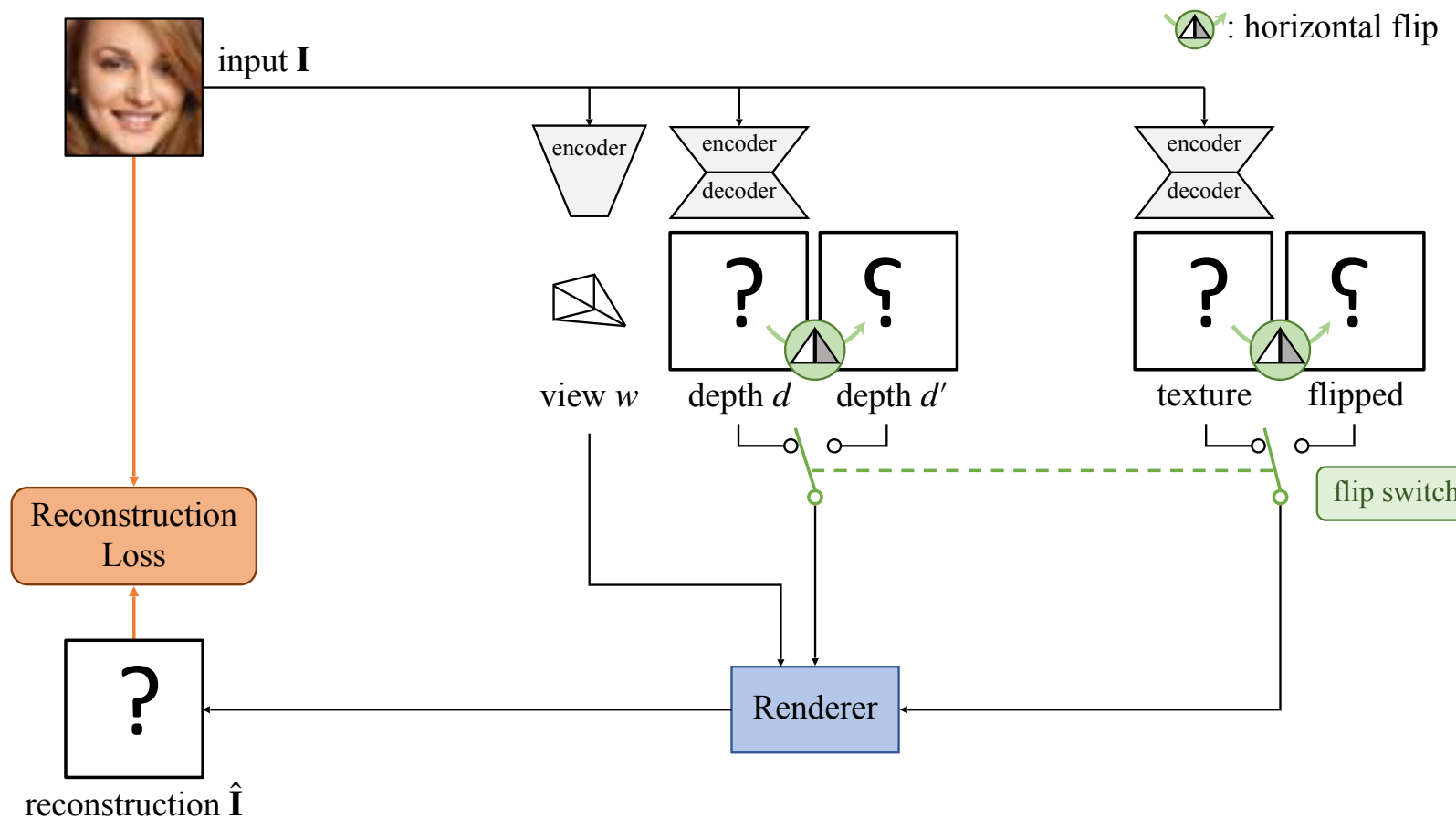
Symmetry is enforced by randomly flipping codes



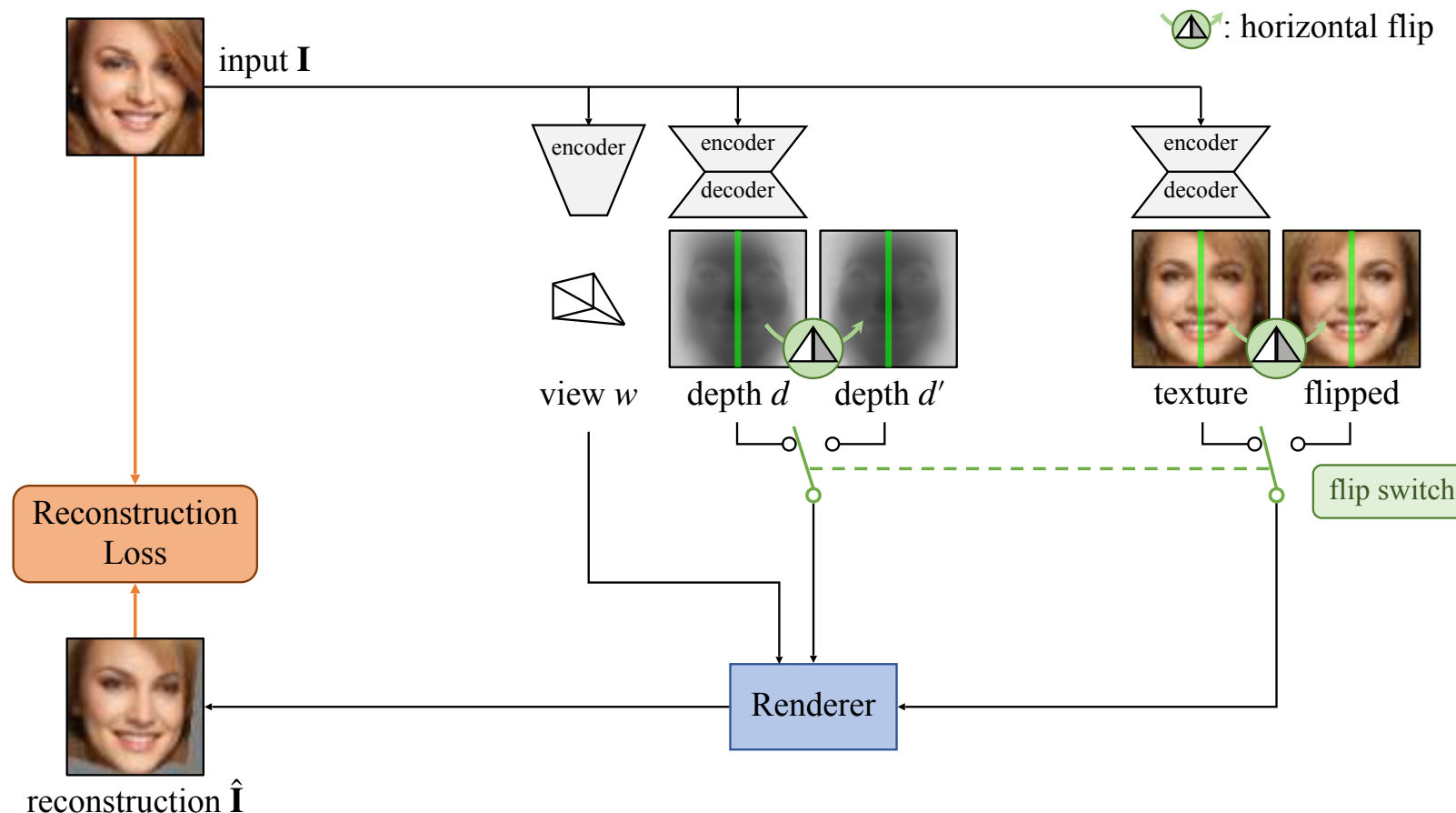
Symmetry is enforced by randomly flipping codes



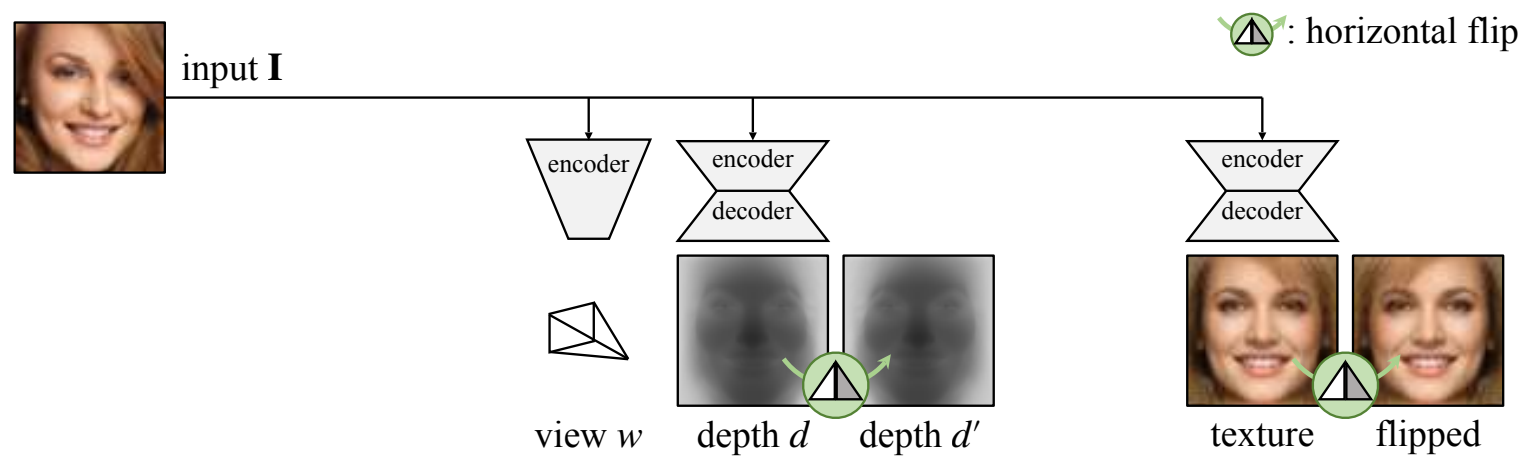
Symmetry is enforced by randomly flipping codes



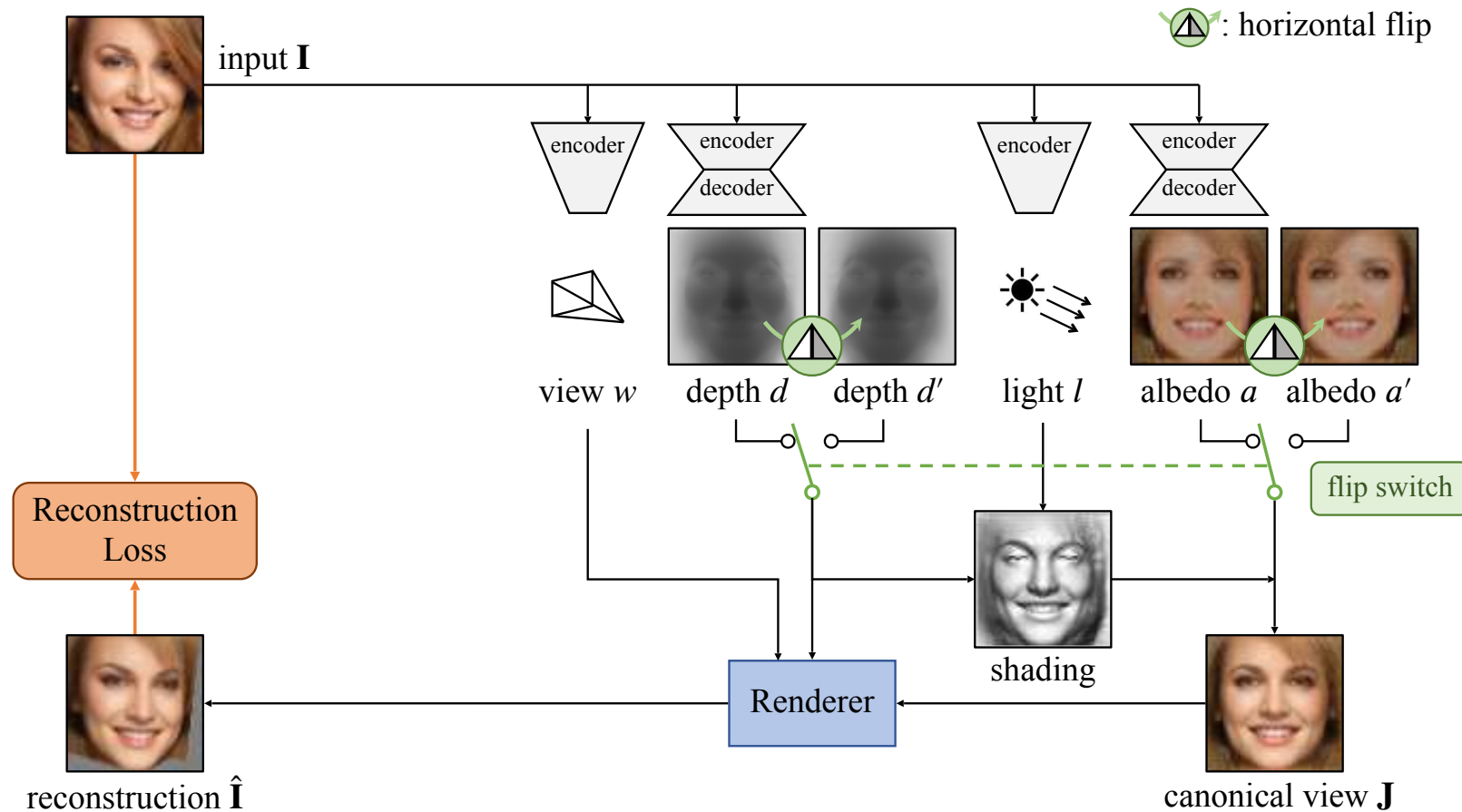
Symmetry is enforced by randomly flipping codes



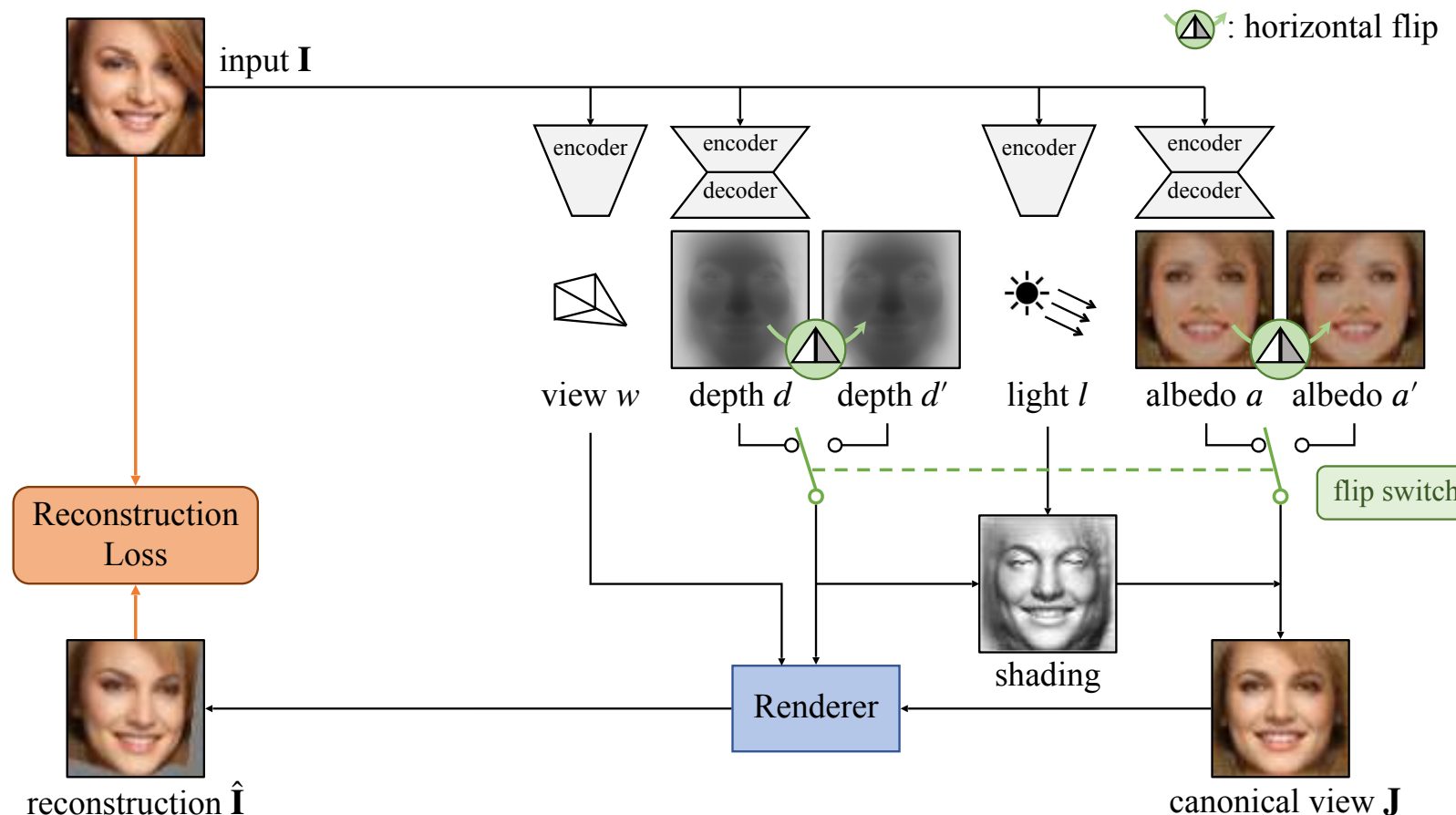
What about non-symmetric lighting?



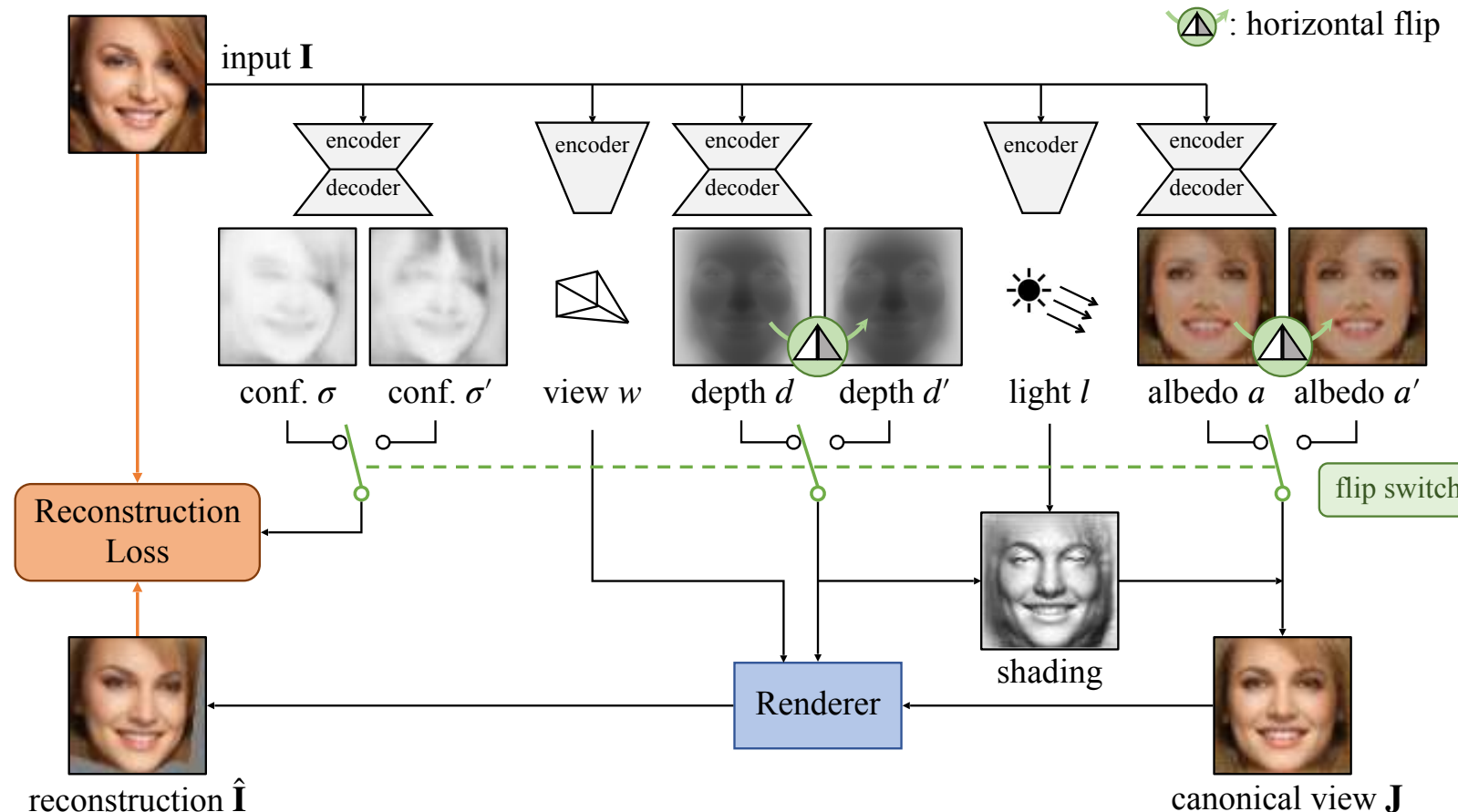
What about non-symmetric lighting? Enforce symmetry on albedo



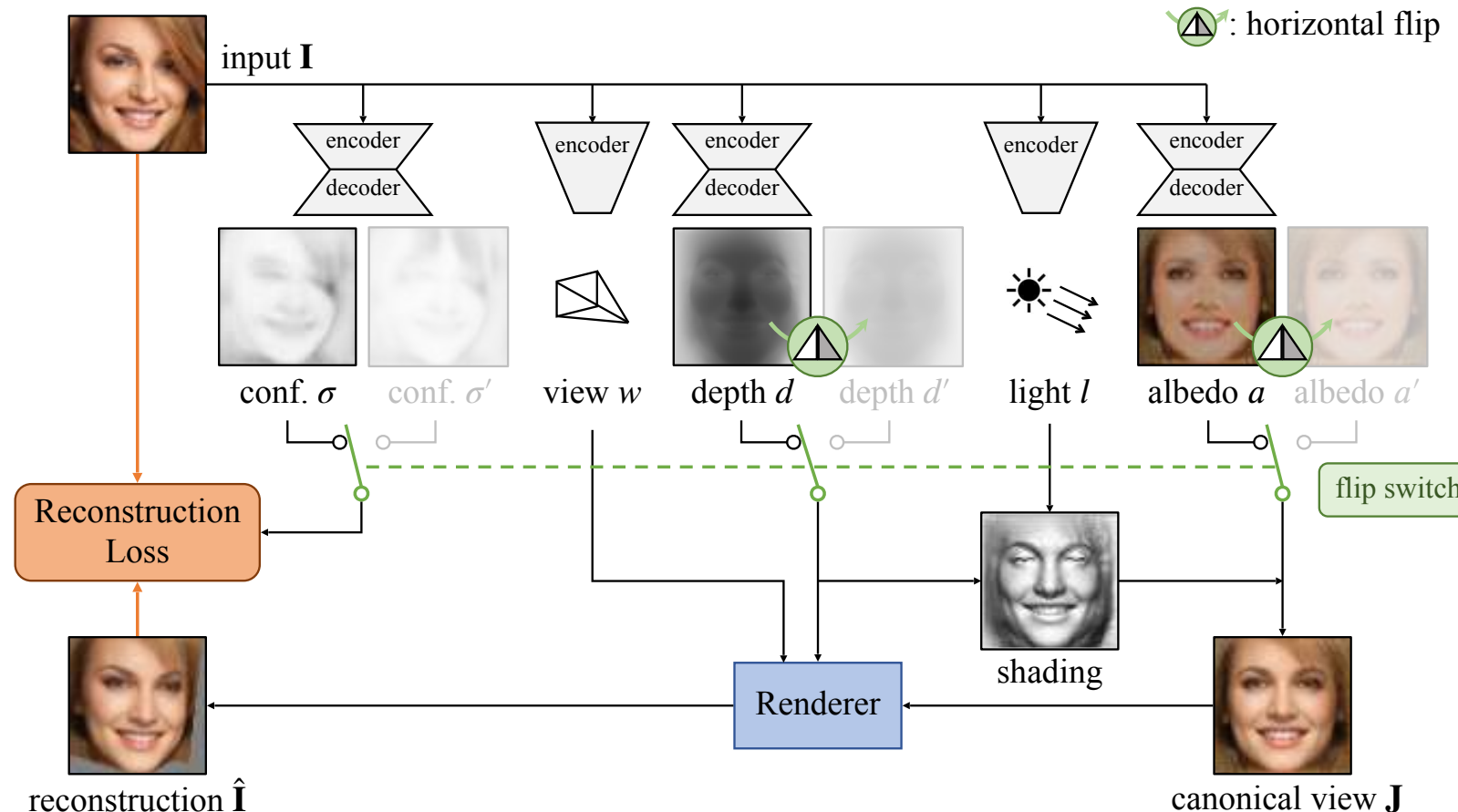
Non-symmetric albedo, deformation, etc?



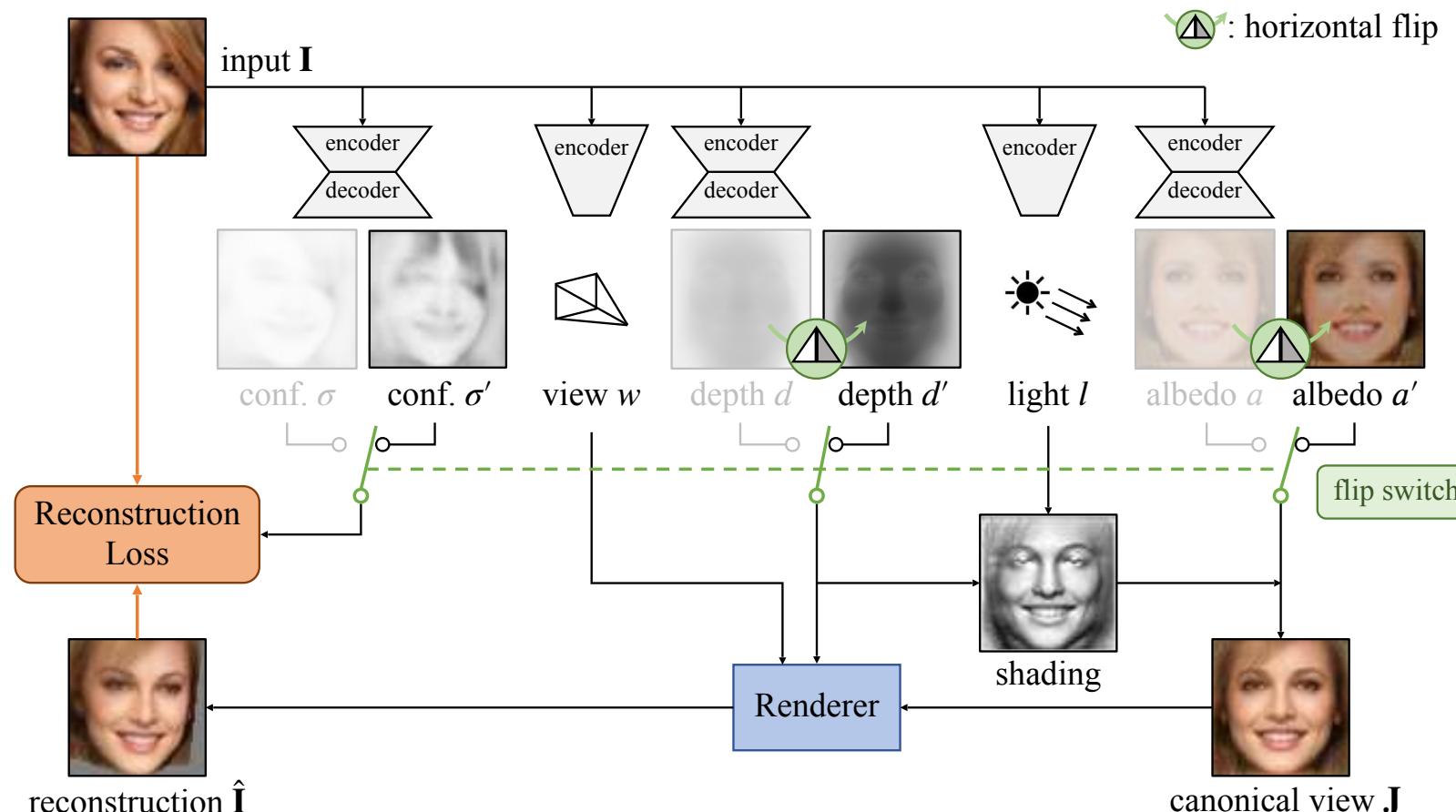
Non-symmetric albedo, deformation, etc? Predict uncertainty



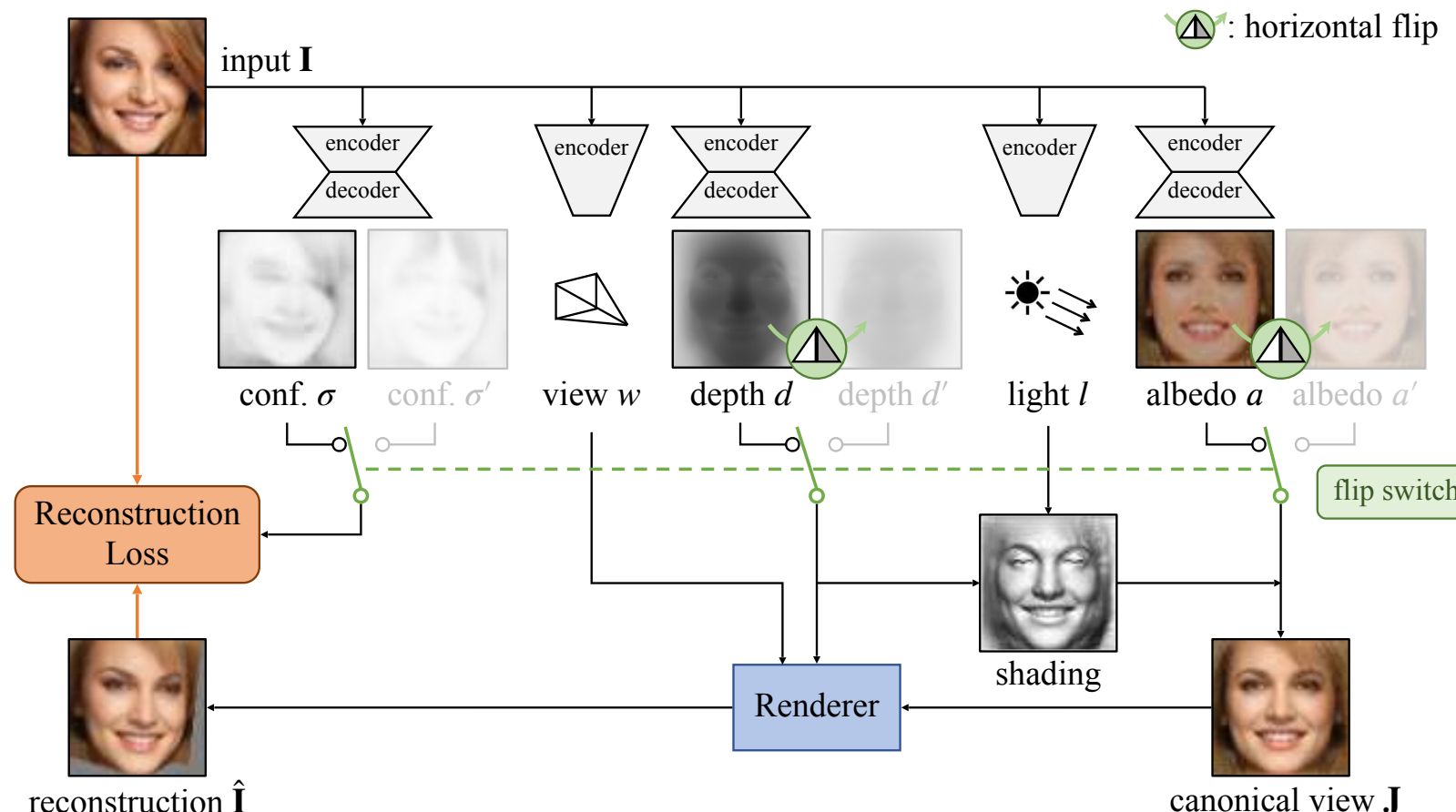
Non-symmetric albedo, deformation, etc? Predict uncertainty



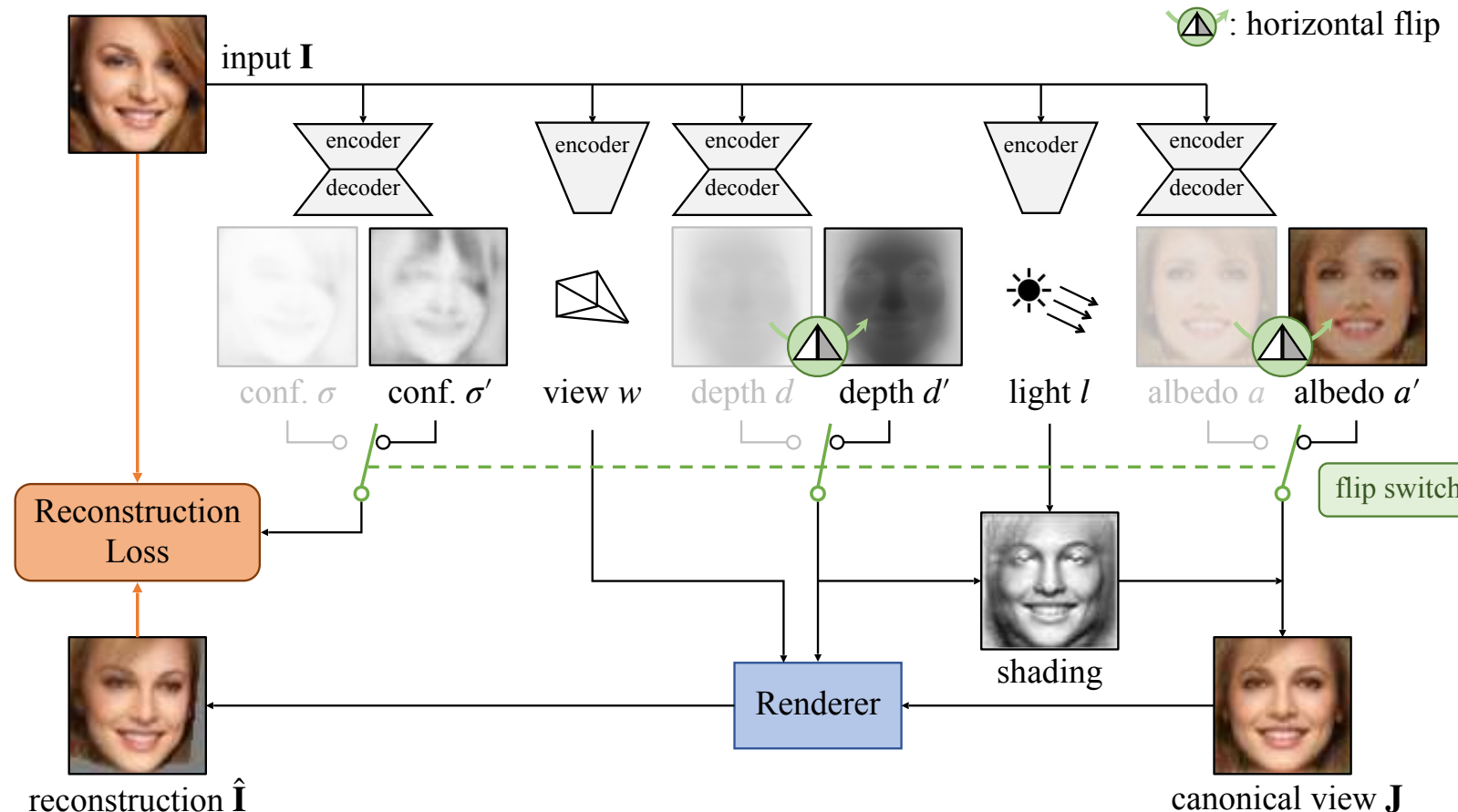
Non-symmetric albedo, deformation, etc? Predict uncertainty



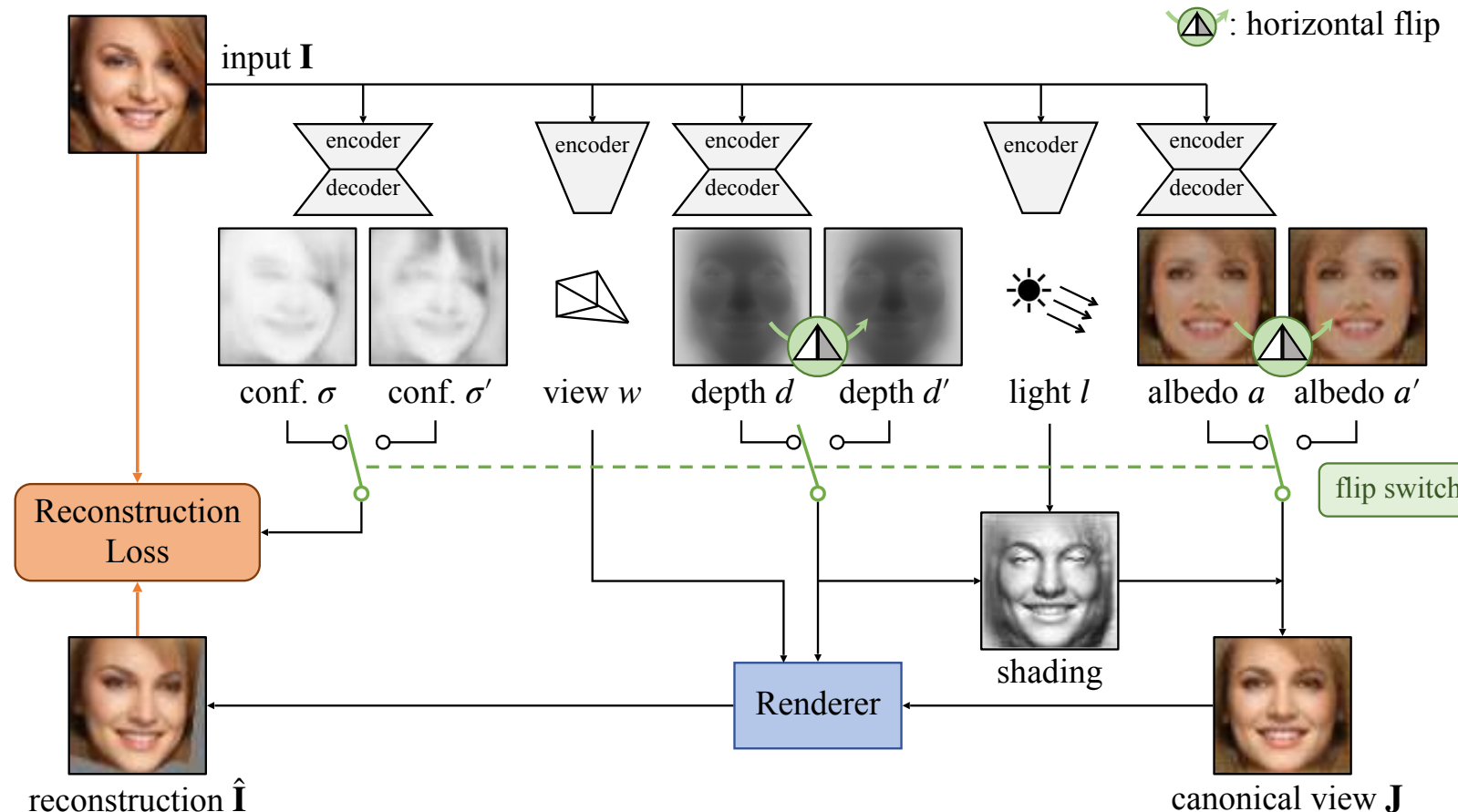
Non-symmetric albedo, deformation, etc? Predict uncertainty



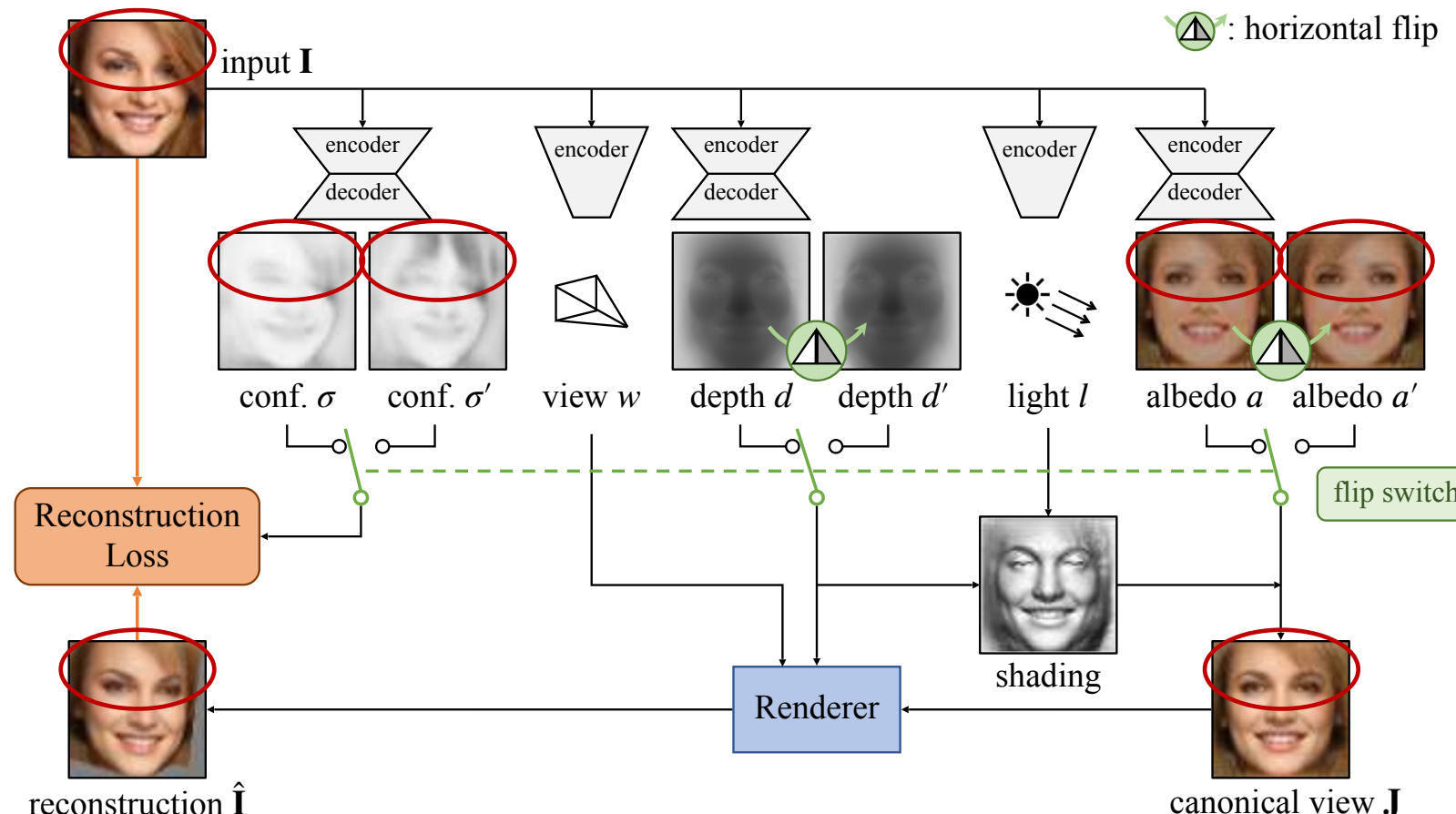
Non-symmetric albedo, deformation, etc? Predict uncertainty

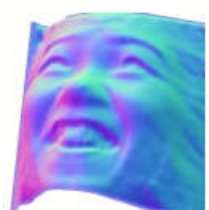
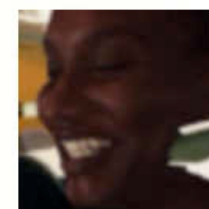
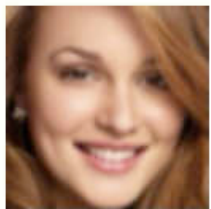


Non-symmetric albedo, deformation, etc? Predict uncertainty



Non-symmetric albedo, deformation, etc? Predict uncertainty



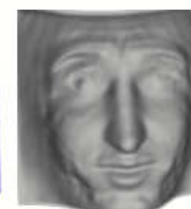
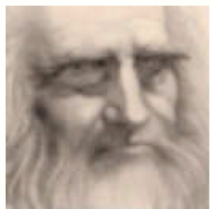


input

reconstruction

input

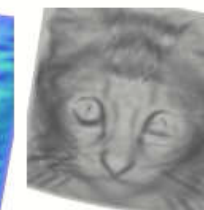
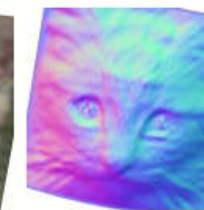
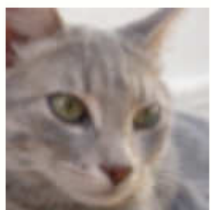
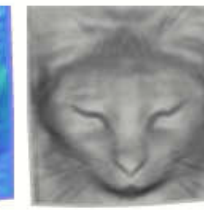
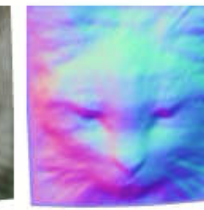
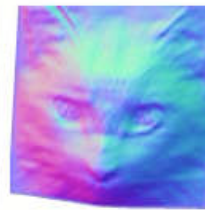
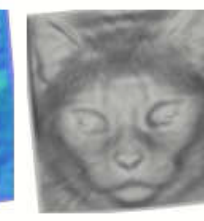
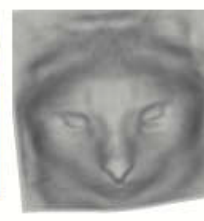
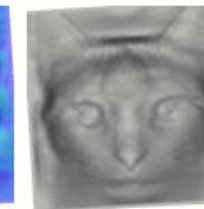
reconstruction



input



reconstruction



input

reconstruction

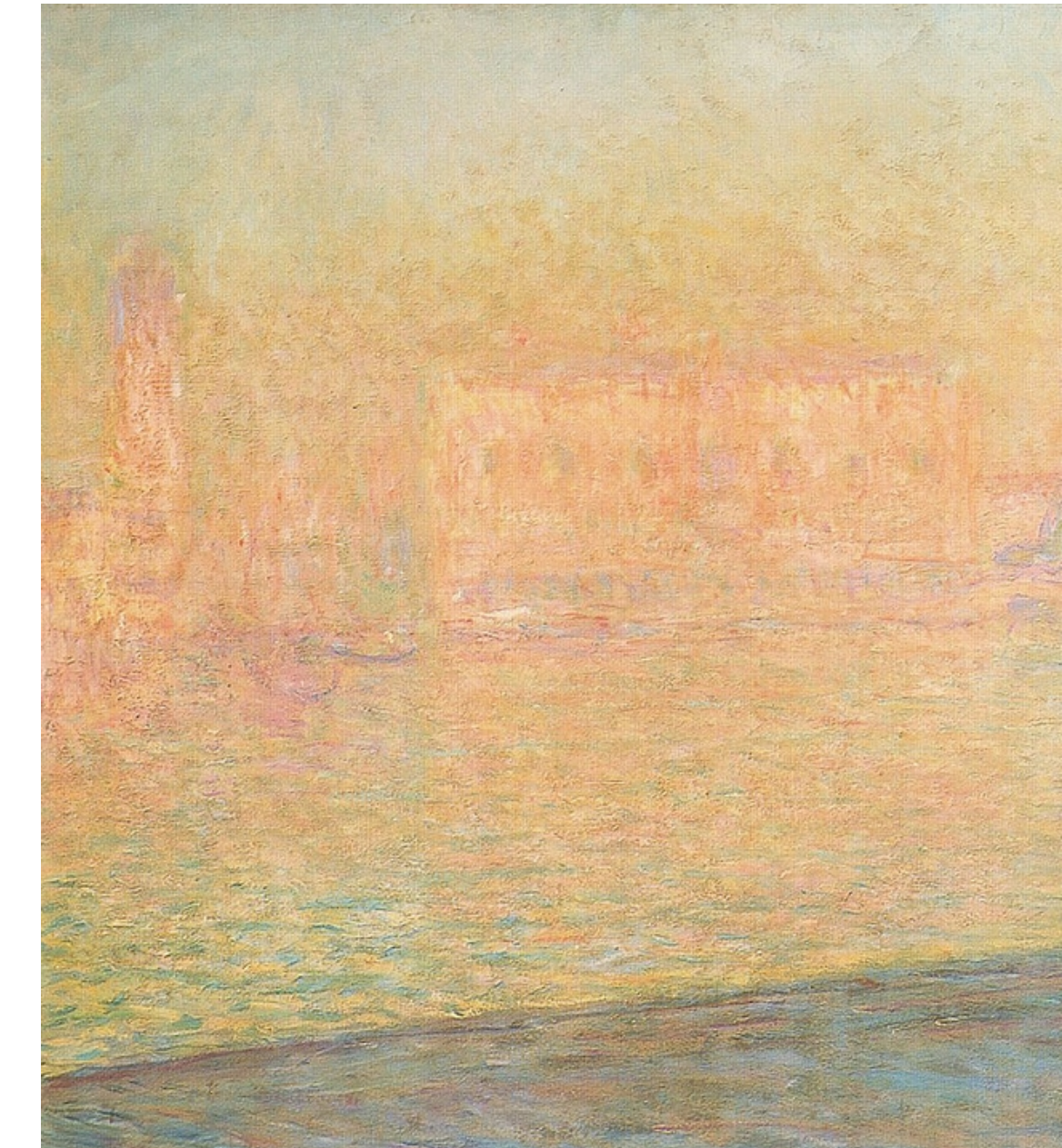
input

reconstruction

Radiance fields

High-quality reconstruction & rendering
as a learning problem

Claude Monet, The Palais Palazzo Ducal as Seen from San Giorgio Maggiore [Wikimedia Commons]



Learned radiance fields

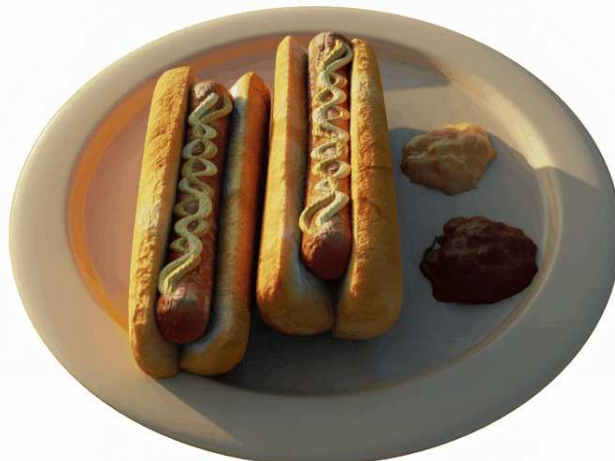


Image formation and radiometry

An image is **formed** by the interaction of light, matter and sensor

Radiometry is a simplified model of light-matter interaction

matter

light

sensor / image



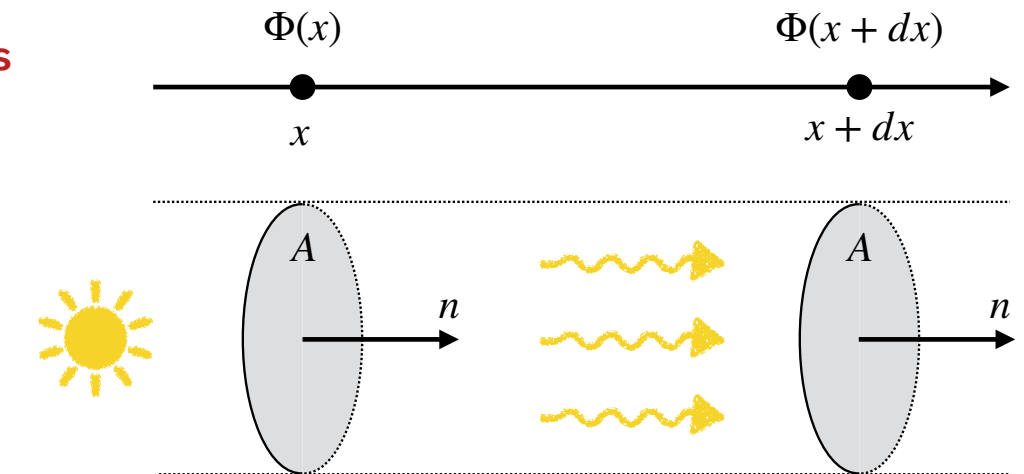
Luminous flux

A planar light wave is characterised by the **luminous flux**:

$\Phi(x)$ (luminous power flowing through A)

If the medium is **transparent** (air, void), the flux is constant

$$\Phi(x) = \Phi(x + dx)$$



Absorption

Given a **translucent** medium:

dx thickness

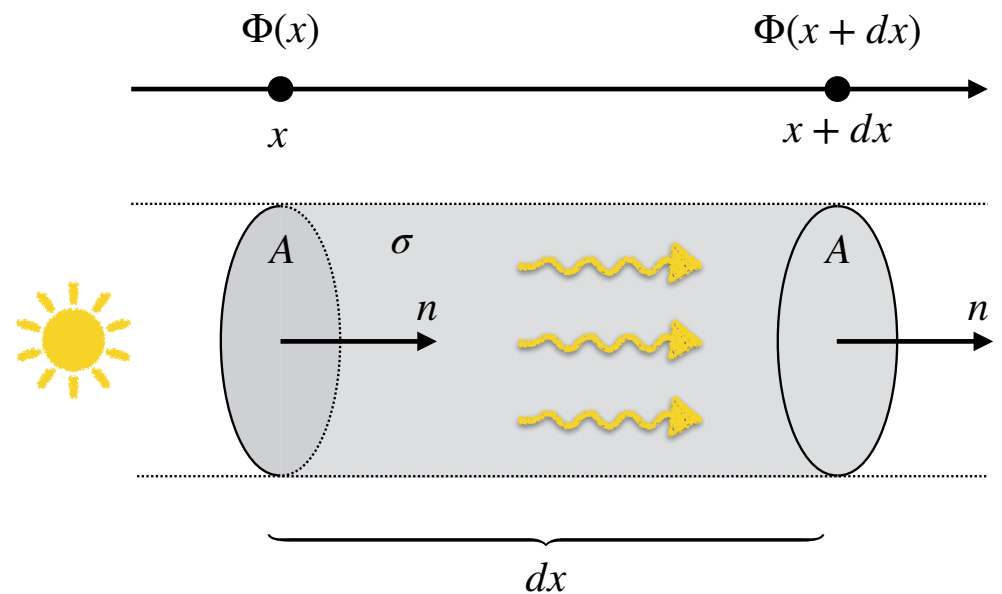
$\sigma(x)$ absorption coefficient

$\sigma(x)dx$ fraction of power **absorbed**

$1 - \sigma(x)dx$ fraction of power **transmitted**

Hence:

$$\Phi(x + dx) = (1 - \sigma(x)dx) \Phi(x) \quad (\text{decreasing})$$



Absorption integral

We have:

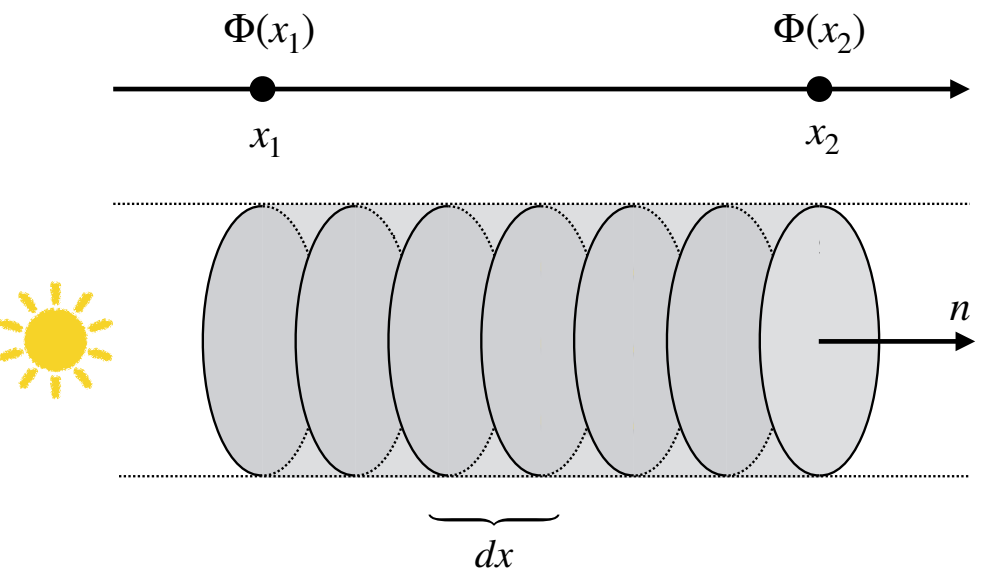
$$\Phi(x + dx) = (1 - \sigma(x)dx) \Phi(x)$$

$$\frac{\Phi(x + dx) - \Phi(x)}{dx} = -\sigma(x)\Phi(x)$$

$$\frac{d\Phi(x)}{dx} = -\sigma(x)\Phi(x)$$

Hence:

$$\Phi(x_2) = \Phi(x_1) \exp\left(-\int_{x_1}^{x_2} \sigma(u) du\right)$$



Emission

Emitting medium:

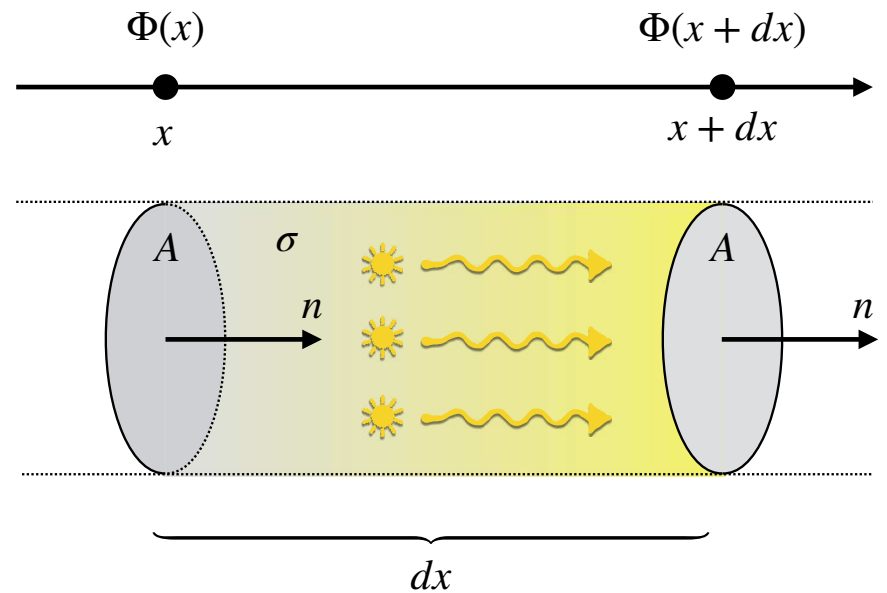
dx thickness

$\epsilon(x)$ emission coefficient

$\epsilon(x)dx$ power emitted

Hence:

$$\Phi(x + dx) = \Phi(x) + \epsilon(x)dx \quad (\text{increasing})$$



Emission & absorption

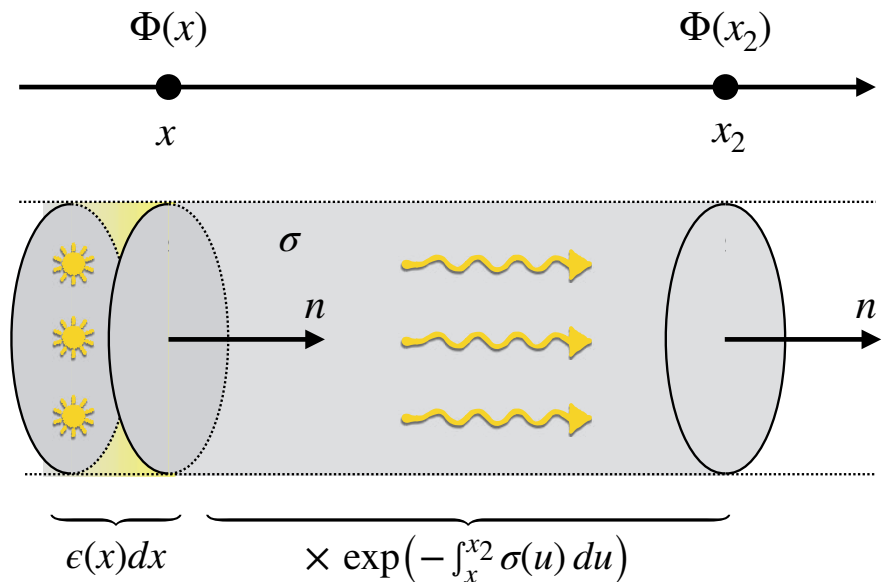
$$\epsilon(x_1)dx$$

power emitted in dx at x_1

$$\exp\left(-\int_{x_1}^{x_2} \sigma(u) du\right) \text{ transmitted through } x_1 \rightarrow x_2$$

Hence, the flux at the other side is:

$$\Phi(x_2) = \exp\left(-\int_x^{x_2} \sigma(u) du\right) \epsilon(x)dx$$



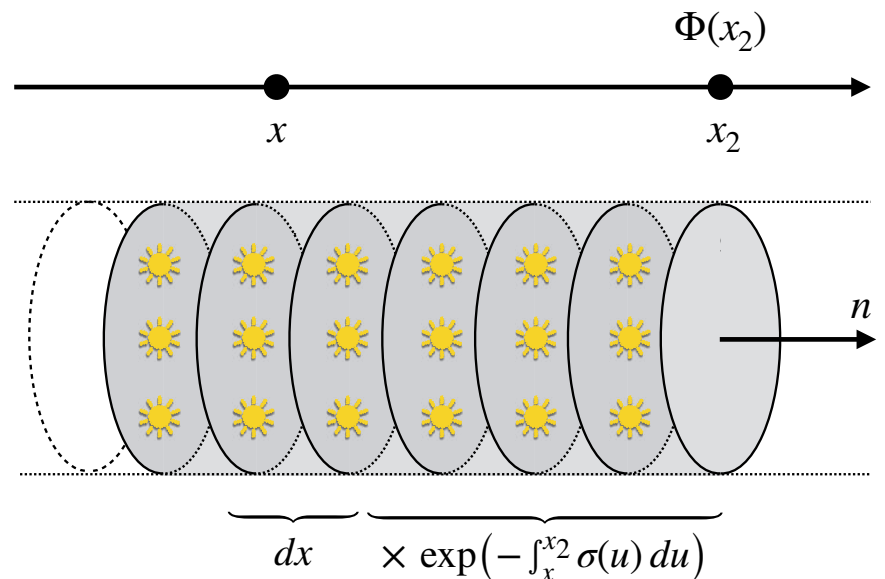
Emission & absorption integral

Each element dx contributes to the flux at x_2 :

$$\exp\left(-\int_x^{x_2} \sigma(u) du\right) \epsilon(x) dx$$

Hence the total flux at x_2 is:

$$\Phi(x_2) = \int_{-\infty}^{x_2} \exp\left(-\int_x^{x_2} \sigma(u) du\right) \epsilon(x) dx$$



Normalised variant

Let emission be proportional to absorption:

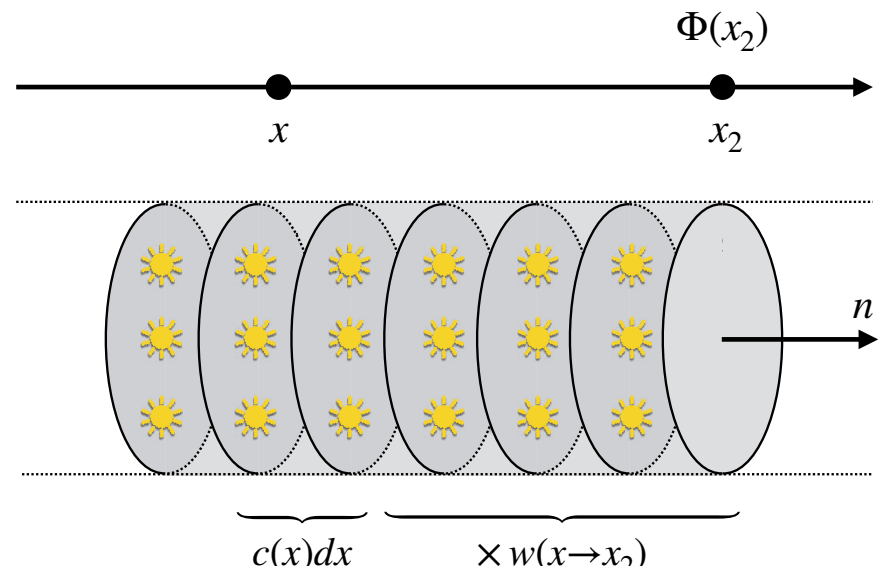
$$\epsilon(x) = c(x)\sigma(x)$$

Hence:

$$\Phi(x_2) = \int_{-\infty}^{x_2} c(x)w(x \rightarrow x_2) dx \quad \text{where}$$

$$w(x \rightarrow x_2) = \sigma(x)\exp\left(-\int_x^{x_2} \sigma(u) du\right)$$

w is a **probability density**: $\int_{-\infty}^{x_2} w(x \rightarrow x_2) dx = 1$



Discretisation

Continuous:

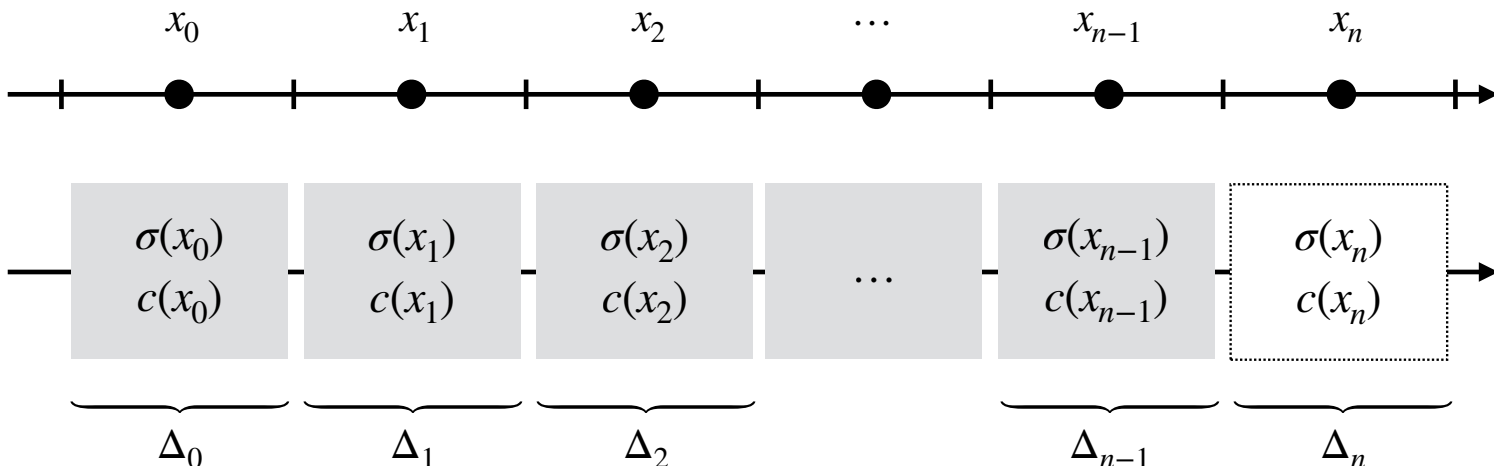
$$\Phi(x_2) = \int_{-\infty}^{x_2} c(x) w(x \rightarrow x_2) dx$$

$$w(x \rightarrow x_2) = \sigma(x) \exp \left(- \int_x^{x_2} \sigma(u) du \right)$$

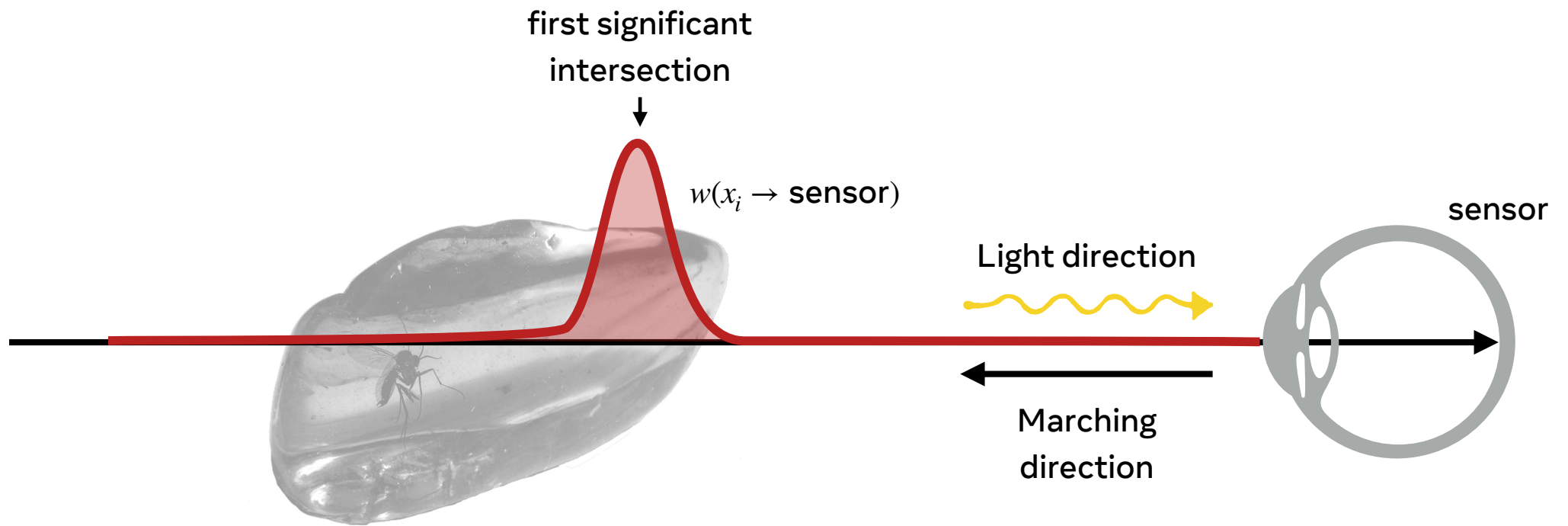
Discrete:

$$\Phi(x_n) = \sum_{i=0}^n c(x_i) w(x_i \rightarrow x_n)$$

$$w(x_i \rightarrow x_n) = \left(1 - \exp(-\sigma(x_i)\Delta_i) \right) \exp \left(- \sum_{j=i+1}^n \sigma(x_j)\Delta_j \right)$$



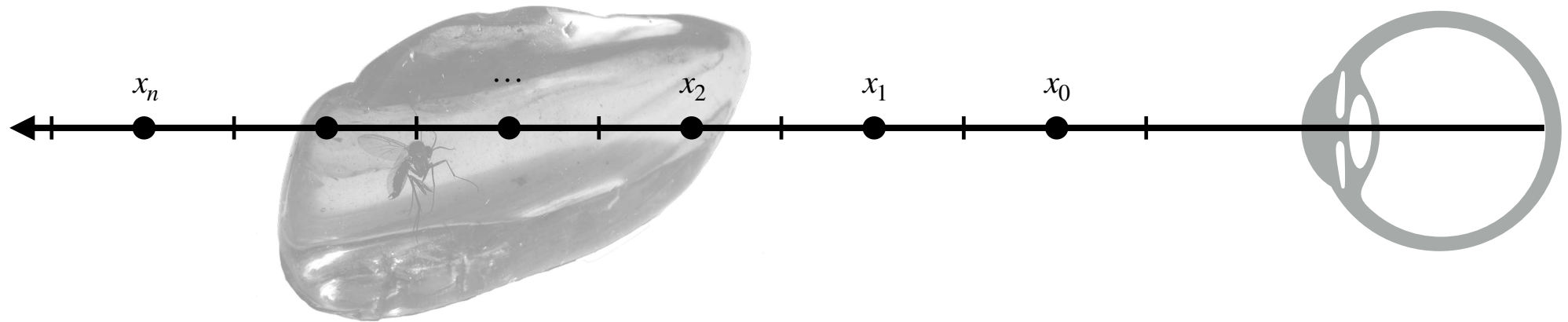
Ray marching



Ray marching

$$\Phi(\text{sensor}) = \sum_{i=0}^n c(x_i) w(x_i)$$

$$w(x_i) = (1 - \exp(-\sigma(x_i)\Delta_i)) \exp\left(-\sum_{j=0}^{i-1} \Delta_j \sigma(x_j)\right)$$



Colours

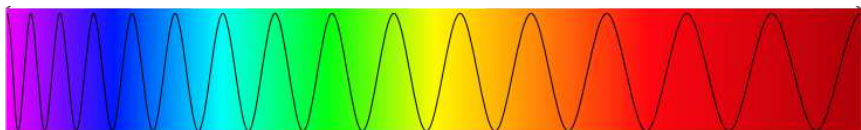
Light is a superposition of waves at different frequencies (colours)

All radiometric quantities have a corresponding **spectral version**

ω frequency

$\Phi(x, \omega)$ spectral flux density

$\Phi(x) = \int \Phi(x, \omega) d\omega$ flux



We only represent a few components (RGB):

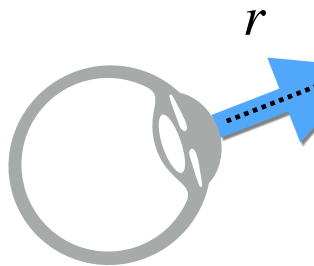
$$\Phi_{\text{rgb}}(x) = \begin{bmatrix} \int \Phi(x, \omega) R(\omega) d\omega \\ \int \Phi(x, \omega) G(\omega) d\omega \\ \int \Phi(x, \omega) B(\omega) d\omega \end{bmatrix}$$

$$c_{\text{rgb}}(x) = \begin{bmatrix} c_r(x) \\ c_g(x) \\ c_b(x) \end{bmatrix}$$

View-dependency of colour

The light emitted by a material depends on the emission direction r :

$$c_{\text{rgb}}(x, r) = \begin{bmatrix} c_r(x, r) \\ c_g(x, r) \\ c_b(x, r) \end{bmatrix}$$



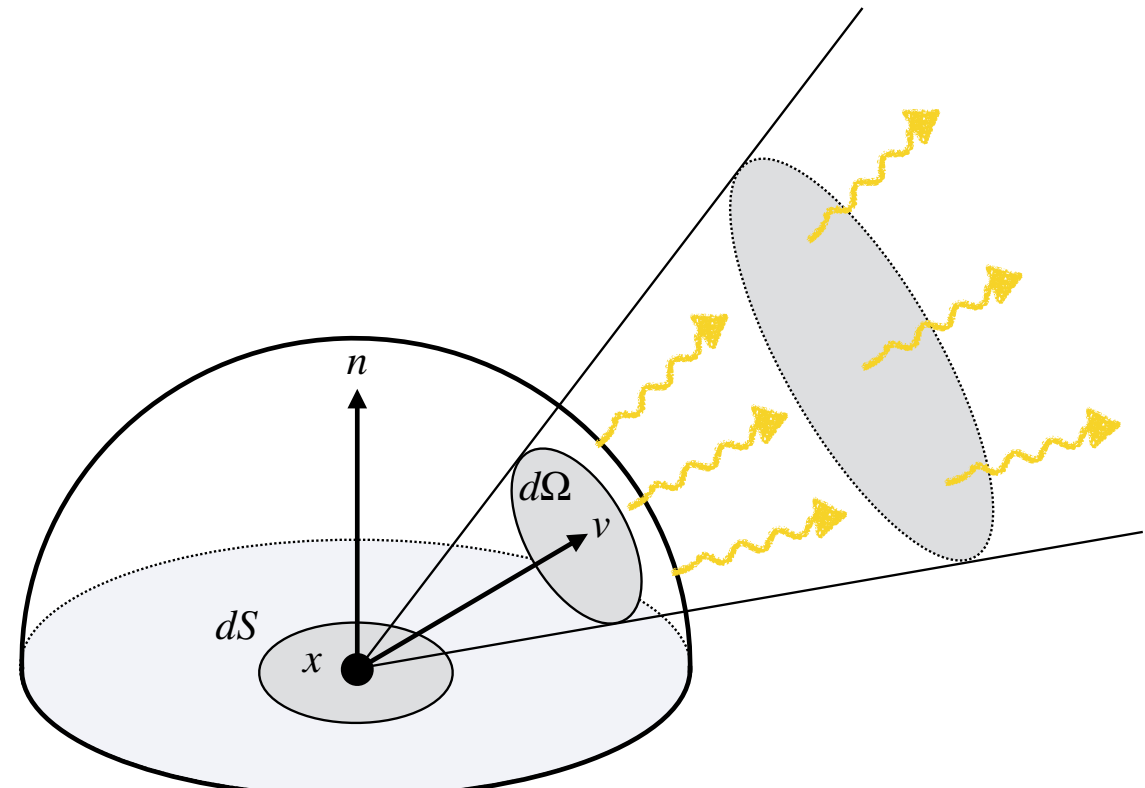
Radiance

Flux is an extensive (global) measure

In practice, we use an intensive (local) description of light:

The **radiance** $L(x, v)$ is

- the flux density x
- at point v
- along direction dS
- through perp. area $| \langle n, v \rangle |$
- through solid angle $d\Omega$



$$L(x, v) | \langle n, v \rangle | dS d\Omega$$

Radiance fields (RFs)

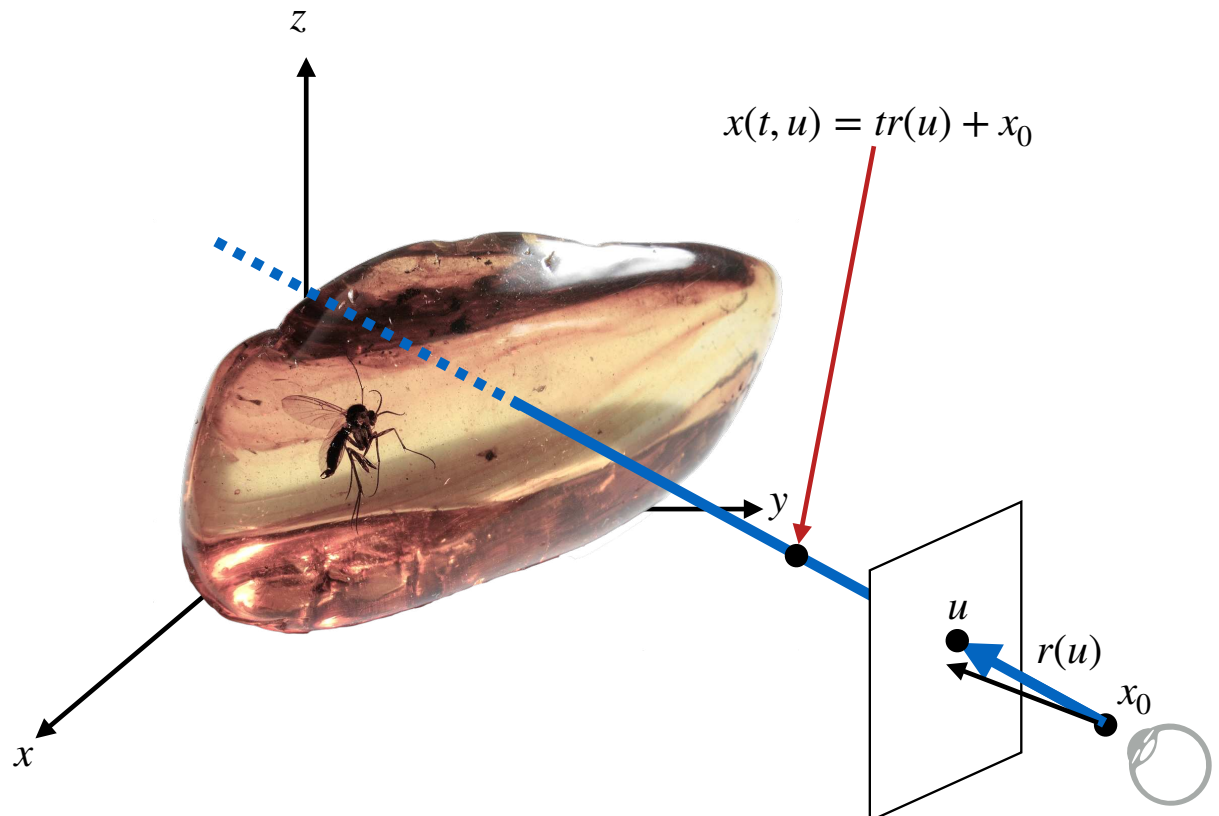
A **radiance field** is a pair of functions:

- $\sigma(x)$ absorption (non-neg. scalar)
- $c(x, r)$ color (RGB vector)

together with the **rendering equation**:

$$I(u) = \int_0^{\infty} c(x(t, u), r(u)) w(t, u) dt$$

$$w(t, u) = \sigma(x(t, u)) e^{-\int_0^t \sigma(x(q, u)) dq}$$



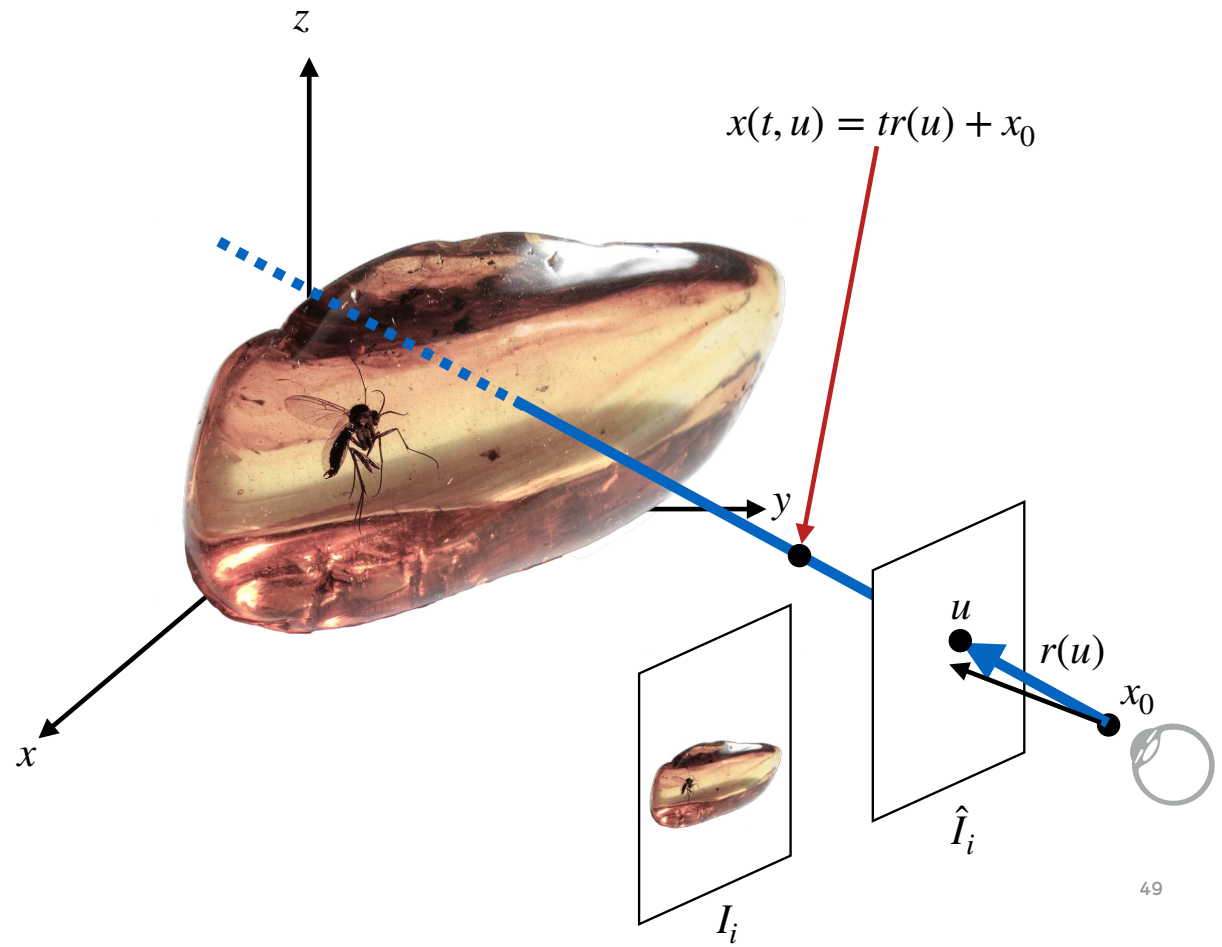
Training RFs

Training data:

- Example images of the object/scene I_i
- Calibration parameters (R_i, T_i)

Rendering function $\hat{I}_i = \text{raycast}(R_i, T_i, \theta)$

$$\text{Training loss } E(\theta) = \sum_{i=1}^n \|\hat{I}_i - I_i\|^2$$

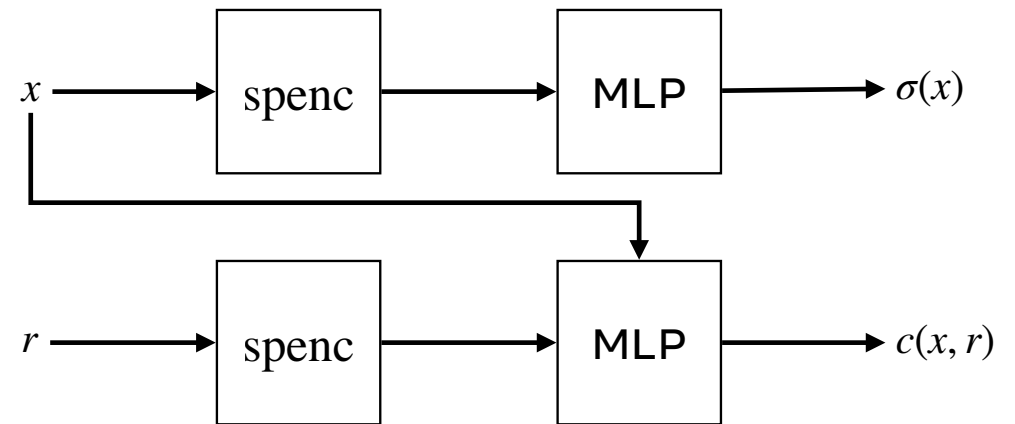


The NeRF idea

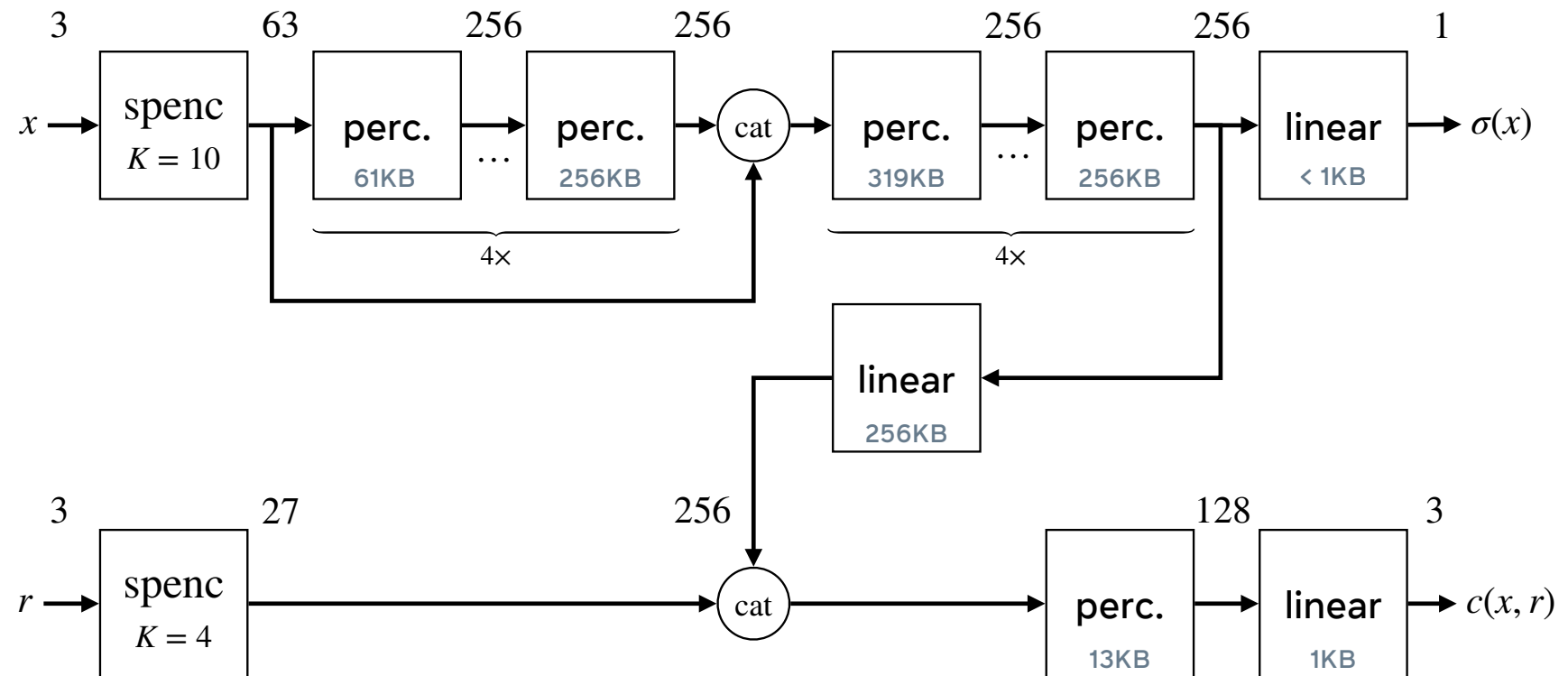
Use **Coordinate Multi-Layer Perceptrons**
(CMLPs) to represent functions $\sigma(x)$ and $c(x)$

CMLP = regular MLP + **coordinate (positional)
encoding**

$$\text{spenc}(a) = \begin{bmatrix} a \\ \sin(2^0 a) \\ \cos(2^0 a) \\ \vdots \\ \sin(2^{k-1} a) \\ \cos(2^{k-1} a) \end{bmatrix}$$



NeRF in real life



Model size: ~2.5MB (or 5MB coarse+fine)

Improving NeRF's computational efficiency

Plenoxels: Radiance fields without neural networks. Yu, Fridovich-Keil, Tancik, Chen, Recht, Kanazawa. arXiv, 2021.

VaxNeRF: Revisiting the classic for voxel-accelerated neural radiance field. Kondo, Ikeda, Tagliasacchi, Matsuo, Ochiai, Gu. CoRR, abs/2111.13112, 2021.

KiloNeRF: Speeding up neural radiance fields with thousands of tiny MLPs. Reiser, Peng, Liao, Geiger. arXiv.cs, abs/2103.13744, 2021.

Direct voxel grid optimization: Super-fast convergence for radiance fields reconstruction. Sun, Sun, Chen. Proc. CVPR, 2022

Instant neural graphics primitives with a multiresolution hash encoding. Müller, Evans, Schied, Keller. Proc. SIGGRAPH, 2022.

Efficient geometry-aware 3D generative adversarial networks. Chan, Lin, Chan, Nagano, Pan, Mello, Gallo, Guibas, Tremblay, Khamis, Karras, Wetzstein. Proc. CVPR, 2022.

TensoRF: Tensorial radiance fields. Chen, Xu, Geiger, Yu, Su. arXiv, 2022.

Direct Voxel Grid

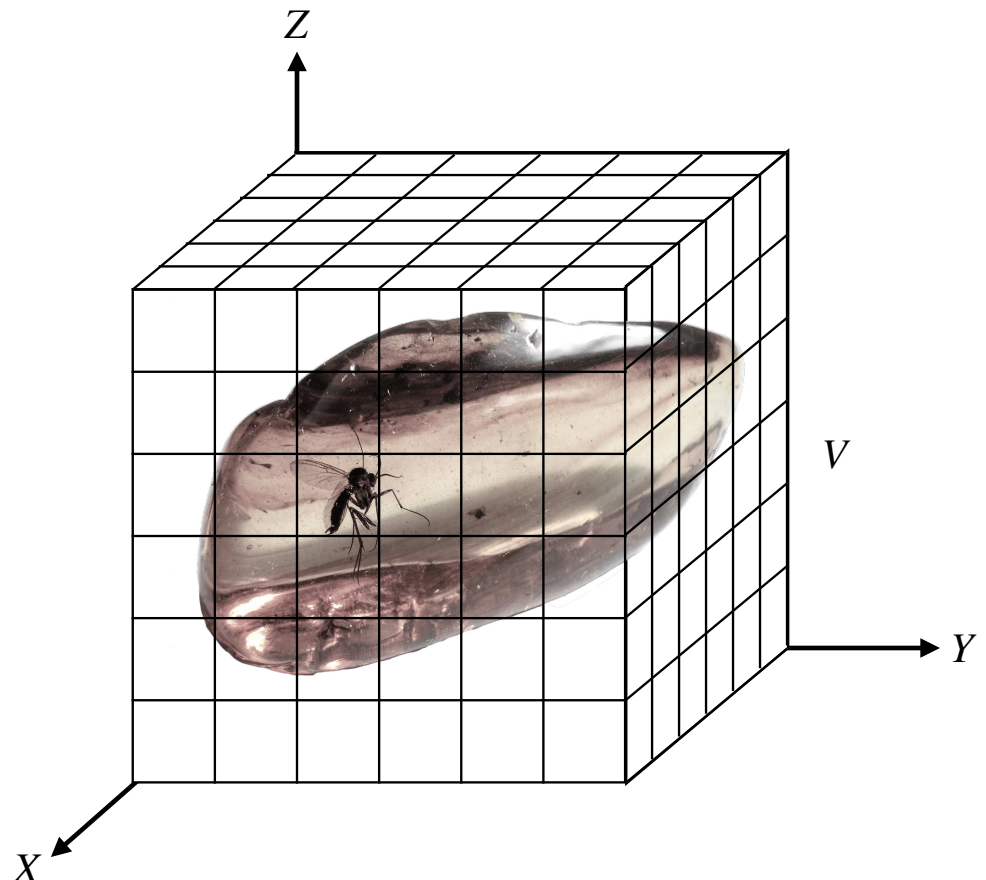
Tabulate σ using a 3D grid:

- $\sigma(x) = G \cdot \log(1 + \exp s(x))$
- $s(x) = \text{interp}(V, x)$ (trilinear)

Softplus makes $\sigma(x) > 0$

The gain G compensates for small Δ_i in the rendering equation:

$$w(x_i \rightarrow \text{sensor}) = (1 - e^{-\sigma(x_i)\Delta_i}) \sum_{j=0}^{i-1} e^{-\Delta_j \sigma(x_j)}$$



Direct Voxel Grid: color

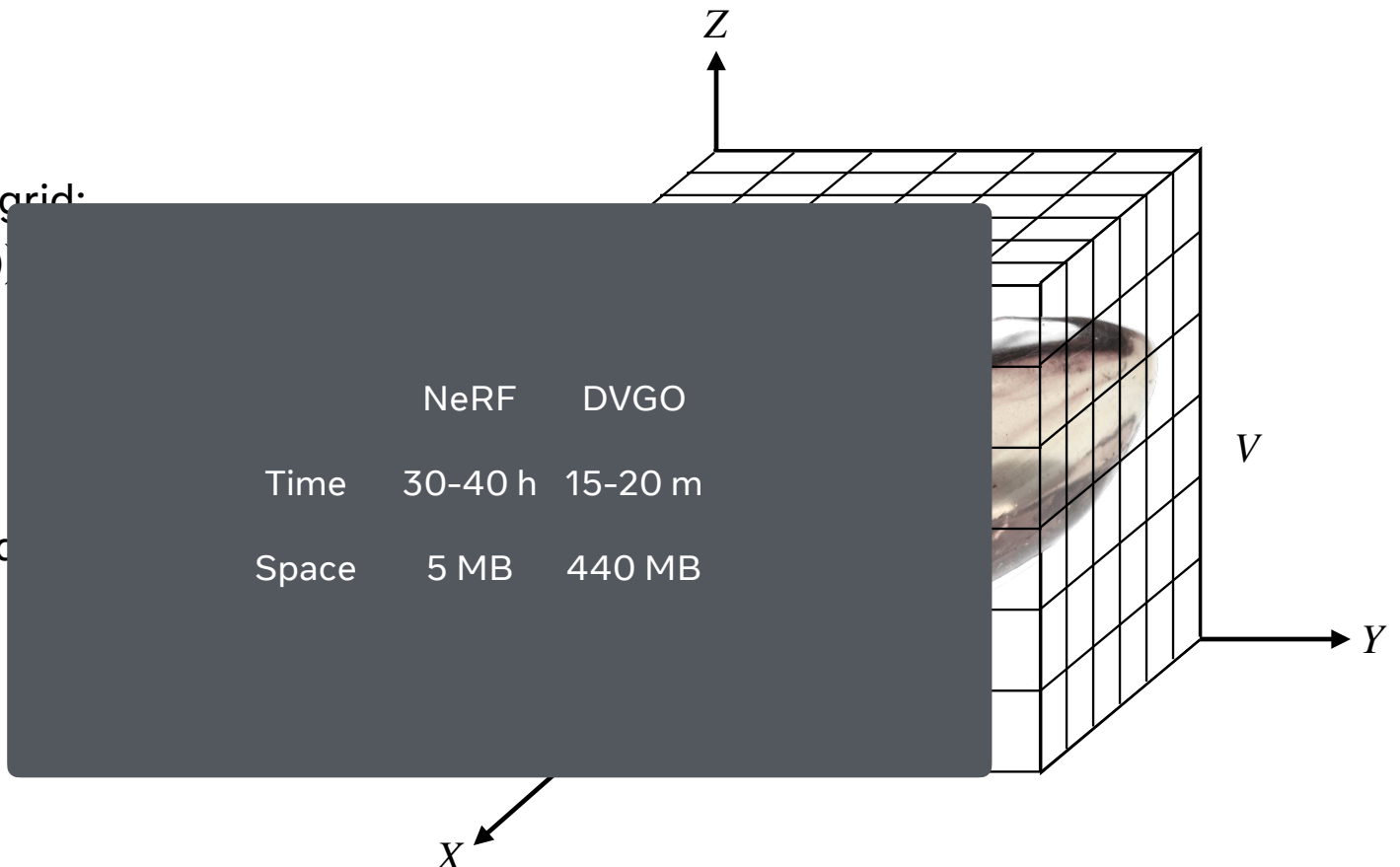
Tabulate $c(x, r)$ using a 3D grid:

- $c(x, r) = \text{MLP}(x, r; f(x))$
- $f(x) = \text{interp}(V_f, x)$
- $f(x) \in \mathbb{R}^C$

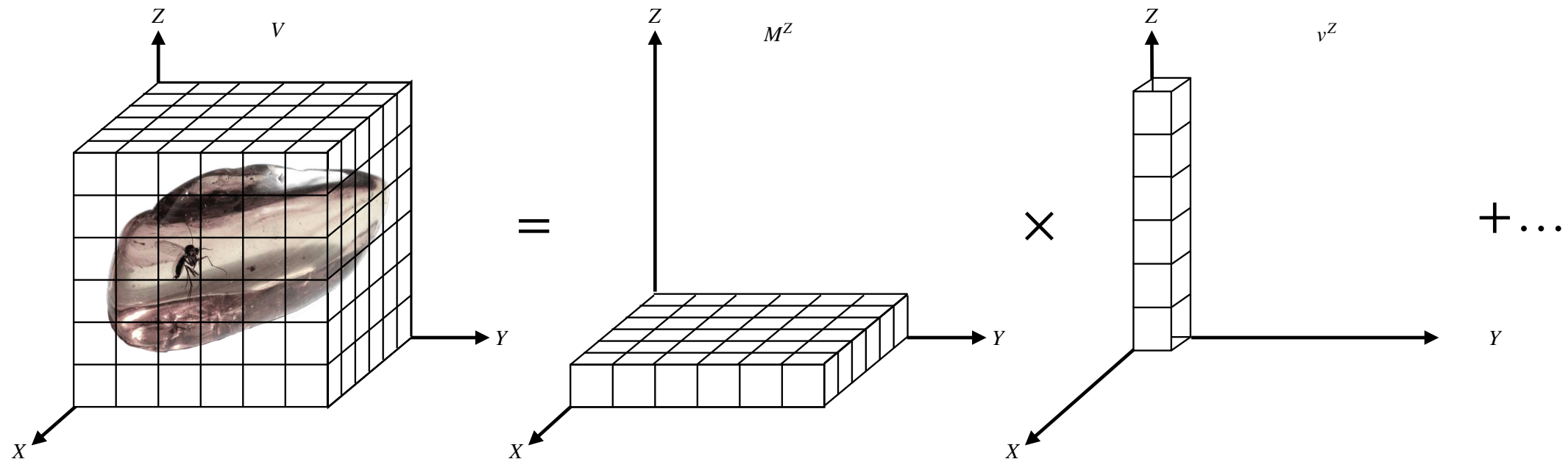
MLPs are much smaller and faster

Parameters:

- $160 \times 160 \times 160$ grid
- 1 + 27 scalars per cell
- 440 MB



TensoRF



$$\sigma(x, y, z) = \sum_{r=1}^R M_{rxy}^Z v_{rz}^Z + M_{ryz}^X v_{rx}^X + M_{rzx}^Y v_{ry}^Y$$

(tensor decomposition)

Voxel Grid:

$$O(CWHD) = O(CW^3)$$

TensoRF:

$$O(3RW^2)$$

$$3R \ll CW$$

NeRF vs DVGO vs TensoRF: Take home messages

Coordinate MLPs are much harder to train than tabular representations

Low-rank factorisation is very effective for volumetric data

No free lunch:

- these reconstruction problems are kind of easy
- MLPs could still win with less or more noisy data

	NeRF	DVGO	TensoRF
Time	30-40 h	15-30 m	15-30 m
Space	5 MB	440 MB	5 MB

Efficient geometry-aware 3D generative adversarial networks. Chan, Lin, Chan, Nagano, Pan, Mello, Gallo, Guibas, Tremblay, Khamis, Karras, Wetzstein. Proc. CVPR, 2022.

TensoRF: Tensorial radiance fields. Chen, Xu, Geiger, Yu, Su. arXiv, 2022.

Scaling geometry

There is more than one object out there!



Training NeRF



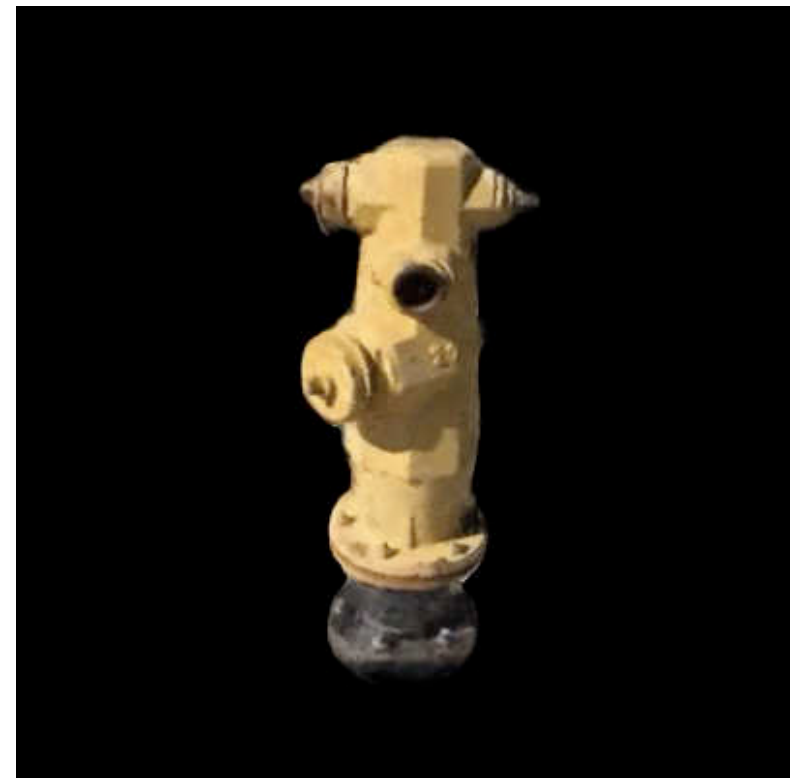
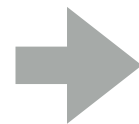
Continue training NeRF...



NeRF's statistical efficiency

NeRF assumes that dozens or even hundreds of view of an objects are available

It then learns a different model for each object



Improving NeRF statistical efficiency

Scene representation networks: Continuous 3D-structure-aware neural scene representations. Sitzmann, Zollhöfer, Wetzstein. Proc. NeurIPS, 2019.

MVSNeRF: Fast generalizable radiance field reconstruction from multi-view stereo. Chen, Xu, Zhao, Zhang, Xiang, Yu, Su. Proc. ICCV, 2021.

Putting NeRF on a diet: Semantically consistent few-shot view synthesis. Jain, Tancik, Abbeel. Proc. ICCV, 2021.

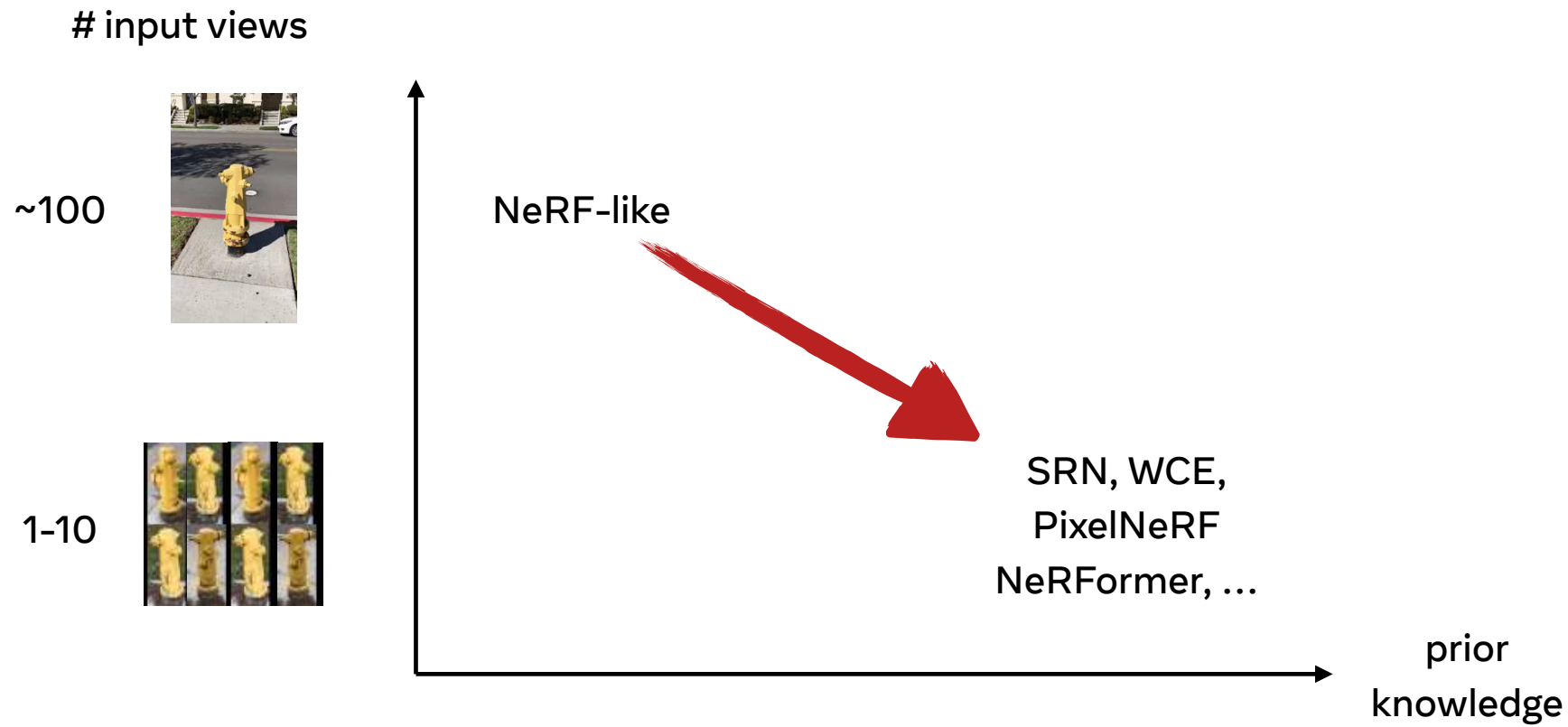
Unsupervised learning of 3D object categories from videos in the wild. Henzler, Reizenstein, Labatut, Shapovalov, Ritschel, Vedaldi, Novotny. CVPR, 2021.

PixelNeRF: Neural radiance fields from one or few images. Yu, Ye, Tancik, Kanazawa. Proc. CVPR, 2021.

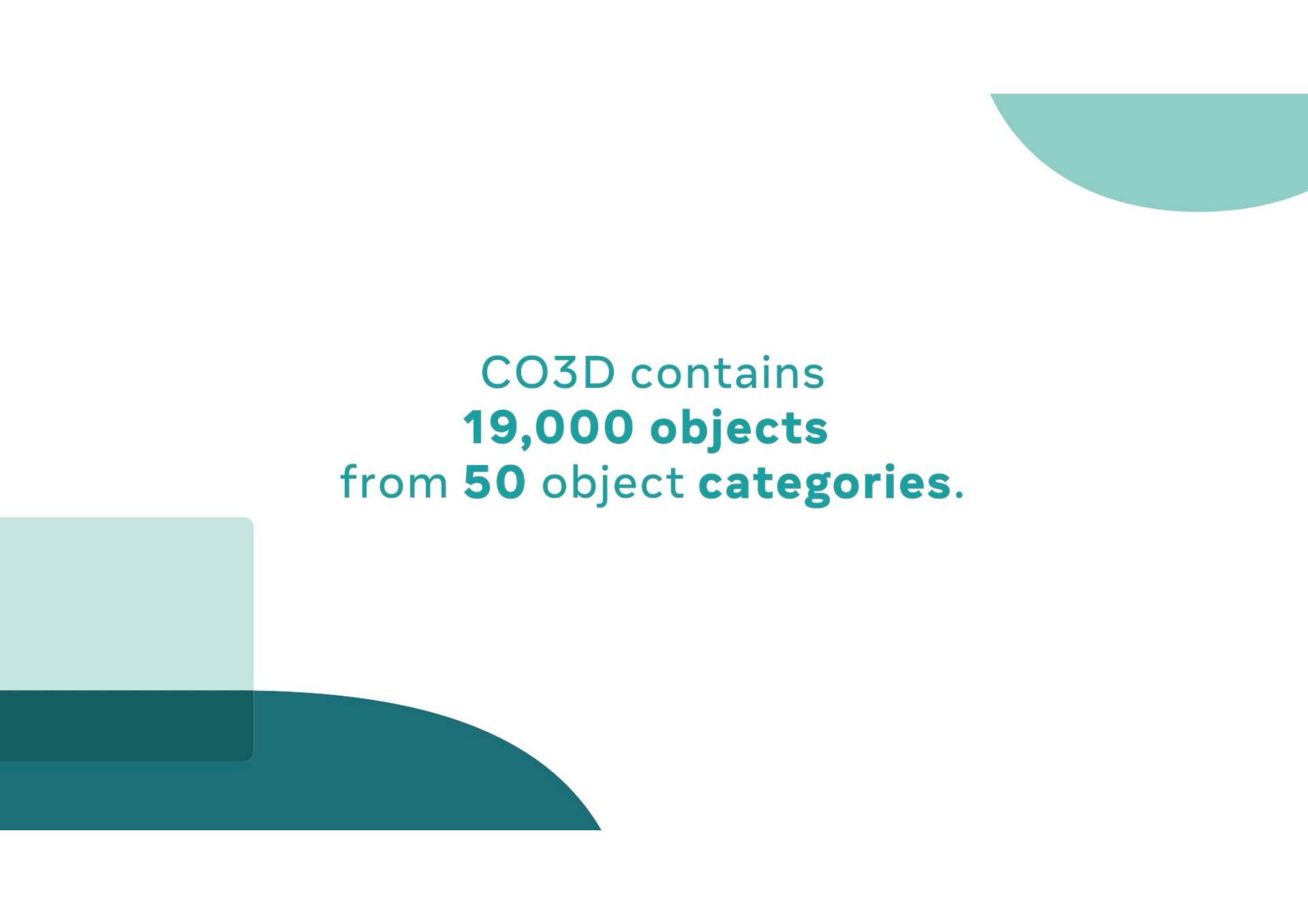
Common Objects in 3D: Large-scale learning and evaluation of real-life 3D category reconstruction. Reizenstein, Shapovalov, Henzler, Sbordone, Labatut, Novotny. Proc. CVPR, 2021.

RegNeRF: Regularizing neural radiance fields for view synthesis from sparse inputs. Niemeyer, Barron, Mildenhall, Sajjadi, Geiger, Radwan. Proc. CVPR, 2022.

Reconstruction from less data



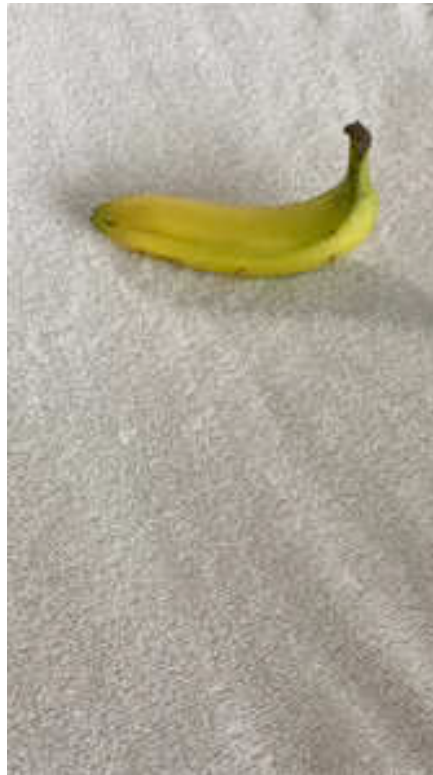
Where are you going to learn a
prior from?



**CO3D contains
19,000 objects
from 50 object categories.**

Crowdsourced videos

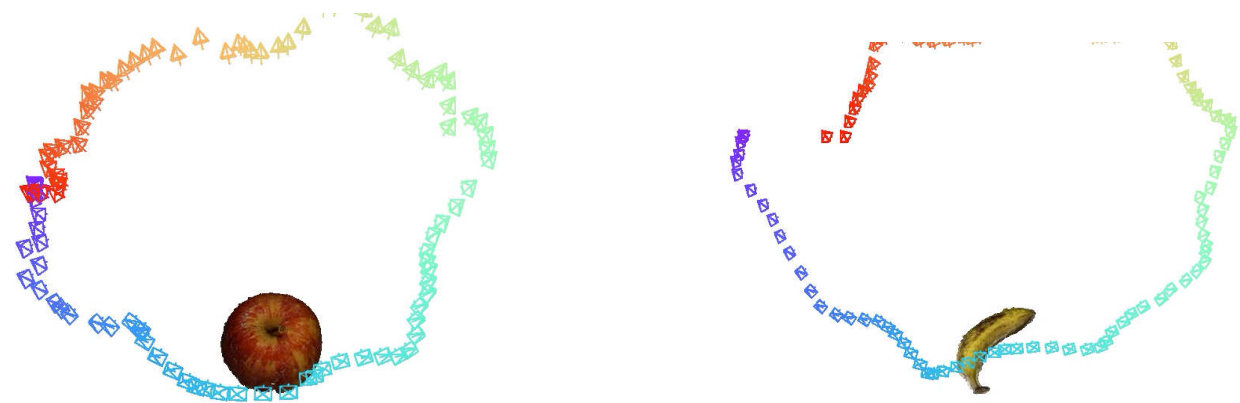
"Turntable" videos
of objects from
Amazon Mechanical
Turk (AMT)



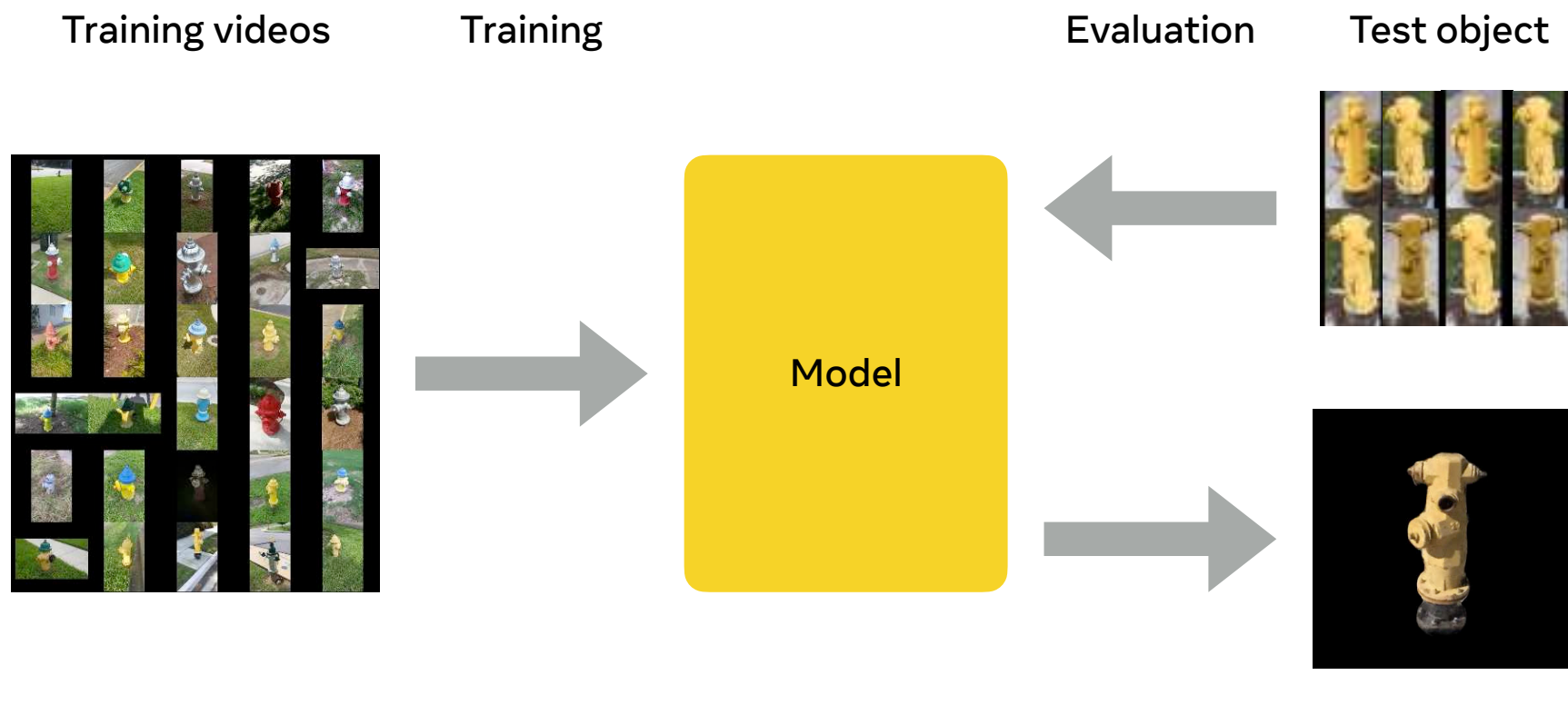
Camera estimates from SfM

COLMAP used to recover

- camera viewpoint
- point cloud



New-view synthesis task



Common Objects in 3D: Large-scale learning and evaluation of real-life 3D category reconstruction. Reizenstein, Shapovalov, Henzler, Sbordone, Labatut, Novotny. Proc. CVPR, 2021.

New views

NeRF-like models

Representation

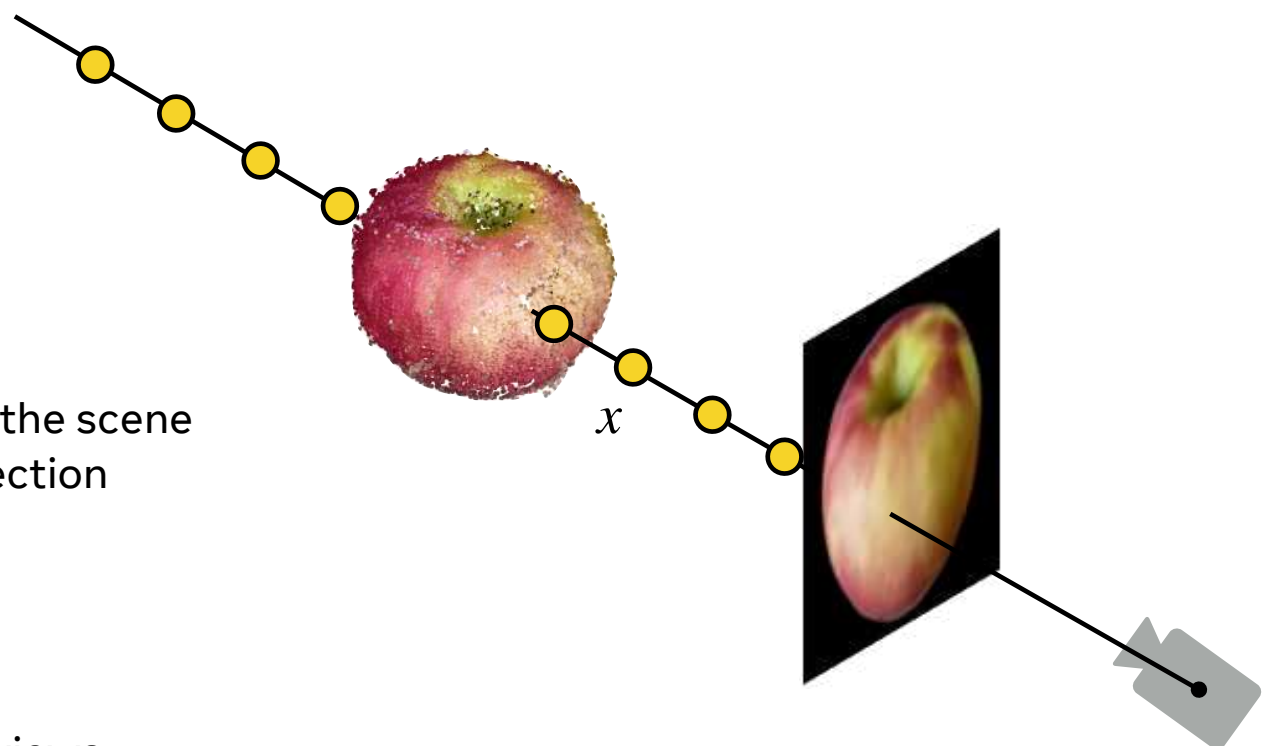
- x 3D point
- $\sigma(x)$ occupancy
- $c(x)$ colour

Rendering

- Shoot a ray from the camera into the scene
- Retrieve the colour of first intersection

Learning

- $\sigma(x) = \text{MLP}_\sigma(x)$
- $c(x) = \text{MLP}_c(x)$
- MLPs parameters fitted to ~100 views



NeRF: Representing scenes as neural radiance fields for view synthesis. Mildenhall, Srinivasan, Tancik, Barron, Ramamoorthi, Ng. Proc. ECCV, 2020

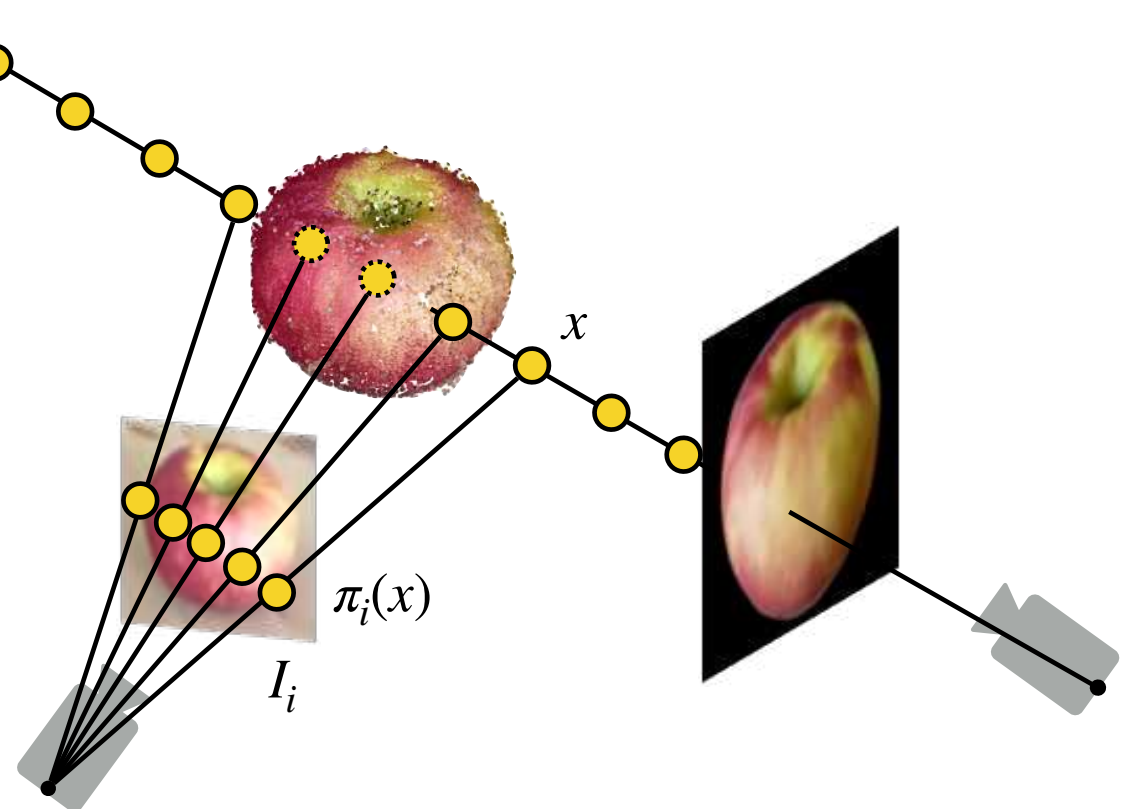
Warped Ray Conditioning (WRC)

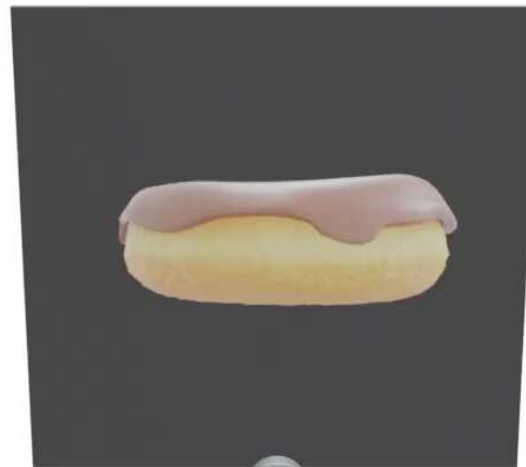
Measure

- Project each ray point x to each input view I_i
- Extract features
 $z_i = \Phi(\pi_i(x), I_i)$
- Pool features
 $z(x) = \text{agg}(z_1(x), \dots, z_K(x))$

Predict

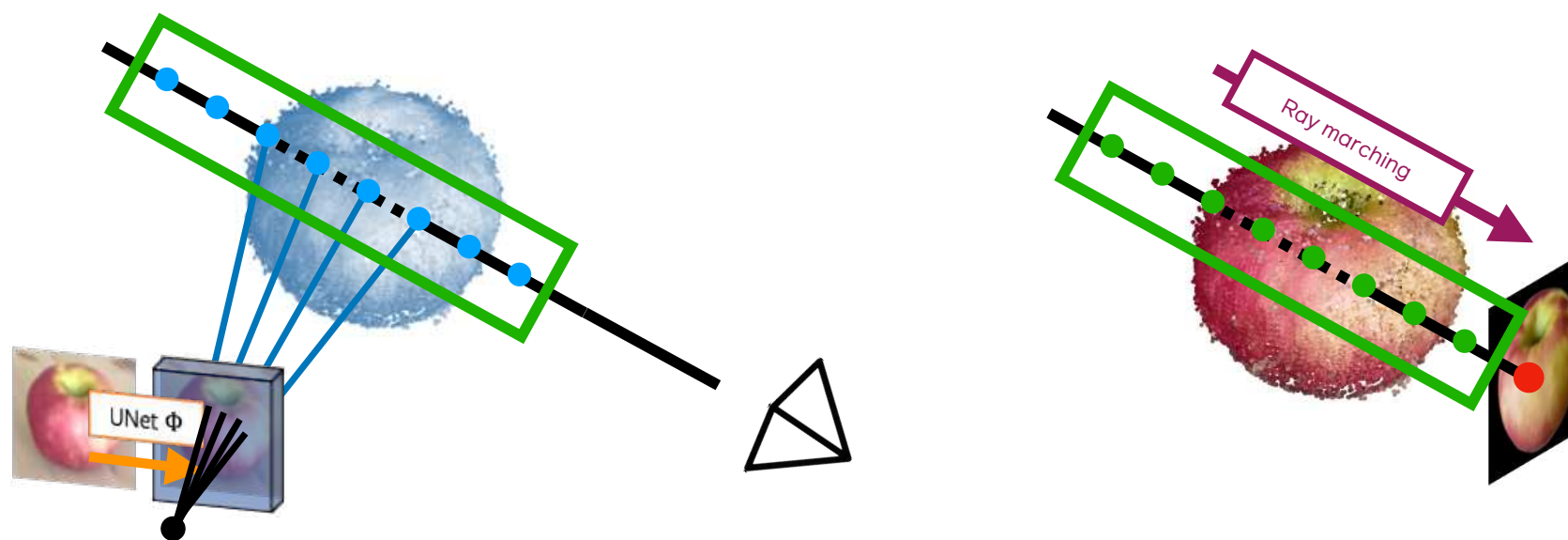
- $\sigma(x) = \text{MLP}_\sigma(x; z(x))$
- $c(x) = \text{MLP}_c(x; z(x))$





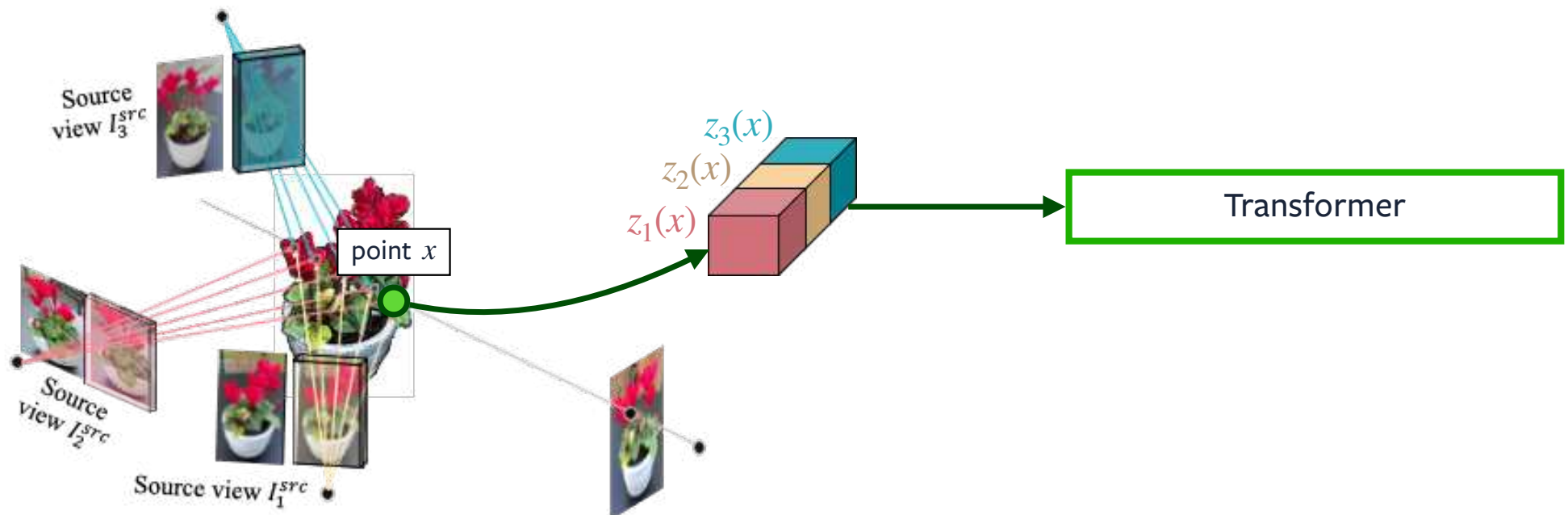
Better ray aggregation

Ray aggregation transformer $T_{\text{ray}}(z(x_1), \dots, z(x_N))$

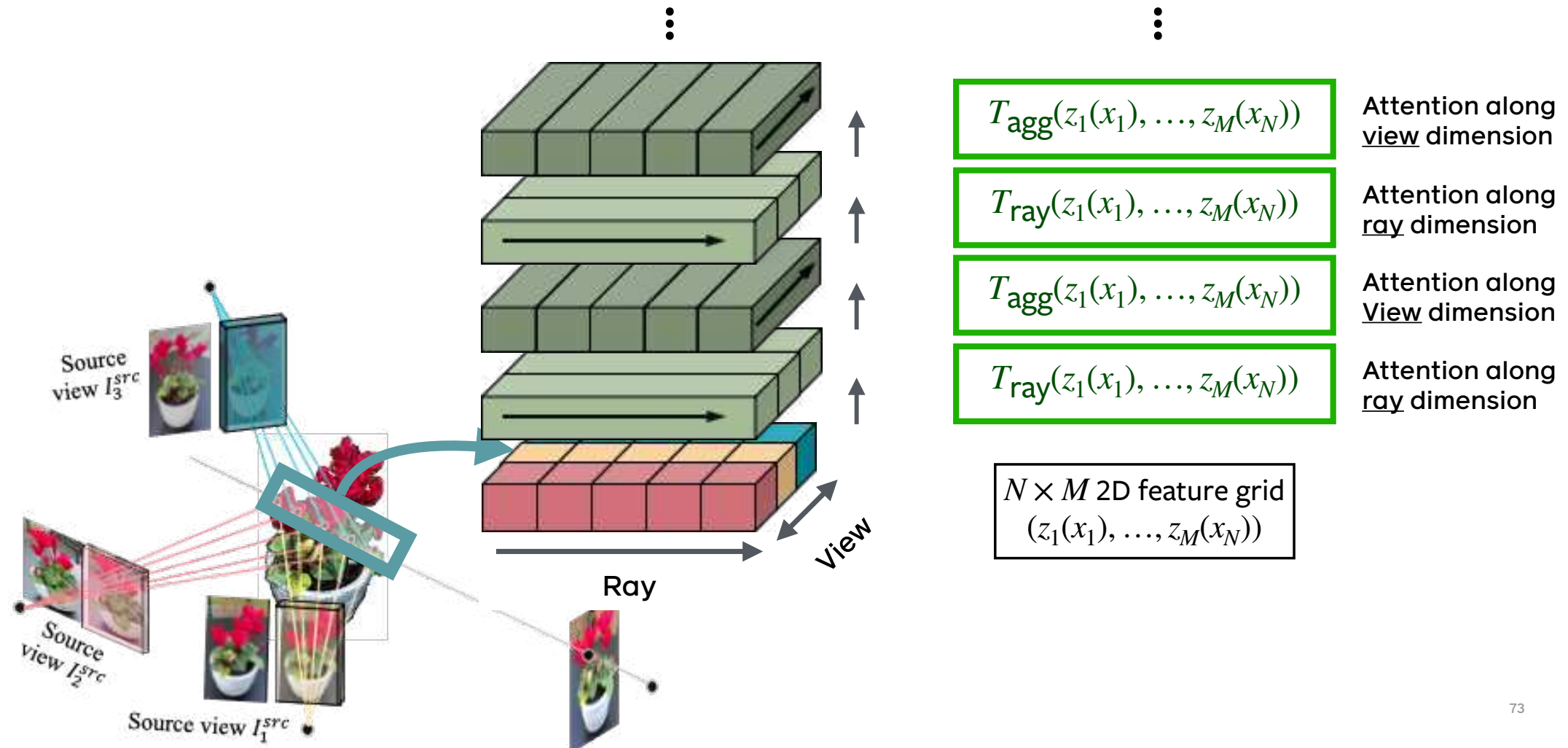


Better view aggregation

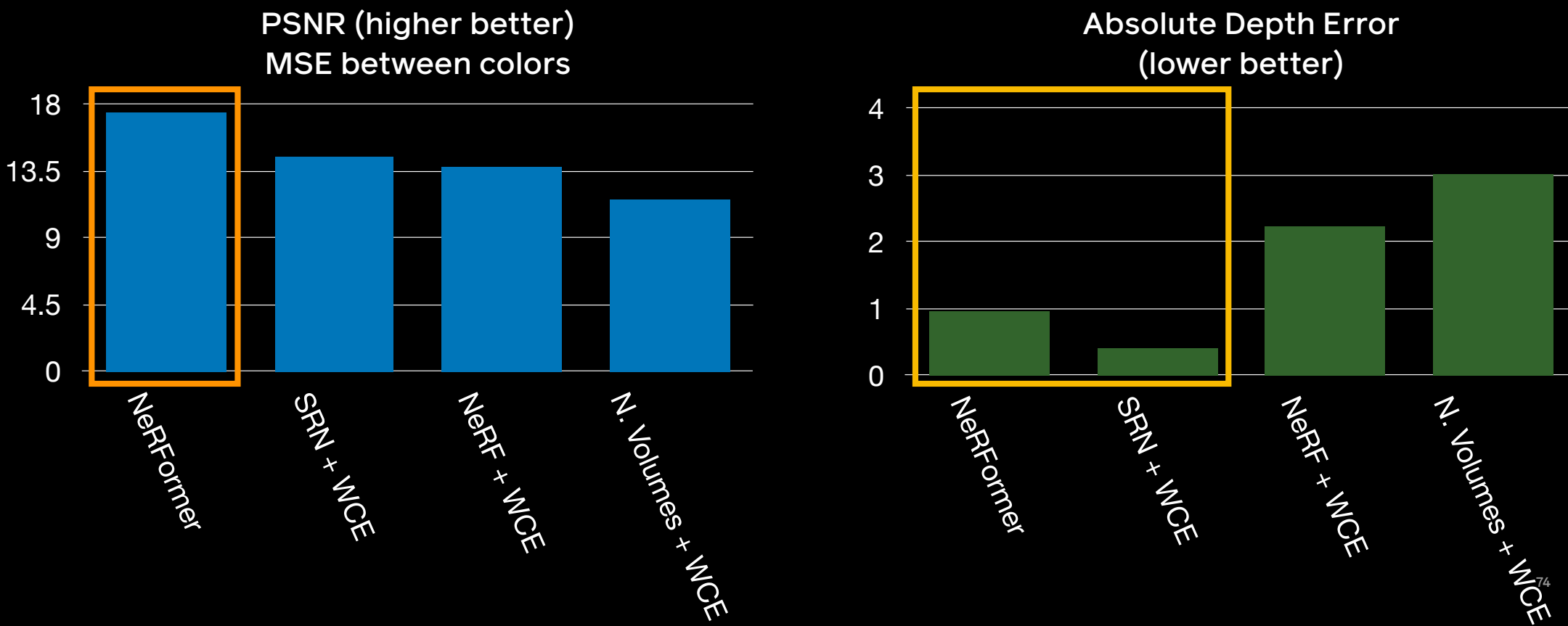
View aggregation transformer $T_{\text{agg}}(\{z_1(x), \dots, z_M(x)\})$



NeRFormer



WCE results



WCE results

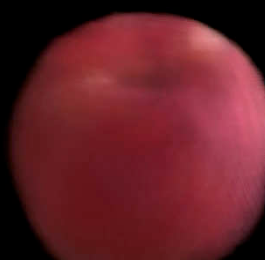
NeRF + WCE



SRN + WCE



NeRFormer



WCE results

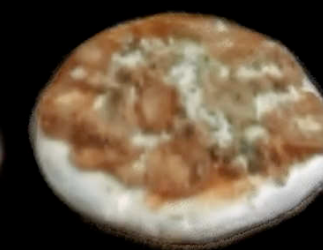
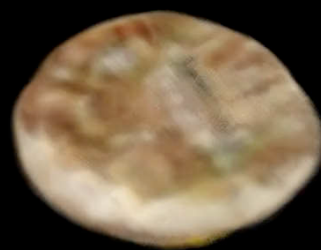
NeRF + WCE



SRN + WCE



NeRFormer



The CO3D Challenge

CO3D V2:

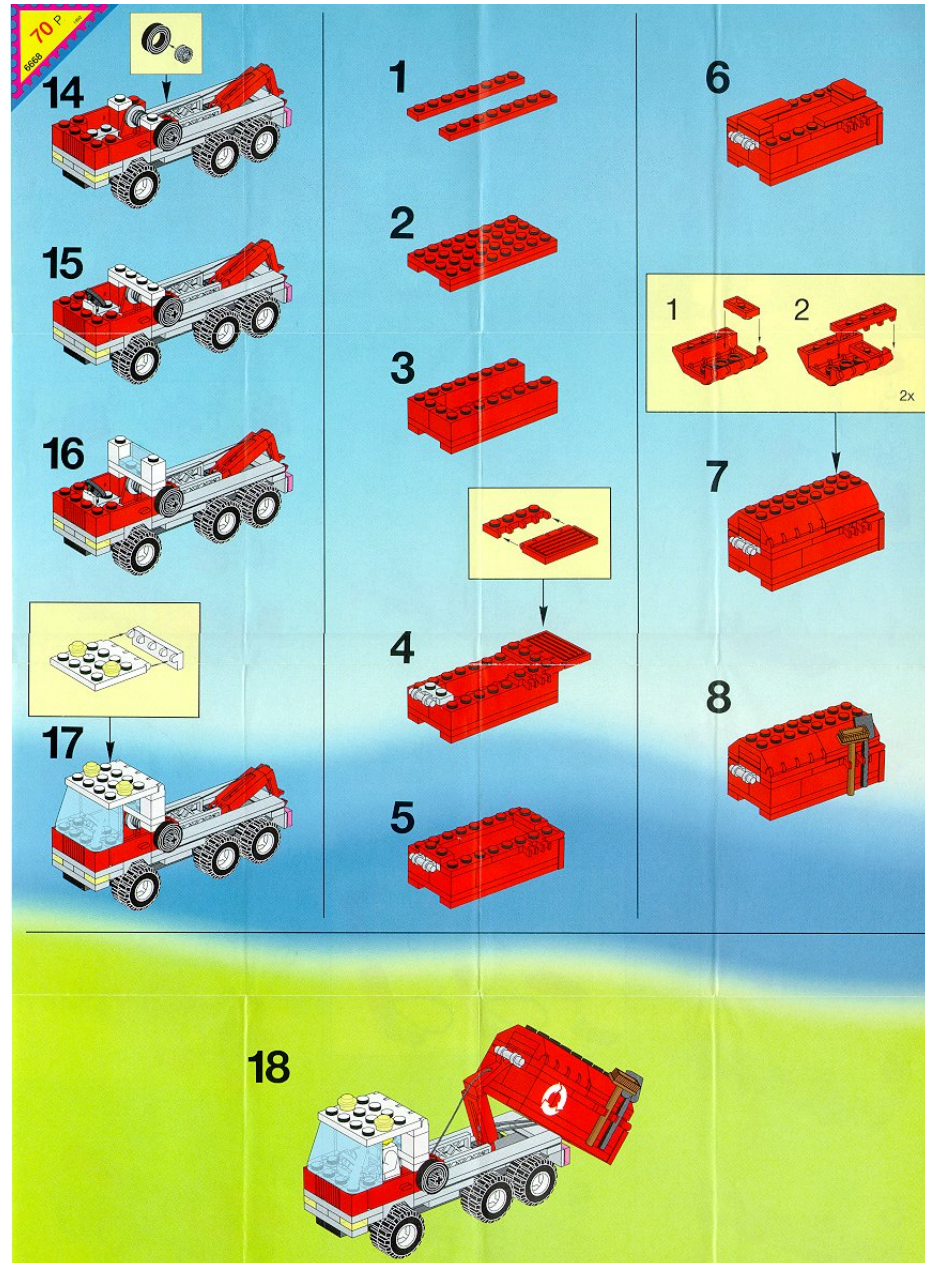
- ~40K viedeos
- Better geometry, masks, image quality
- Evaluation will be done on a hidden test set

Challenge coming at ECCV 2022



Geometry meets meaning

Basing abstract understanding on an understanding of geometry



Viewpoint change



NeuralDiff

Egocentric video



EPIC-KITCHENS

Stabilised, active objects



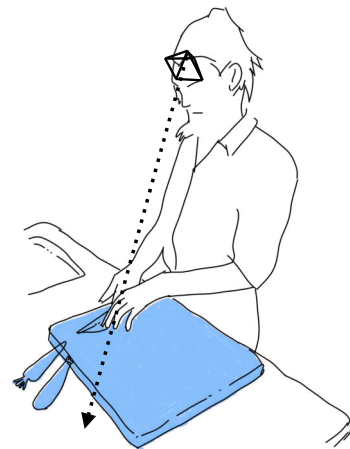
NeuralDiff: Segmenting 3D objects that move in egocentric videos. Tschernezki, Larlus, Vedaldi. 3DV, 2021.

Multiple specialised fields

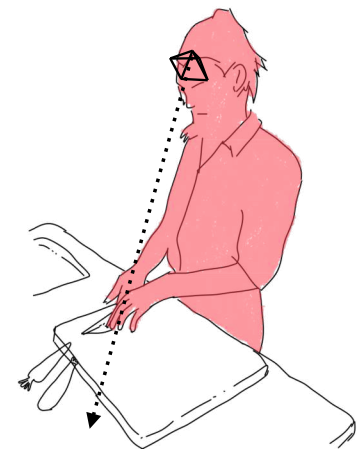
Background (exo)



Foreground (exo)



Actor (ego)



$c, \sigma \leftarrow \text{MLP}_b(x, d)$

$c, \sigma, \beta \leftarrow \text{MLP}_f(x, t)$

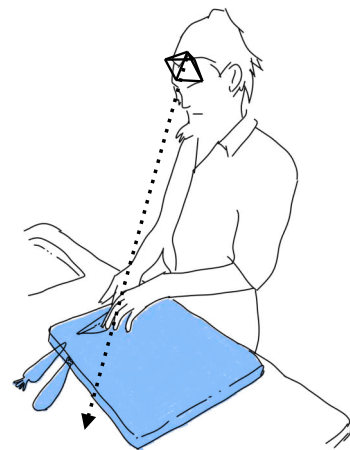
$c, \sigma, \beta \leftarrow \text{MLP}_a(x^*, t)$

Multiple specialised fields

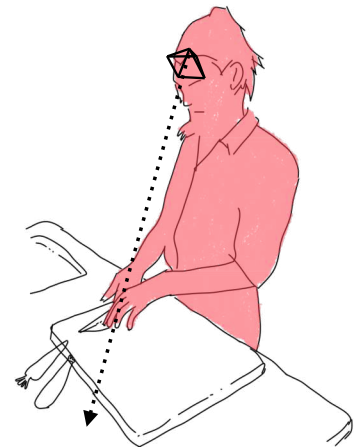
Background (exo)



Foreground (exo)



Actor (ego)



$c, \sigma \leftarrow \text{MLP}_b(x, d)$

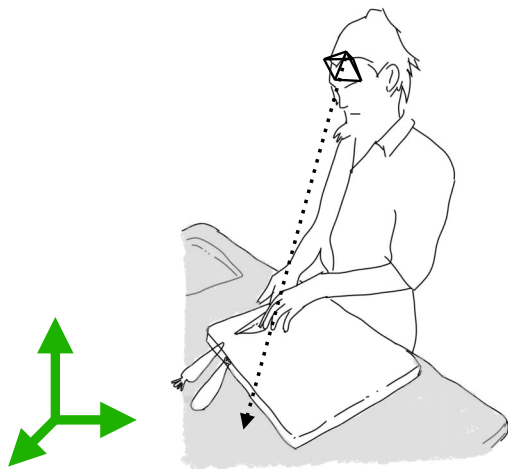
$c, \sigma, \beta \leftarrow \text{MLP}_f(x, t)$

$c, \sigma, \beta \leftarrow \text{MLP}_a(x^*, t)$

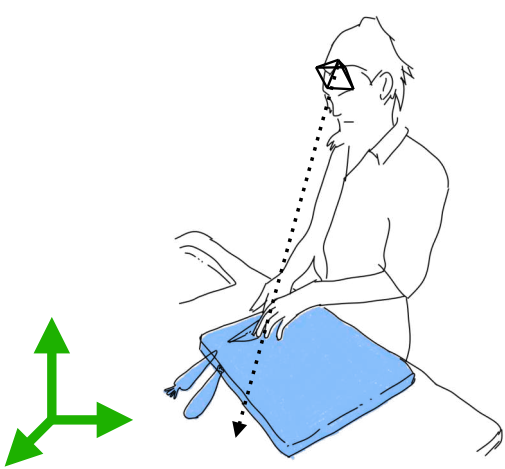
Time

Multiple specialised fields

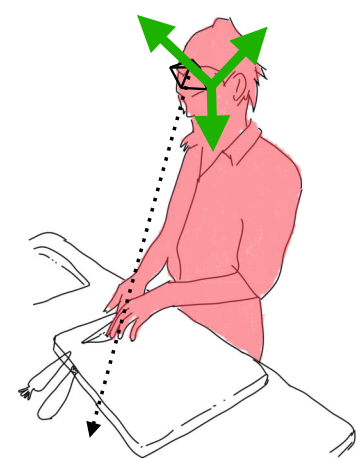
Background (exo)



Foreground (exo)



Actor (ego)



$c, \sigma \leftarrow \text{MLP}_b(x, d)$

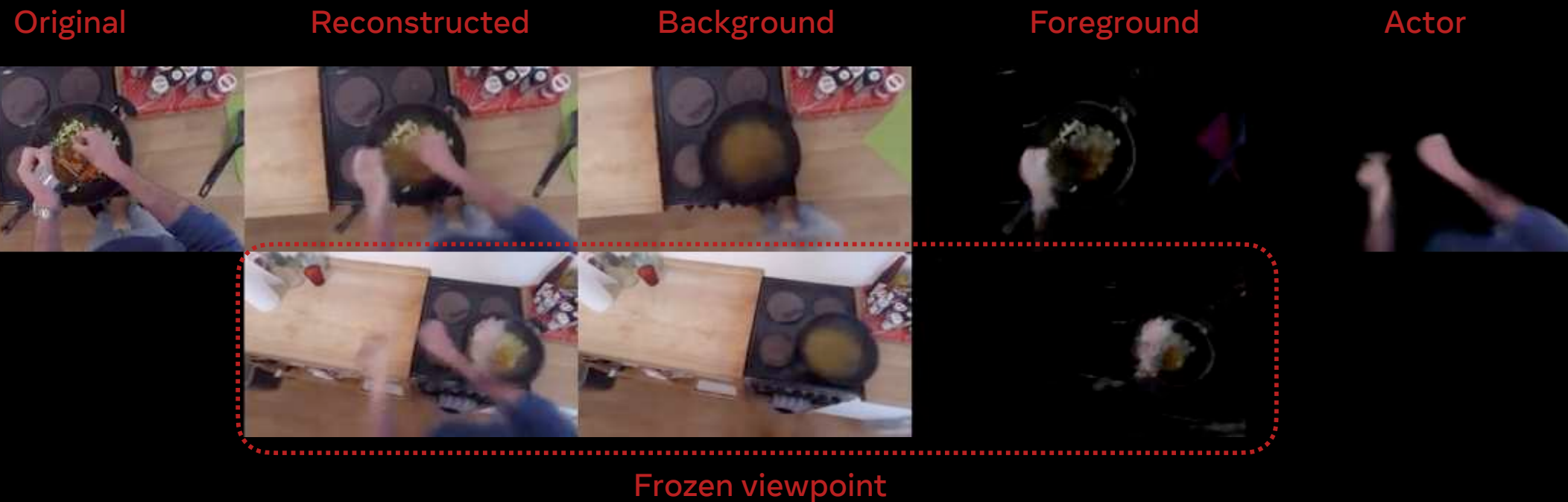
$c, \sigma, \beta \leftarrow \text{MLP}_f(x, t)$

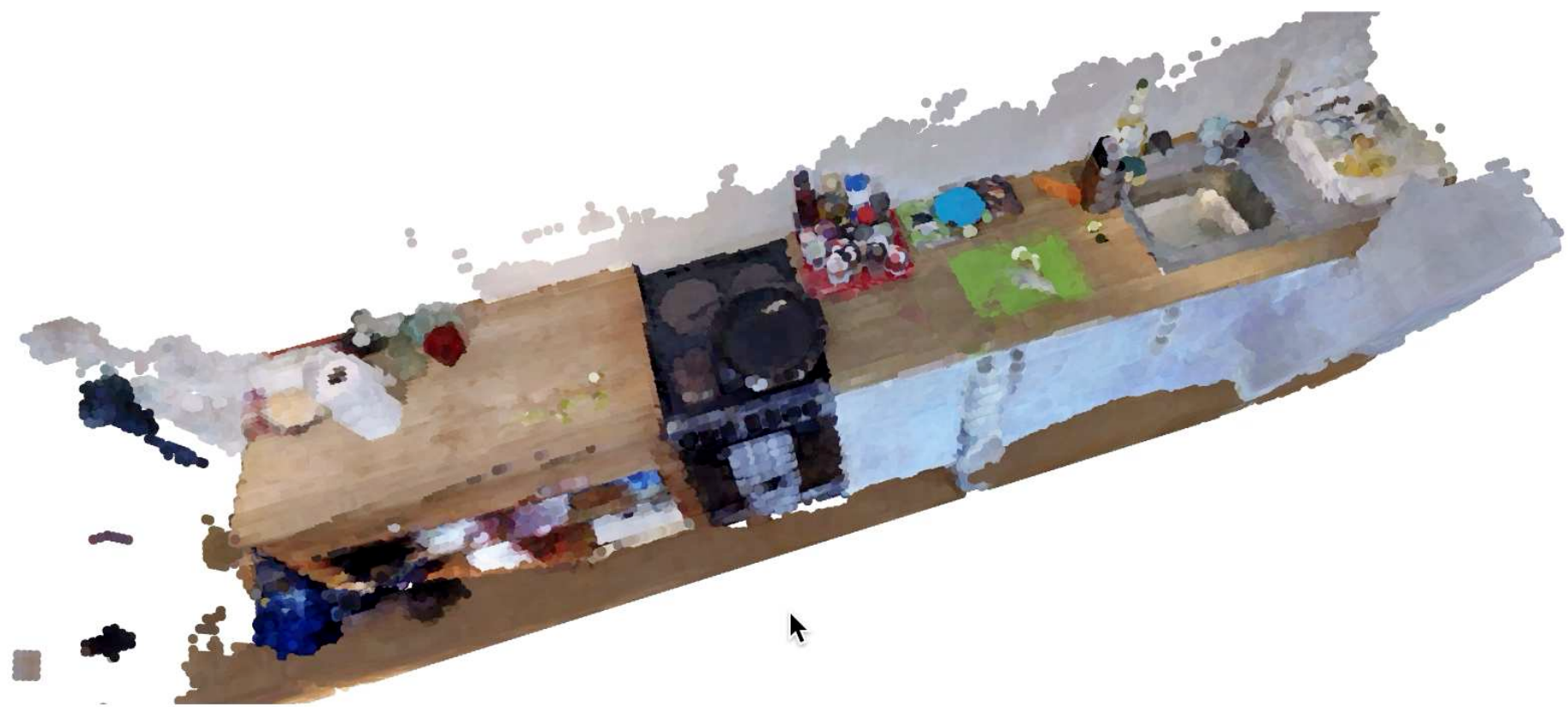
$c, \sigma, \beta \leftarrow \text{MLP}_a(x^*, t)$

World reference

Camera reference

Results



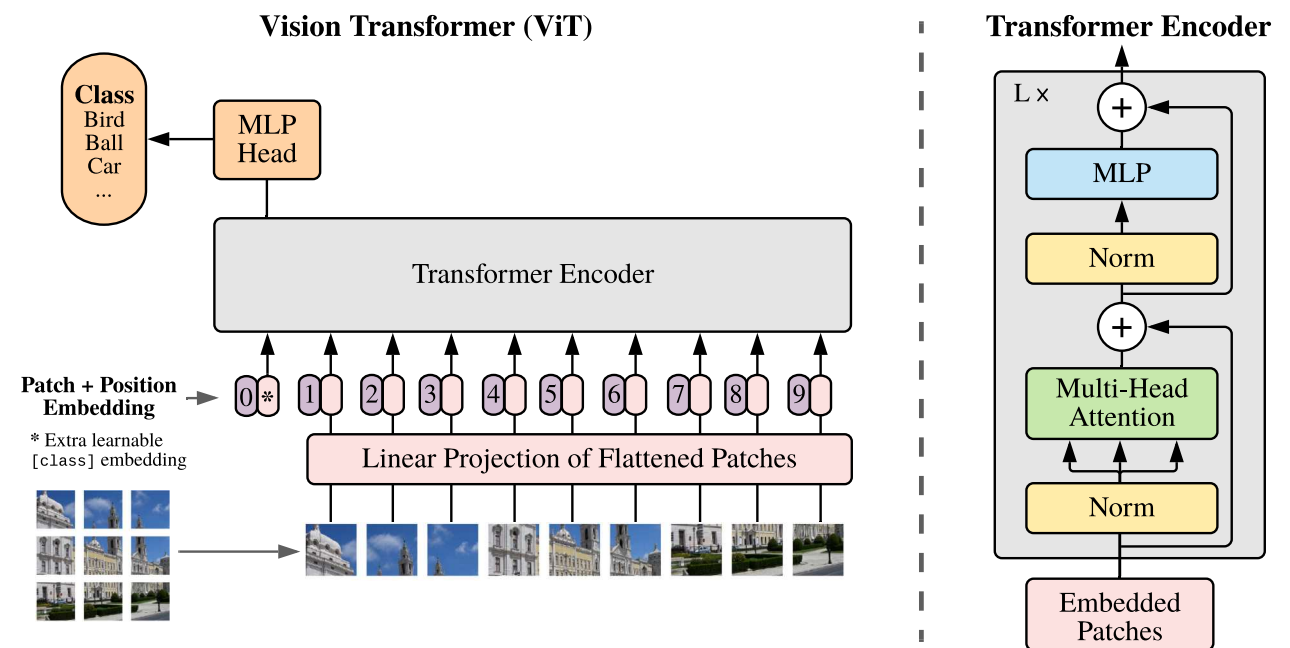


Large-scale 2D self-supervised representations

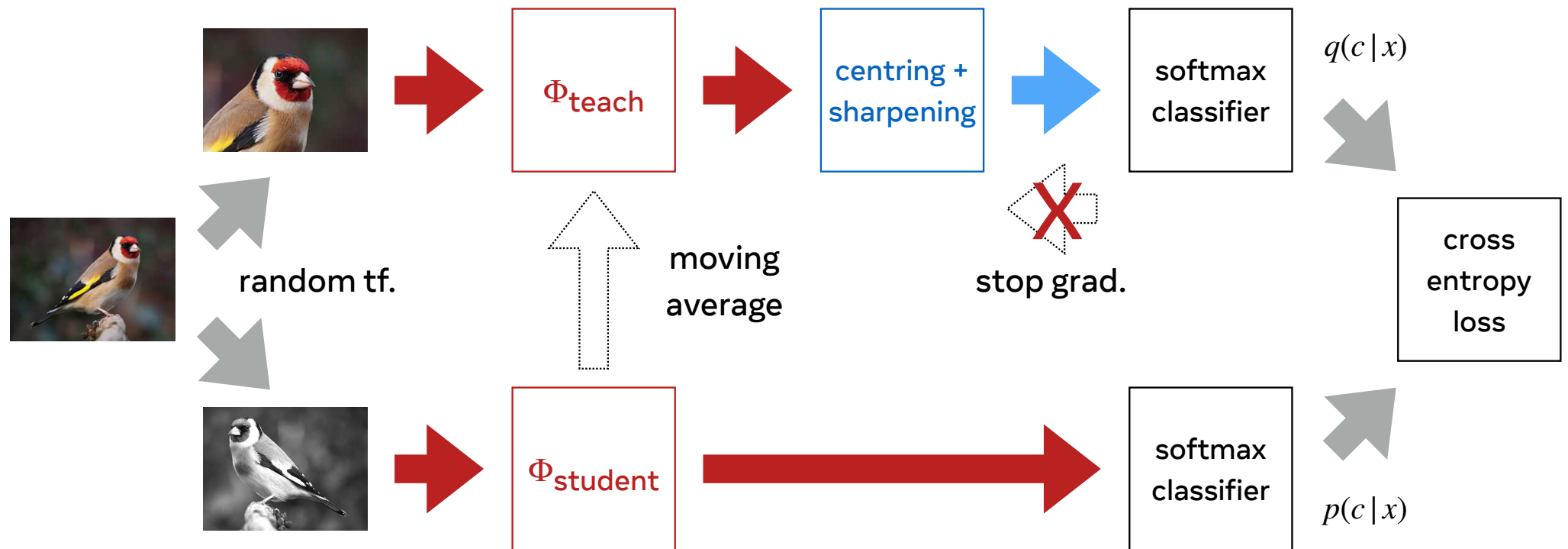
By avoiding the annotation cost,
unsupervised learning allow to scale
to much larder training datasets

High-capacity models can take
advantage of larger datasets

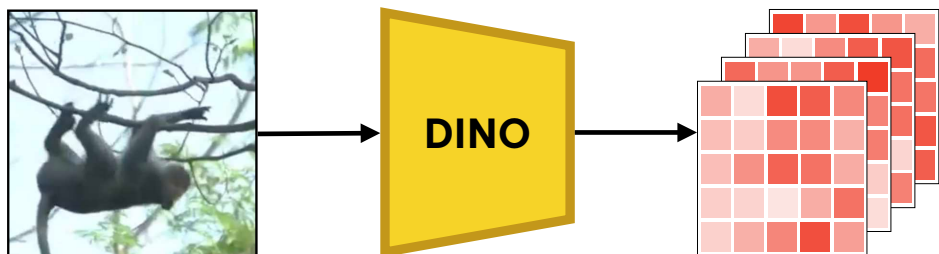
For instance, Vision Transformers
(ViT)



DINO: Self-distillation with no labels



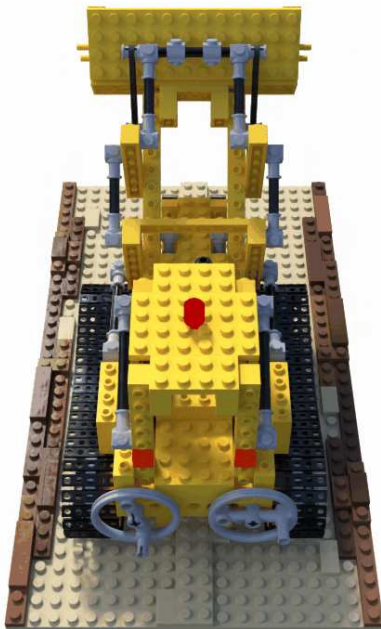
Self-supervised 2D representations



Emerging properties in self-supervised vision transformers. Caron, Touvron, Misra, Jégou, Mairal, Bojanowski, Joulin. Proc. ICCV, 2021

Neural Feature Fusion Fields (N3F)

Unsupervised 3D geometry



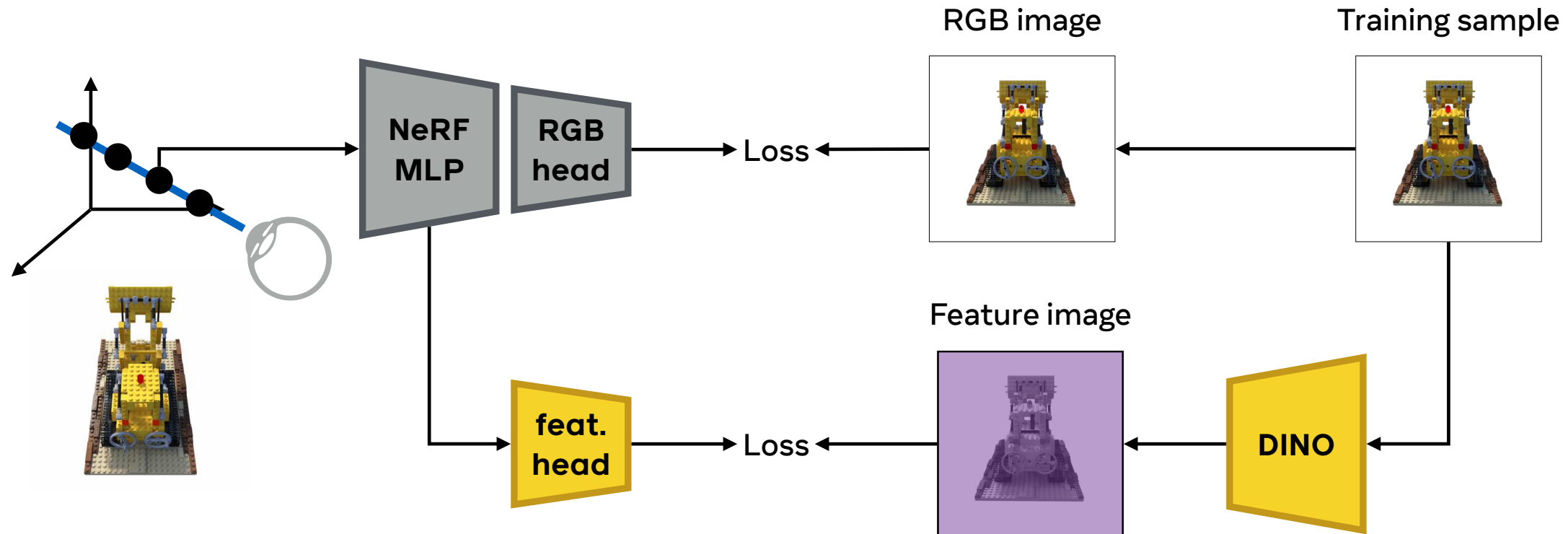
Fusion

N3F

Unsupervised 2D features



Neural Feature Fusion Fields (N3F)



Neural Feature Fusion Fields, Tschernezki, Laina, Larlus, Vedaldi. 3DV, 2022

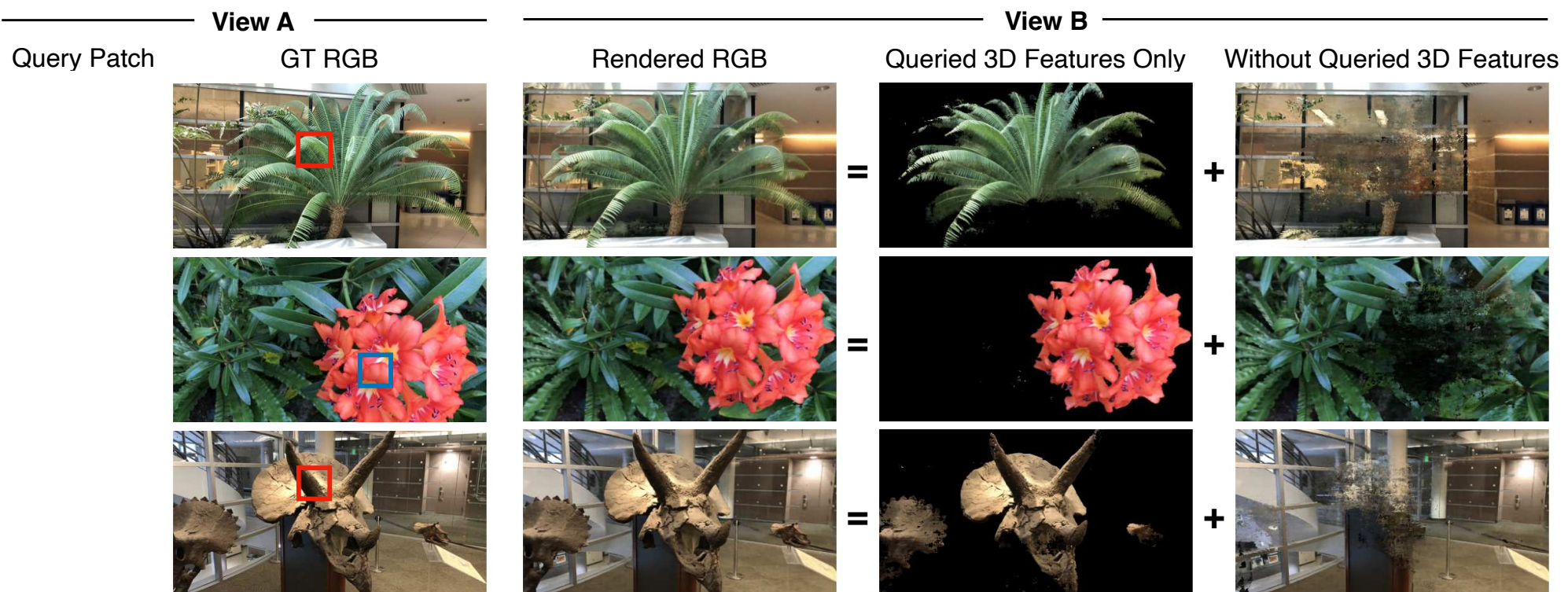
See also: In-place scene labelling and understanding with implicit scene representation. Zhi, Laidlow, Leutenegger, Davison. ICCV, 2021

NeRFs



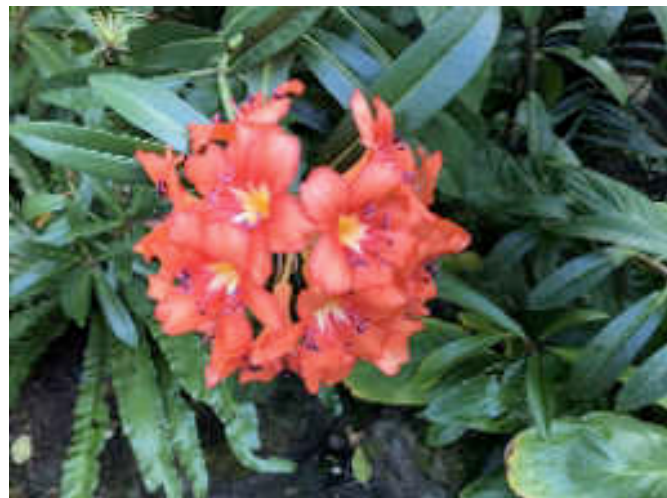
NeRF: Representing scenes as neural radiance fields for view synthesis. Mildenhall, Srinivasan, Tancik, Barron, Ramamoorthi, Ng. Proc. ECCV, 2020

Unsupervised 3D scene decomposition



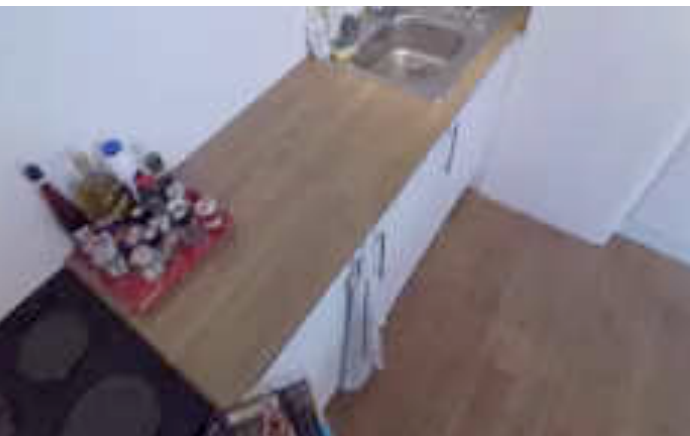
See also concurrent work: **Decomposing NeRF for Editing via Feature Field Distillation**, Kobayashi et al. arXiv, 2022.

In motion



3D distillation leads to more stable, denser features

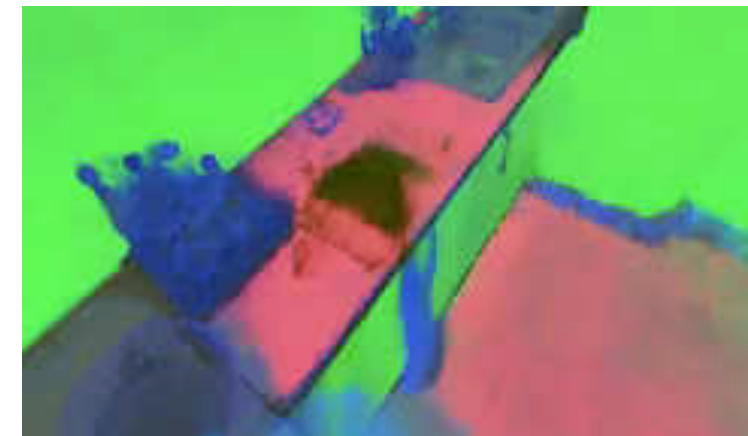
Input frame



DINO

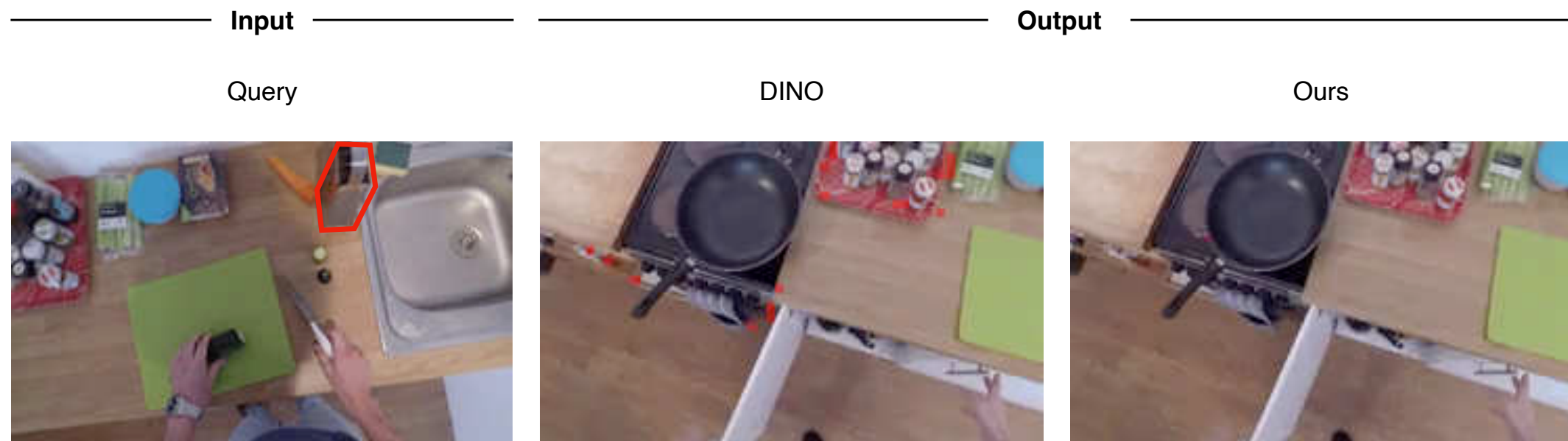


DINO + NeuralFusion

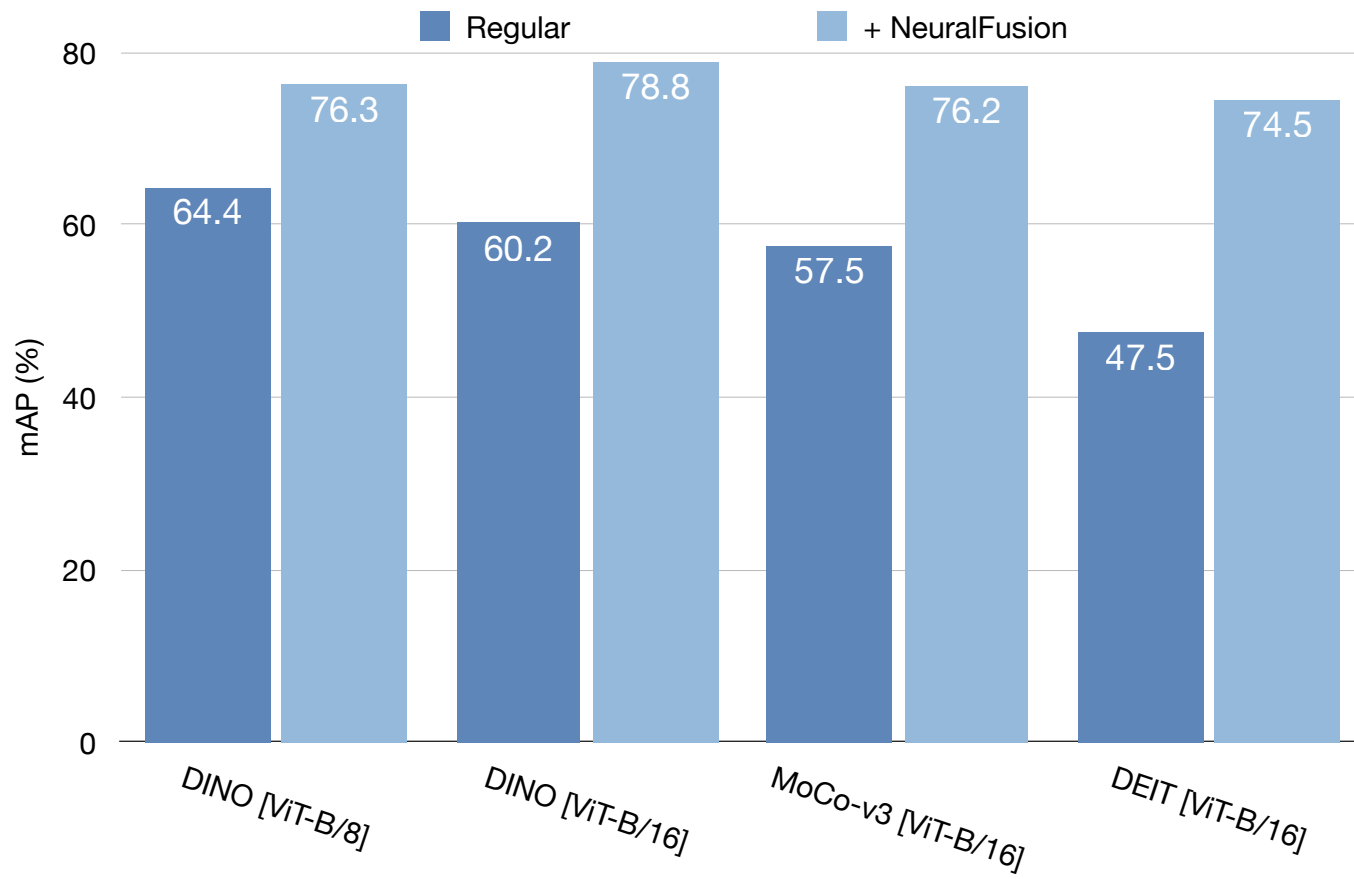


PCA-based coloring of dense DINO features

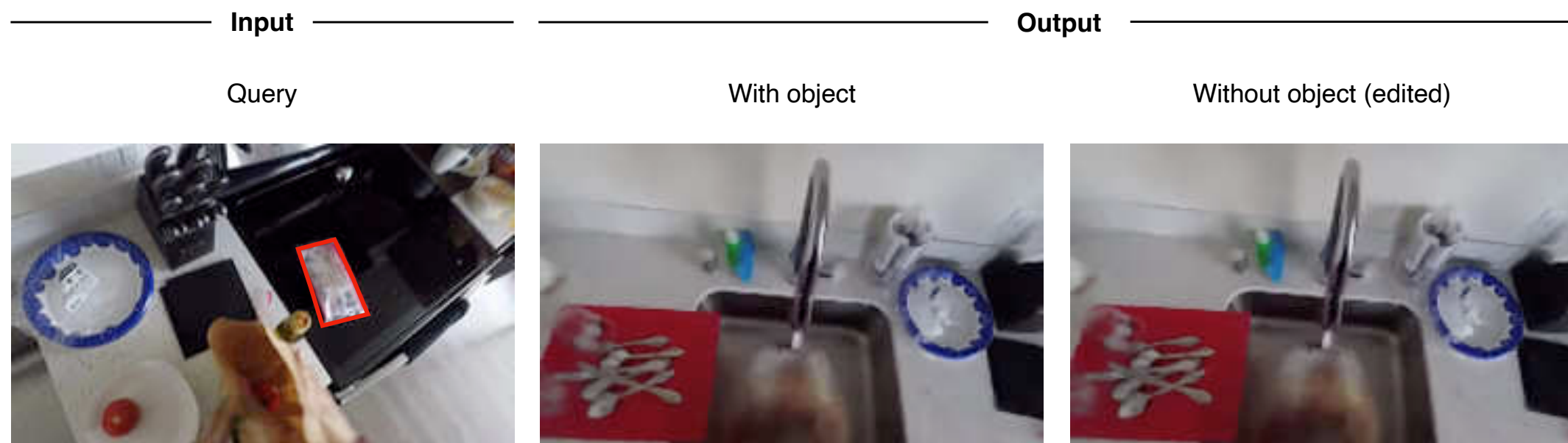
Object retrieval



Object retrieval



Scene editing



Cats: the bane of computer vision

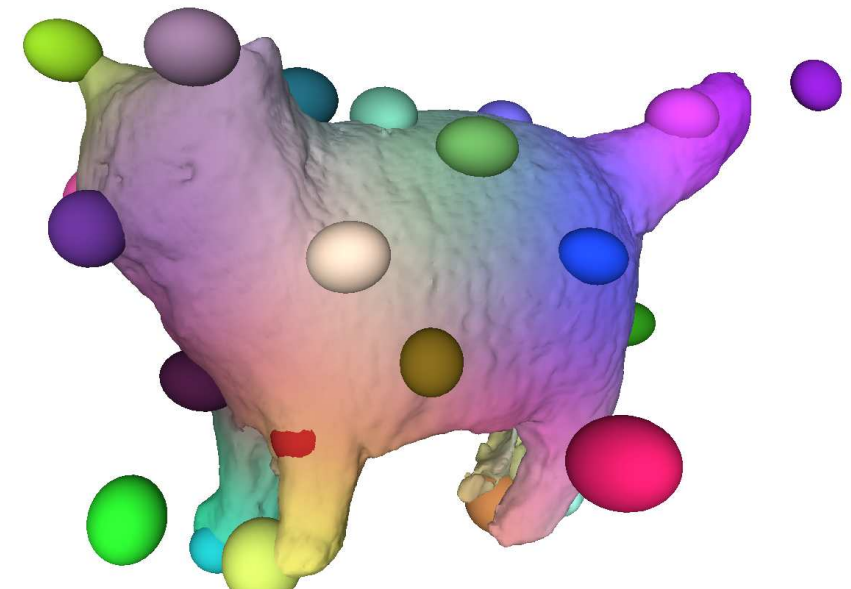
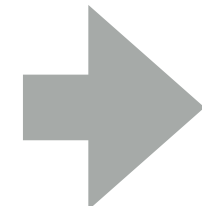


BANMo: Animatable 3D Models from Casual Videos

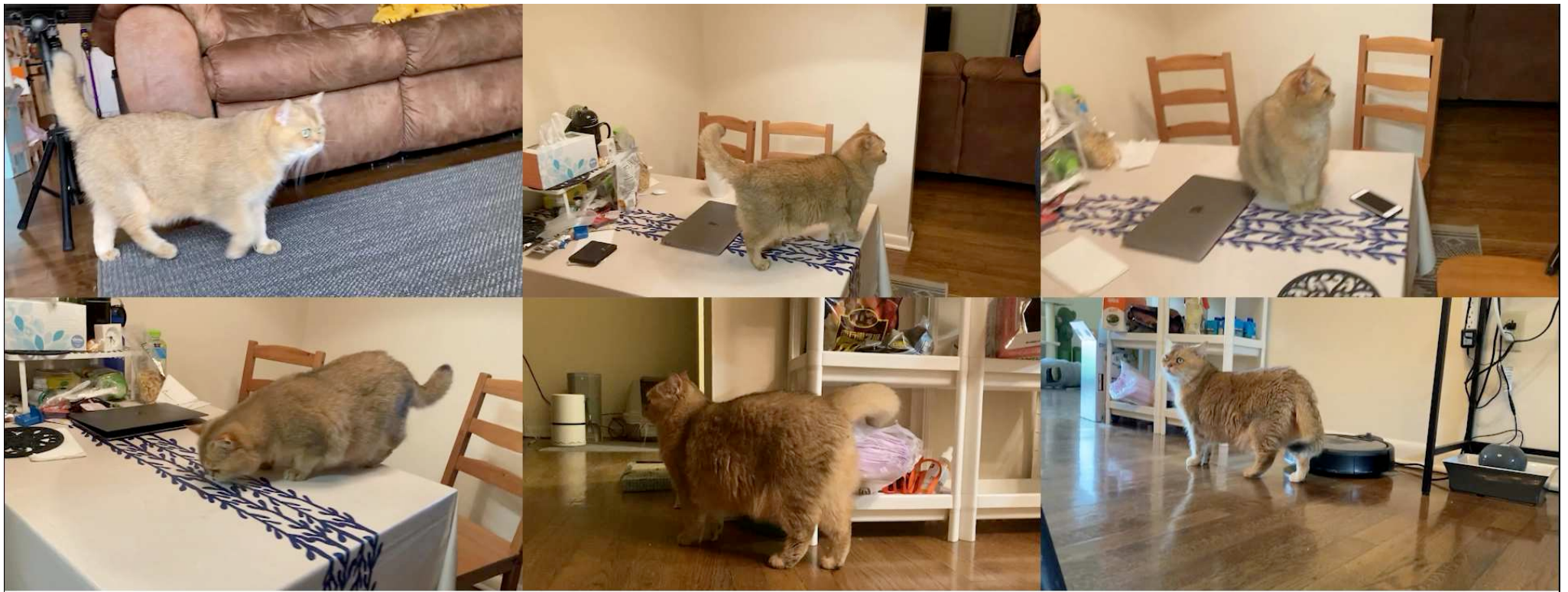
Multiple casual videos



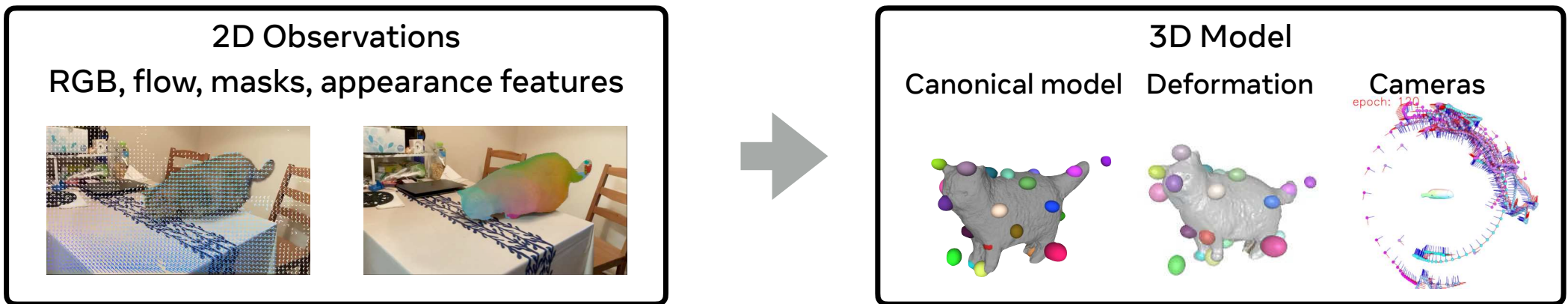
Animatable 3D model



BANMo preview

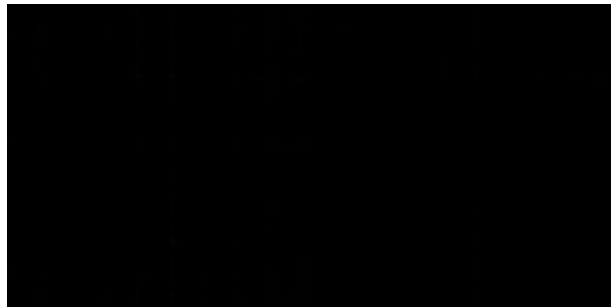


BANMo



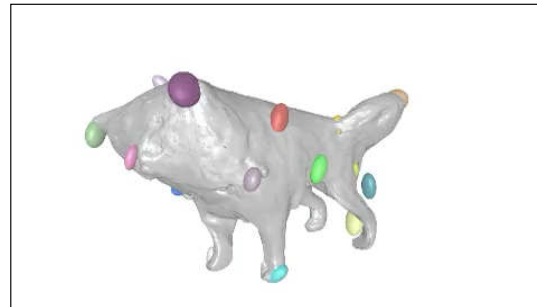
Ingredients

(1) Canonical representation



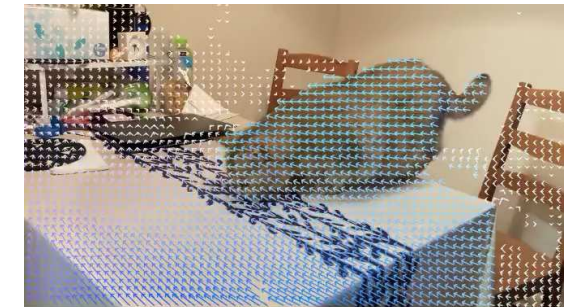
Amenable to gradient-based optimisation

(2) Gaussian bones



Regularise large deformations

(3) Pre-train correspondences



DensePose

Optical flow

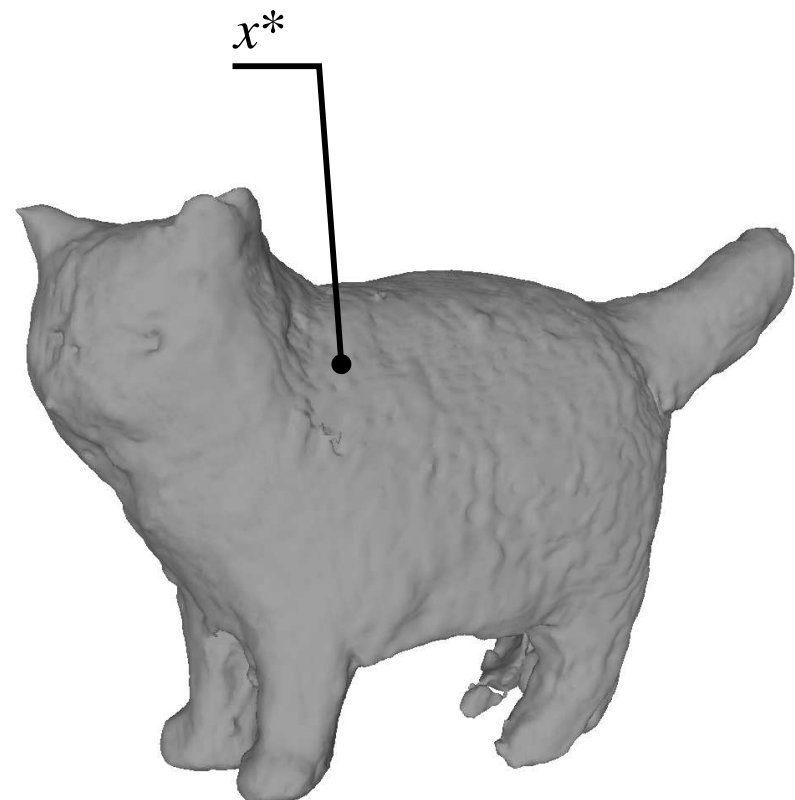
(1) Canonical implicit representation

x^* 3D point in canonical space

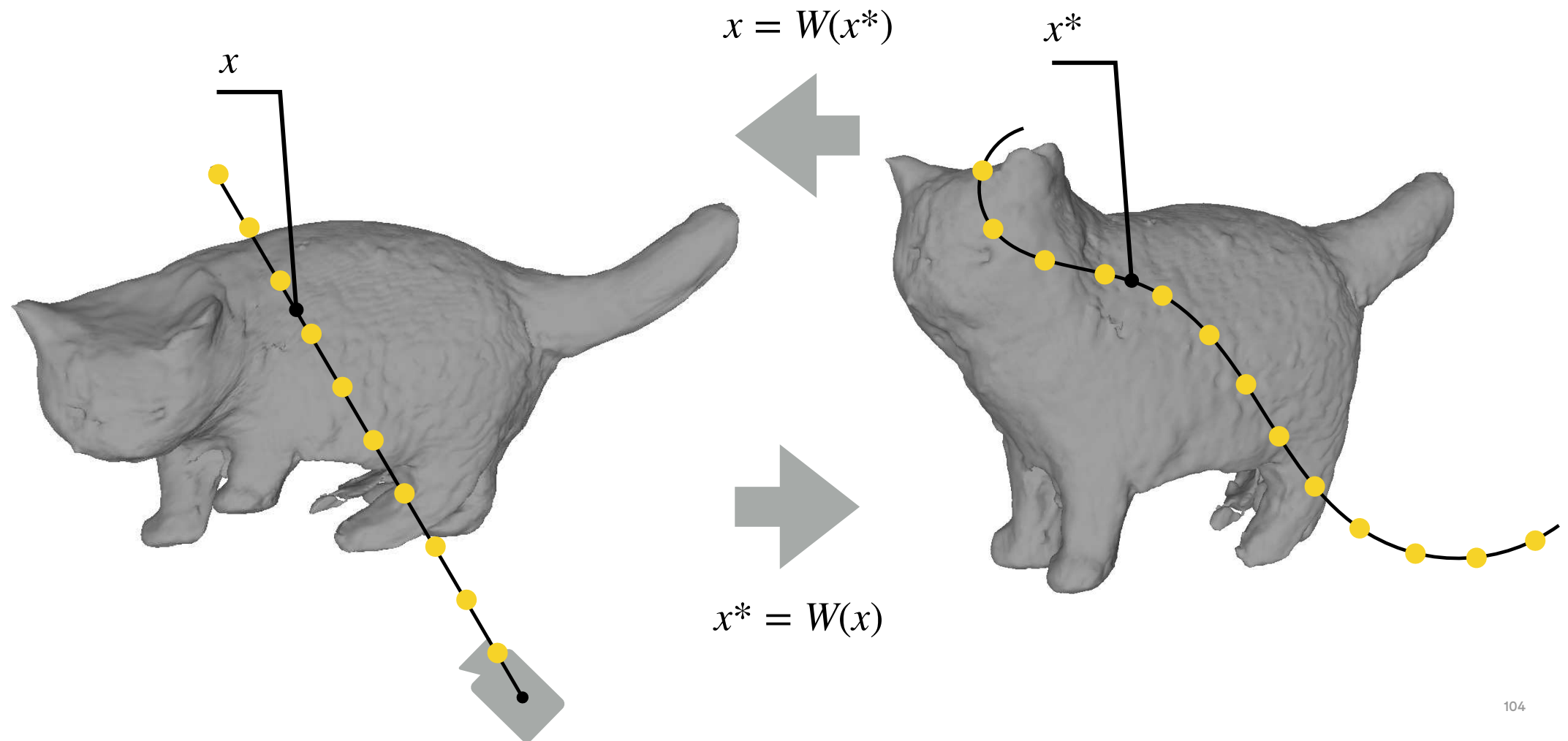
$\sigma(x^*)$ occupancy (SDF-based)

$c(x^*)$ color

$\psi(x^*)$ canonical embedding

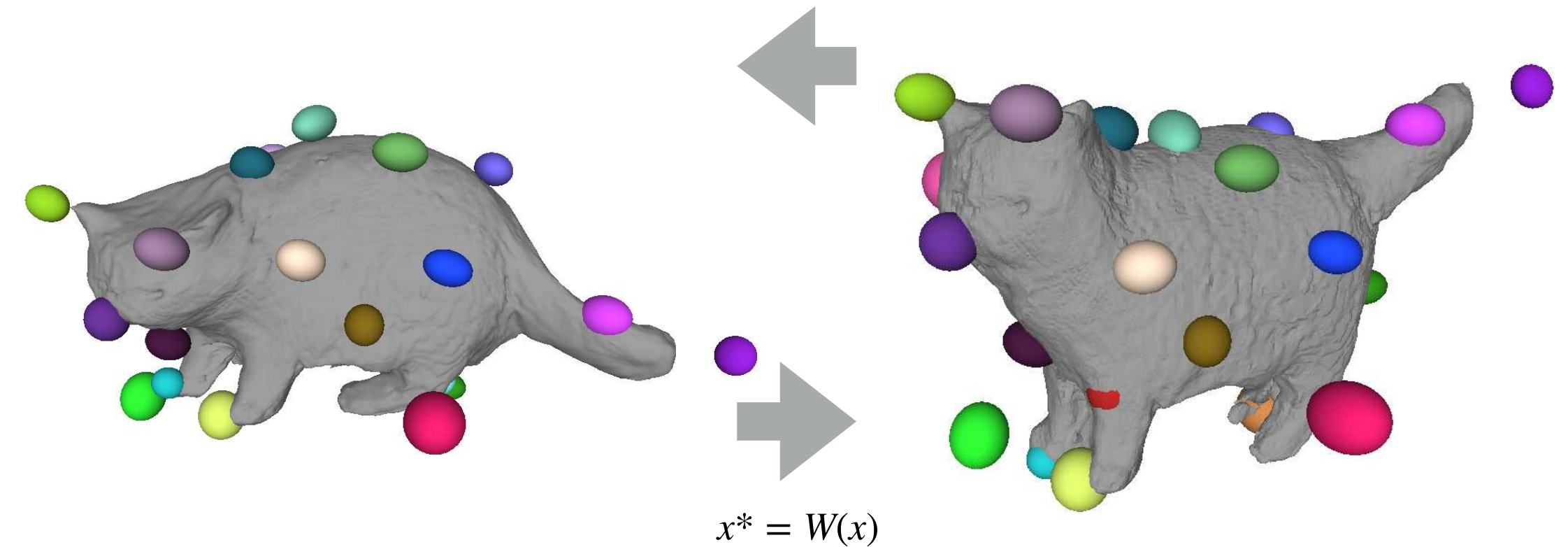


Warped ray casting



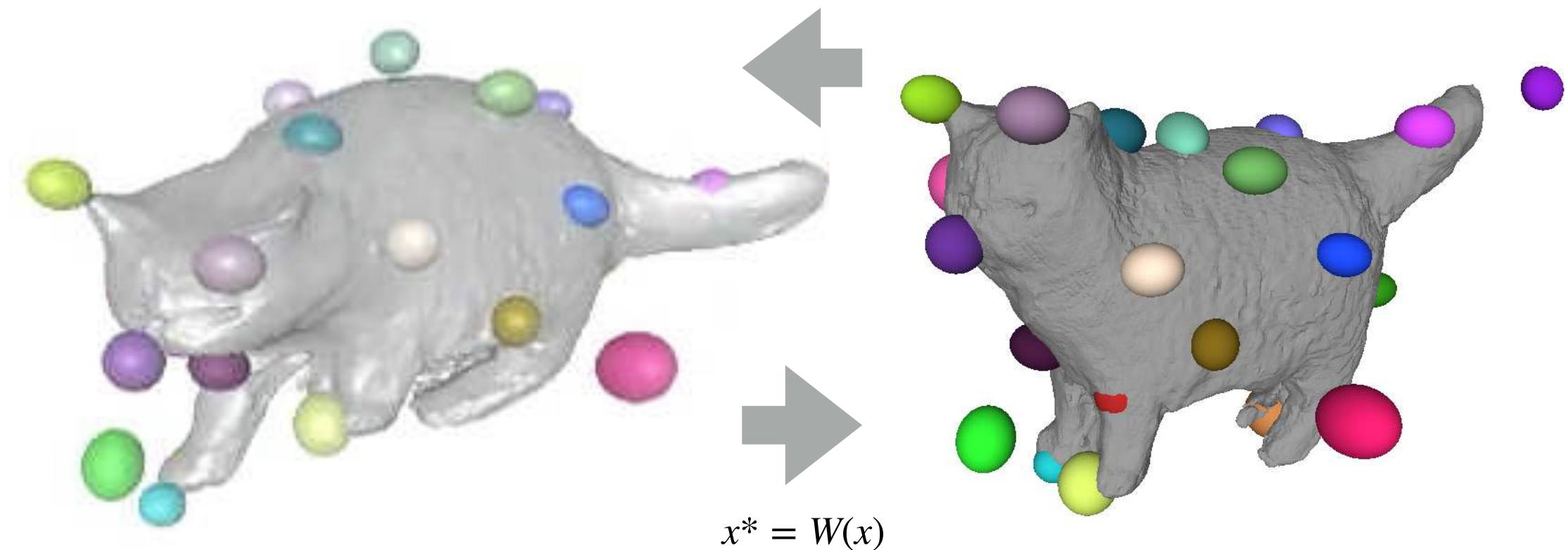
(2) Gaussian bones

$$x = W(x^*)$$



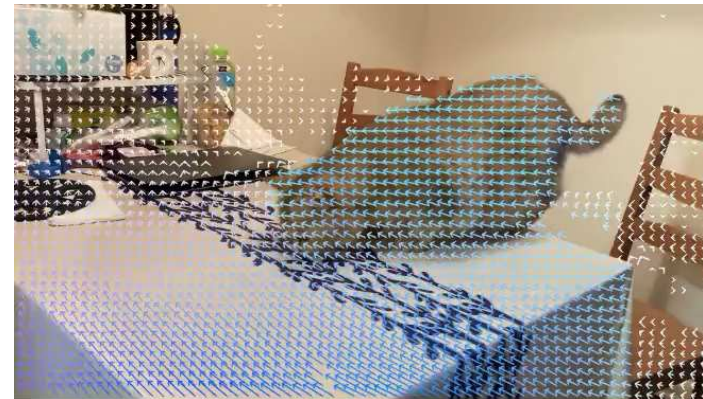
(2) Gaussian bones

$$x = W(x^*)$$

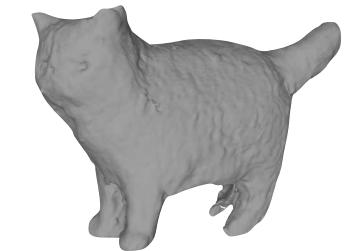


(3) Pre-trained optical flow

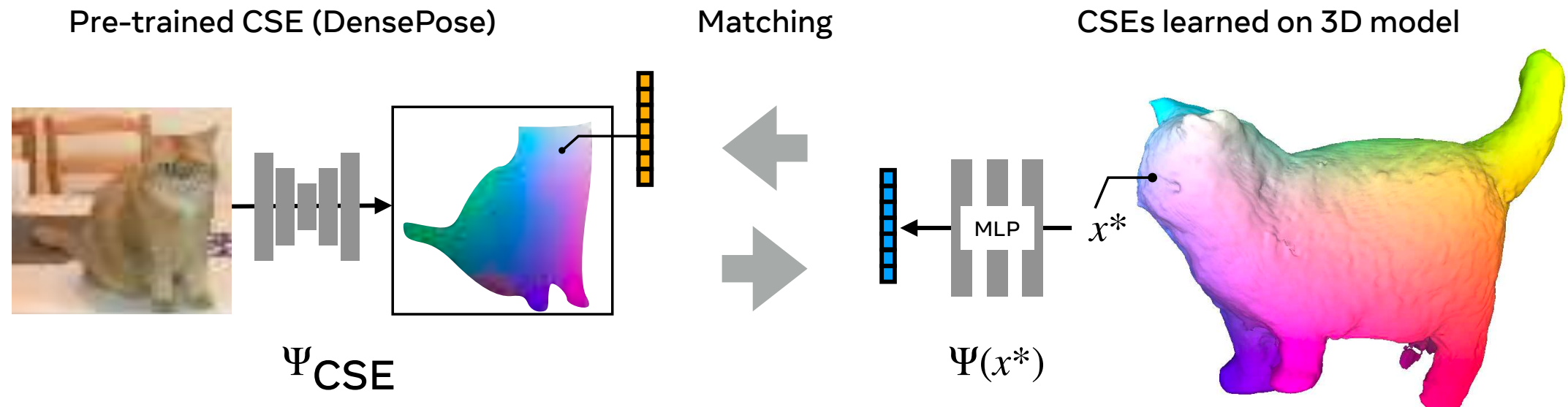
Predict flow from video (e.g., RAFT)



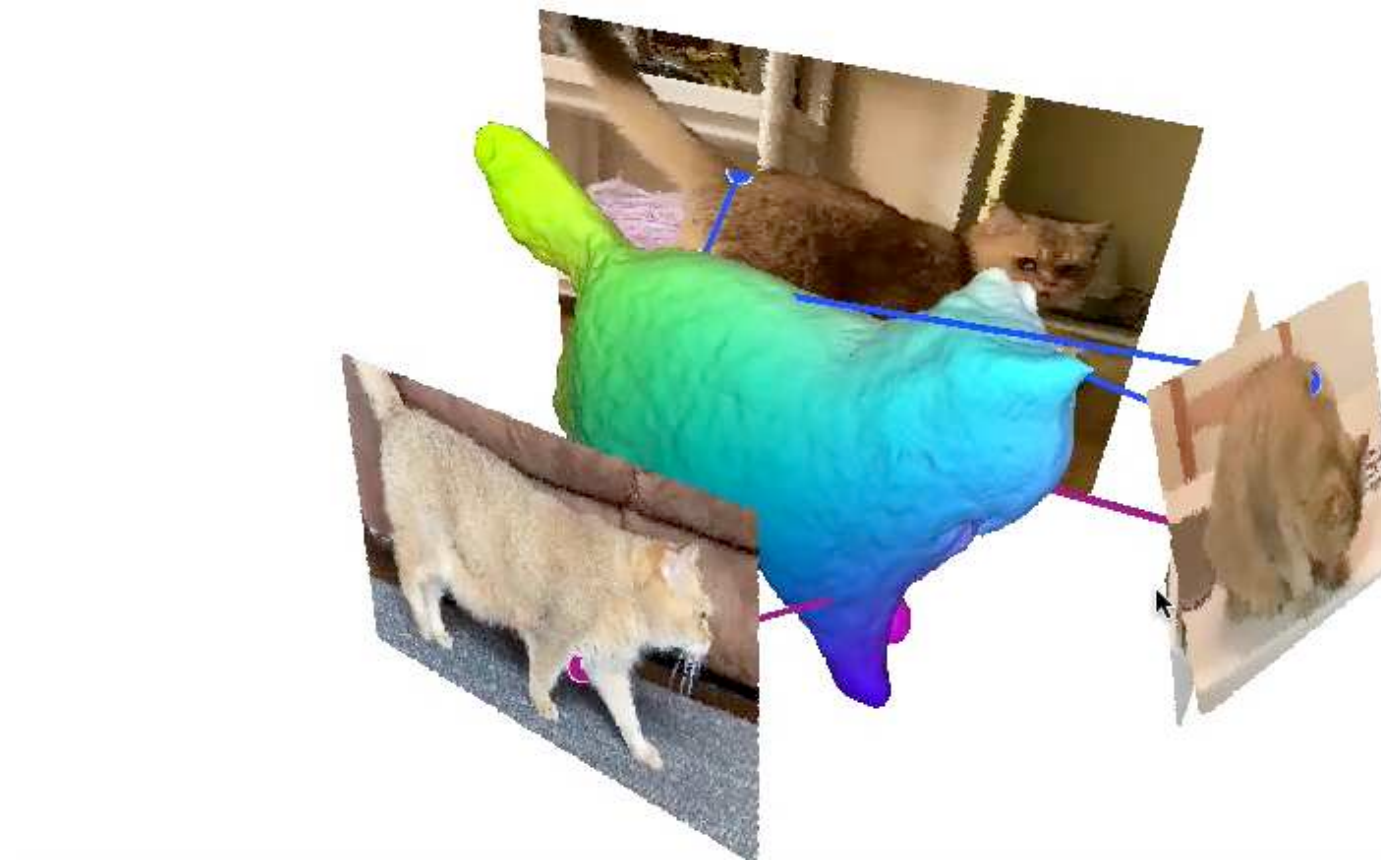
Predict flow from model



(3) Pre-trained continuous surface embeddings (CSEs)



(3) Long-range correspondences



BANMo results



BANMo: Building Animatable 3D Neural Models from Many Casual Videos, Yang, Vo, Neverova, Ramanan, Vedaldi, Joo, CVPR, 2022

BANMo results



111

BANMo: Building Animatable 3D Neural Models from Many Casual Videos, Yang, Vo, Neverova, Ramanan, Vedaldi, Joo, CVPR, 2022

An application: motion retargeting



Single images to articulated objects

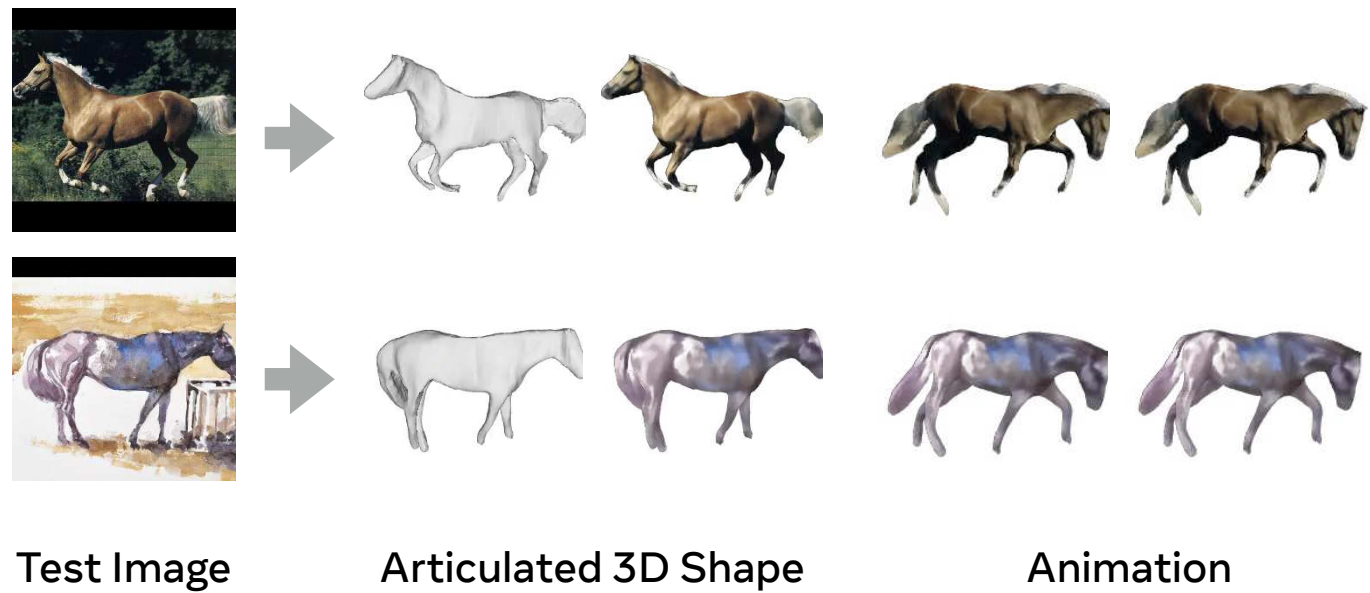
Training



Single-view Images
(+ mask)



Single-Image Inference



Self-supervised correspondences



Single-view Images (+ masks)

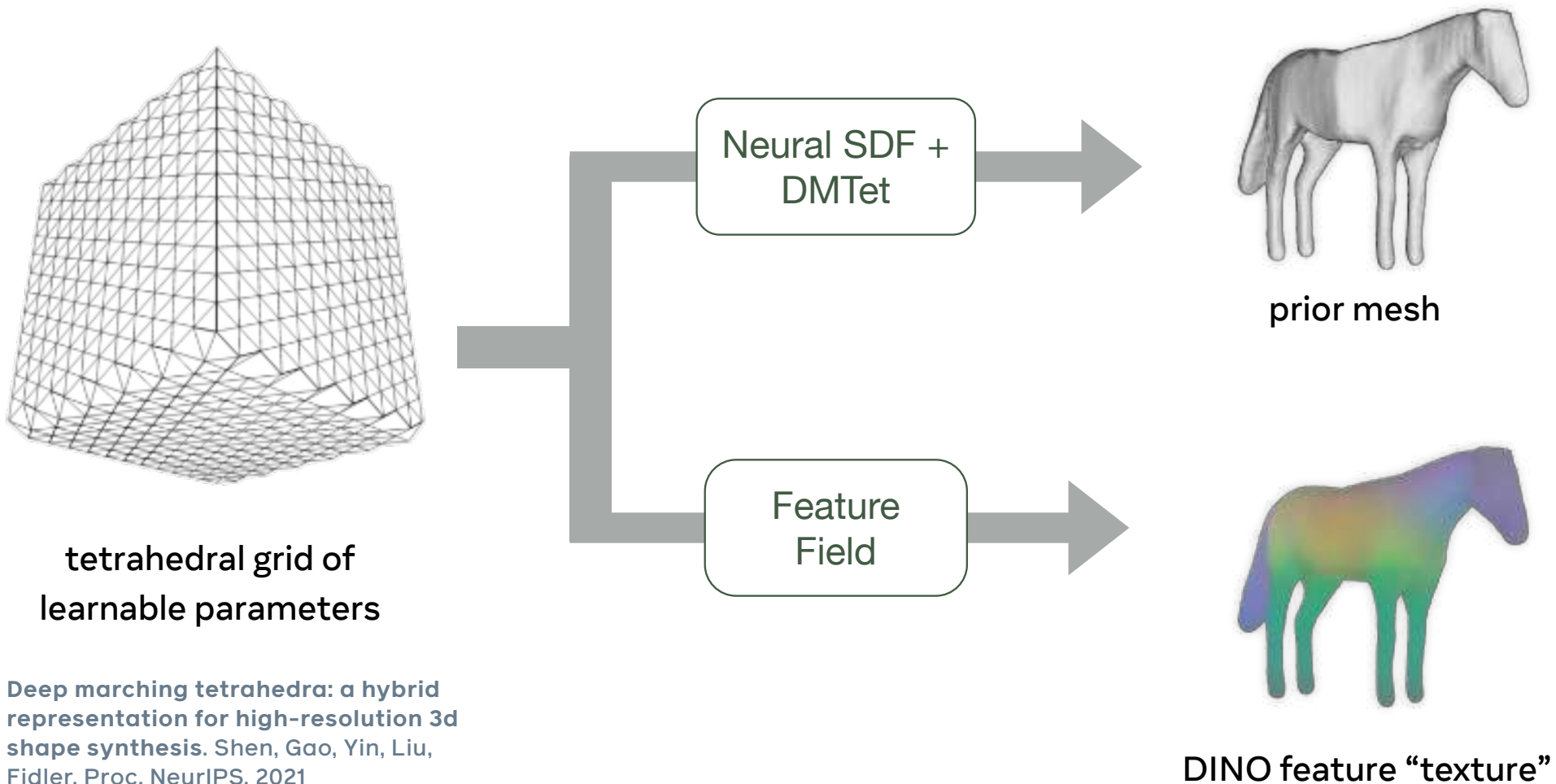
Off-the-shelf
DINO-ViT



Self-Image Features

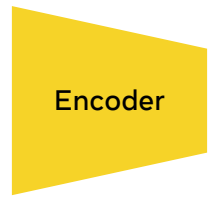
No keypoint or viewpoint supervision, nor template shapes

Implicit-explicit template shape representation

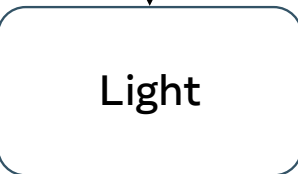
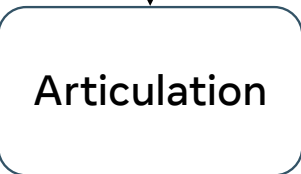
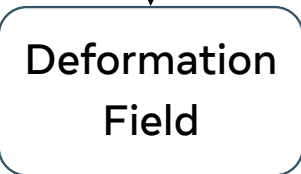


Deep marching tetrahedra: a hybrid representation for high-resolution 3d shape synthesis. Shen, Gao, Yin, Liu, Fidler. Proc. NeurIPS, 2021

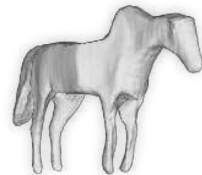
Photo-geometric auto-encoding



feature



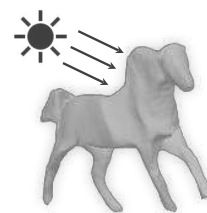
albedo



deformed



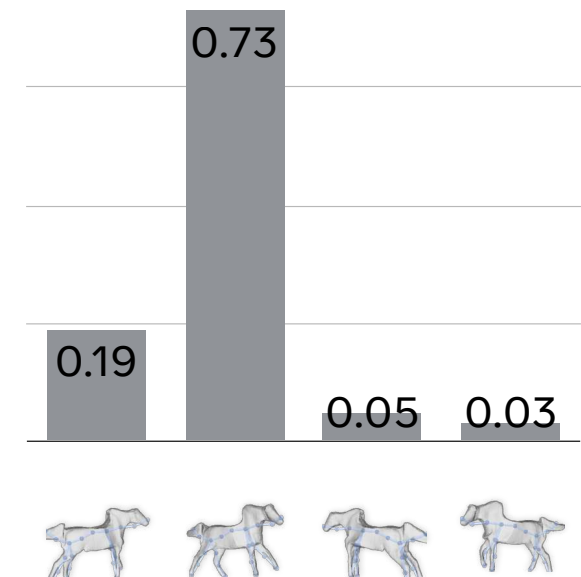
articulated



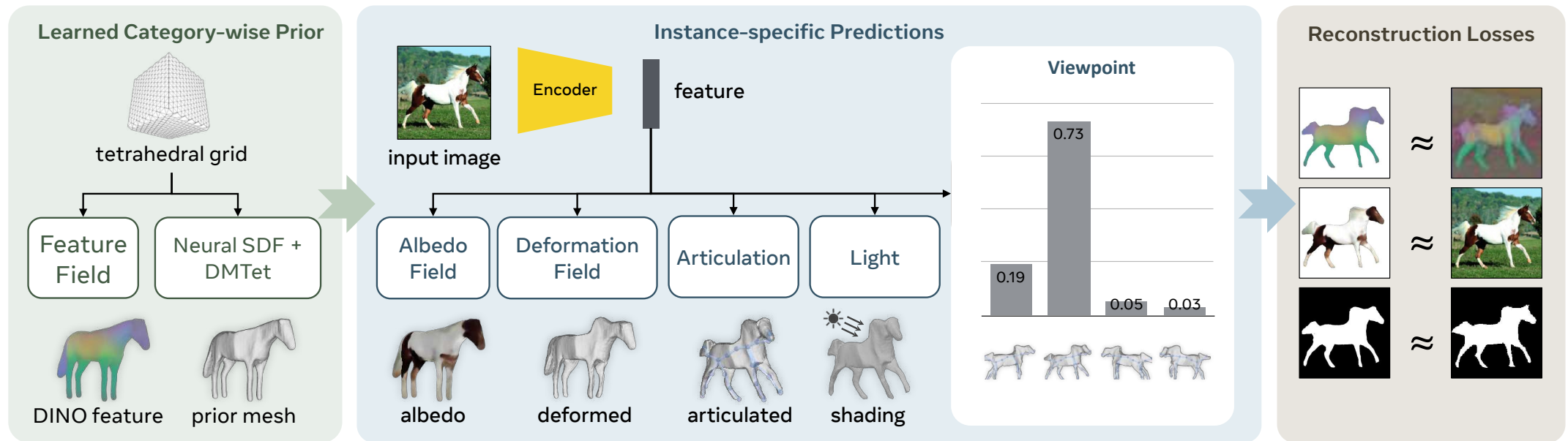
shaded

Viewpoint

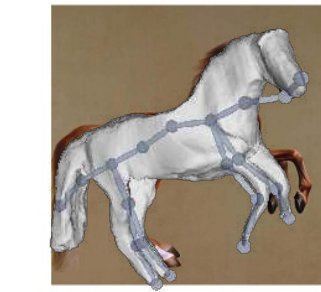
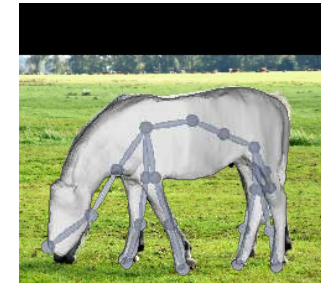
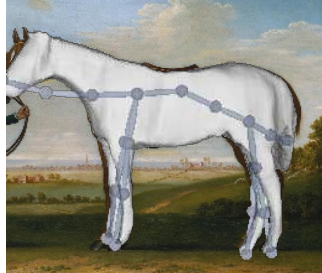
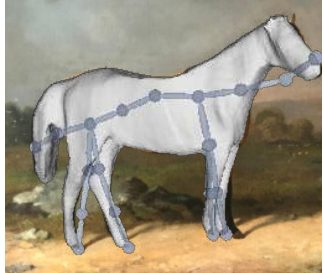
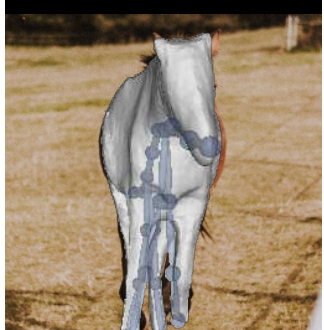
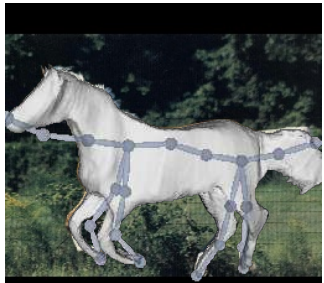
- Sample one of 4 possible viewpoints
- Sampling probability self-supervised by reconstruction loss

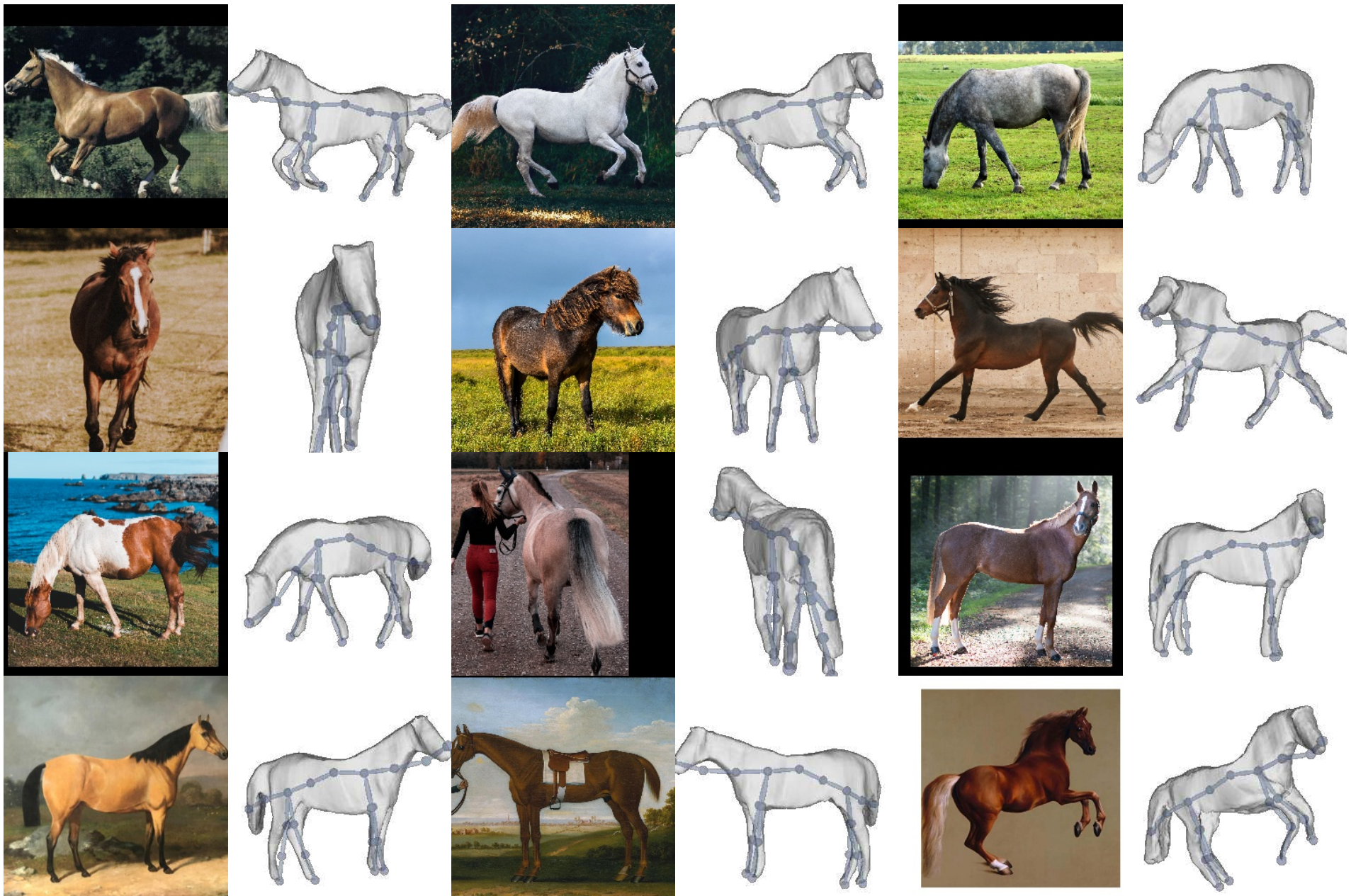


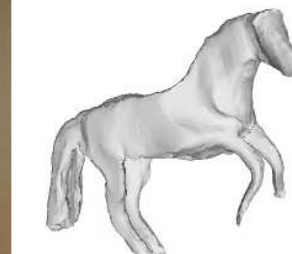
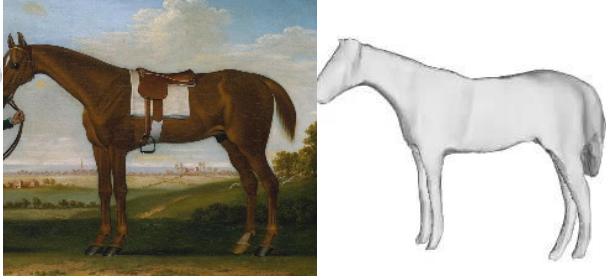
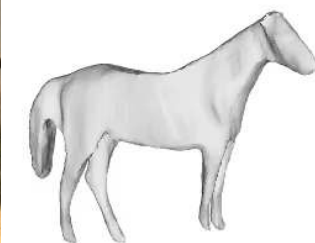
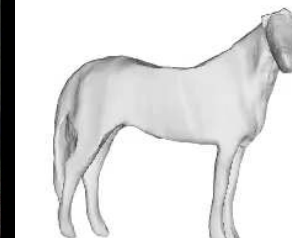
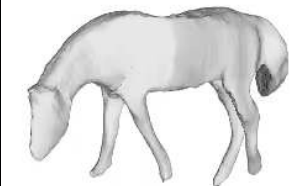
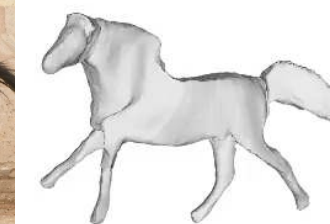
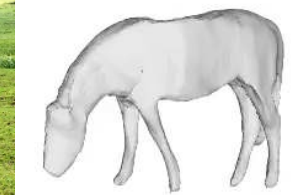
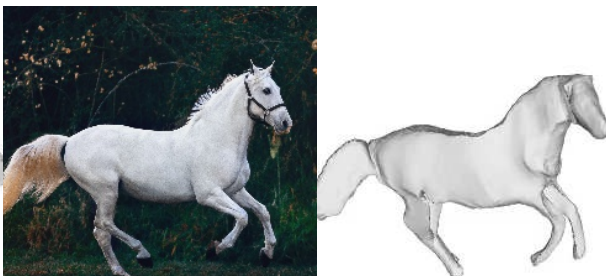
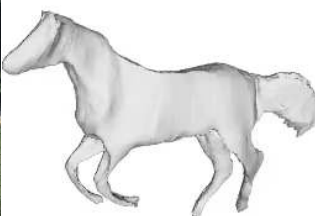
Full model

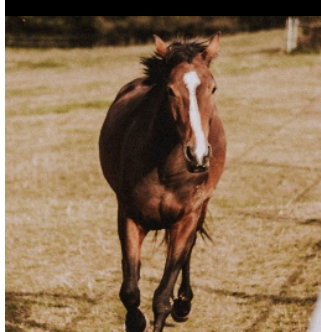


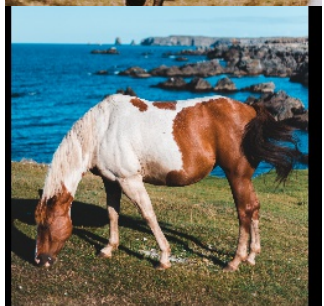
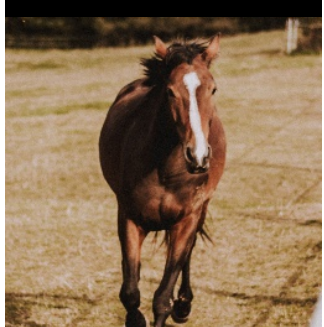
Entire pipeline trained end-to-end with reconstruction losses
(except for frozen DINO-ViT [1] image encoder, pre-trained via self-supervision)

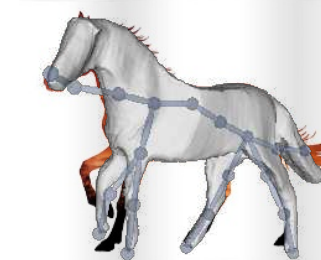
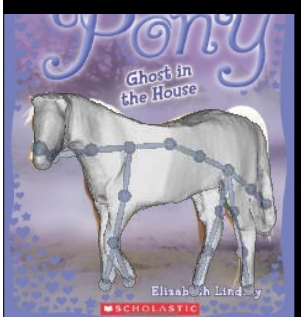
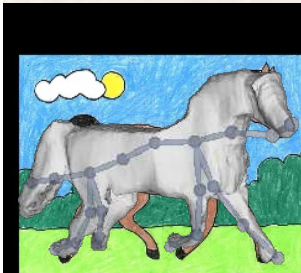
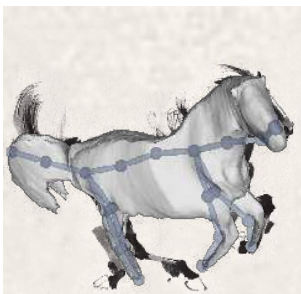


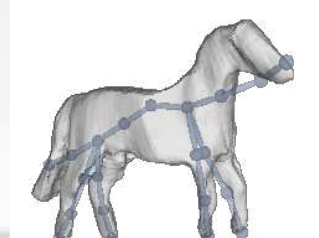
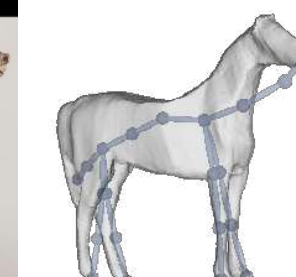
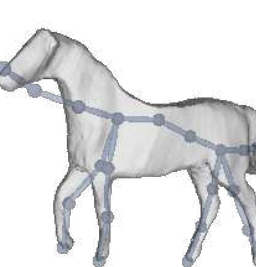
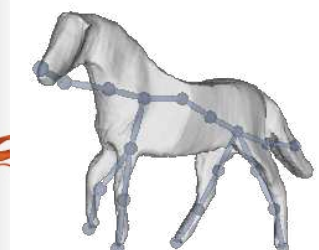
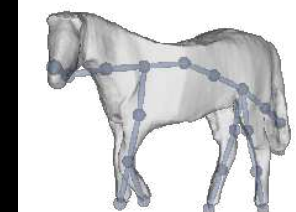
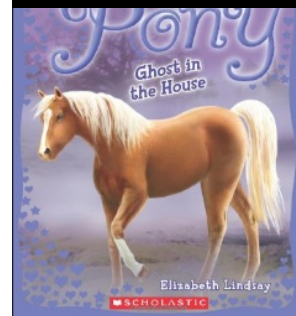
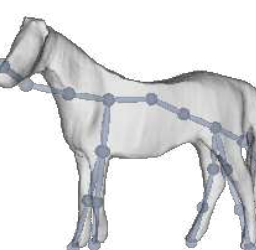
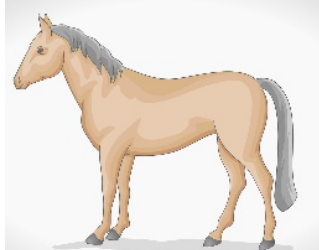
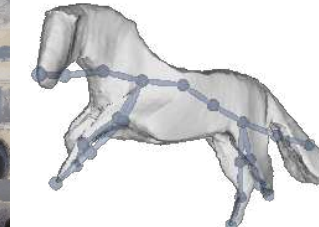
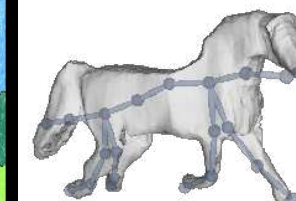
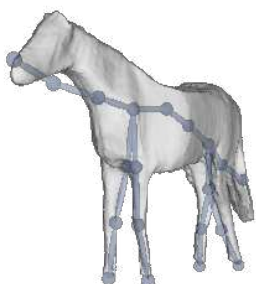
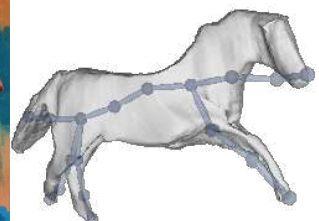
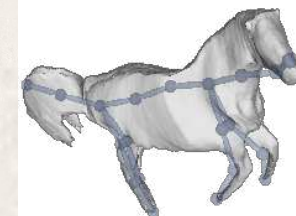
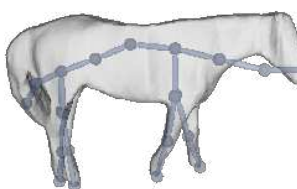


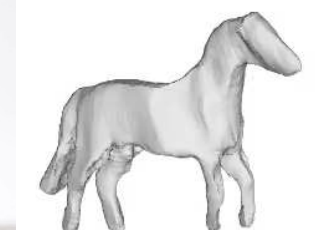
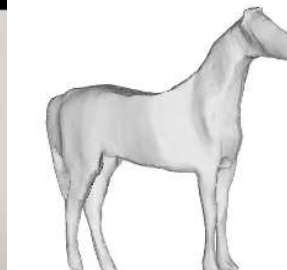
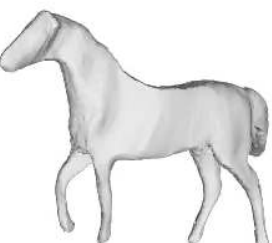
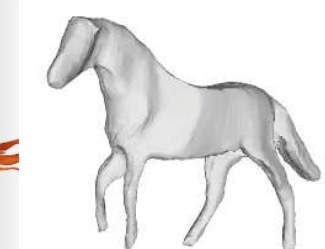
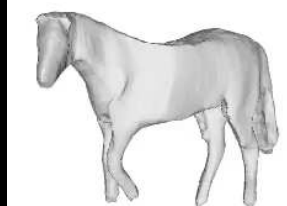
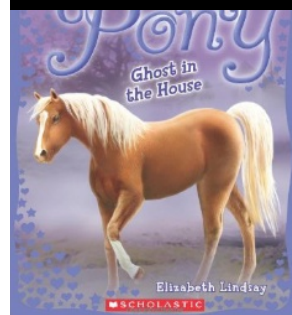
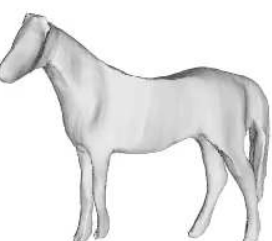
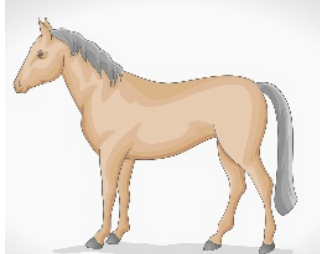
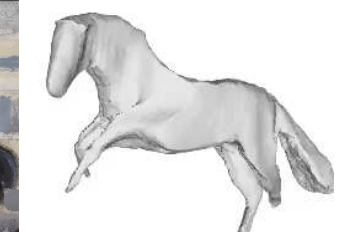
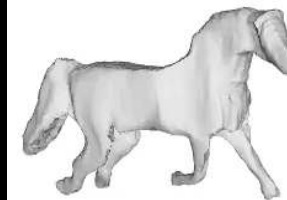
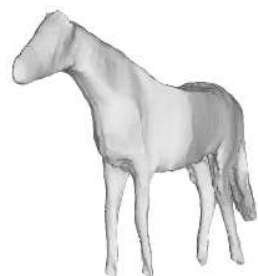
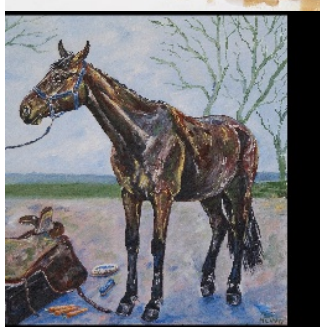
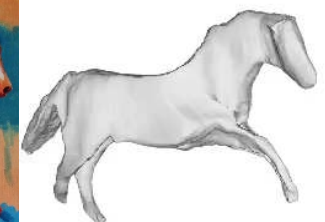
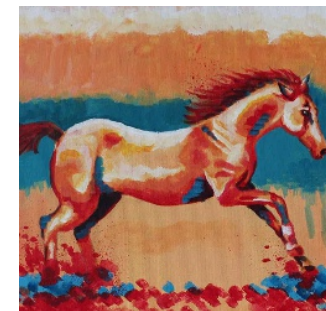
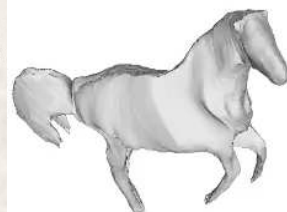
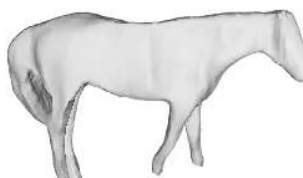


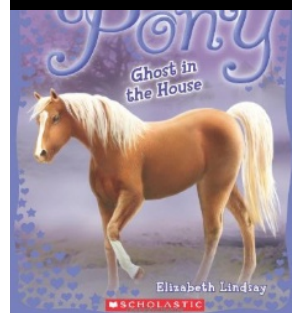
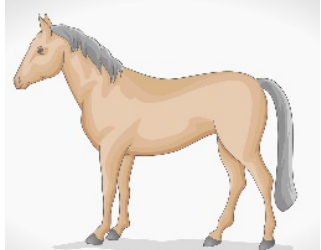
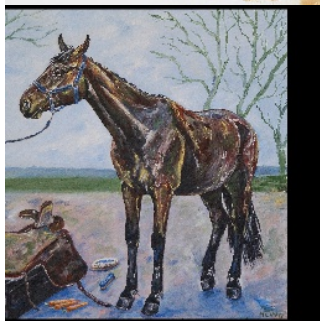
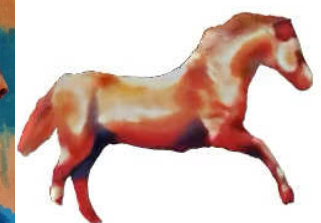
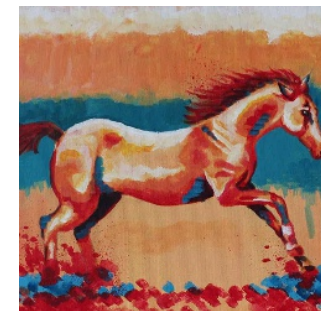


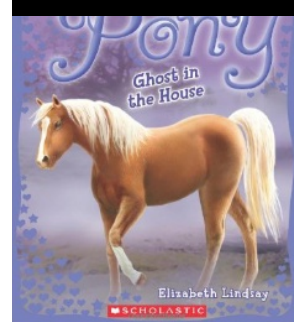
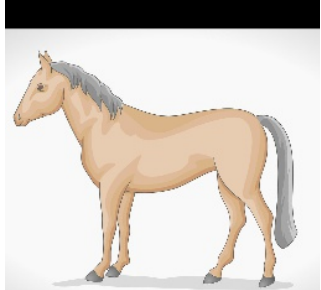
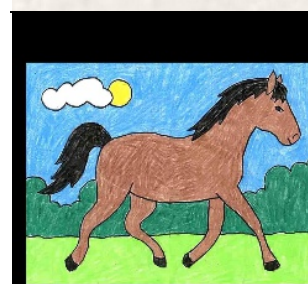
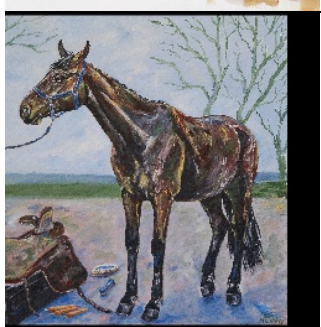
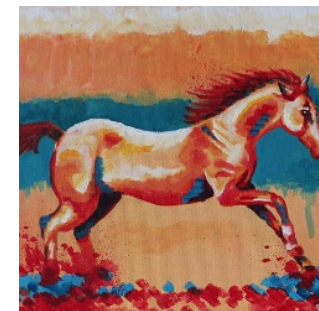
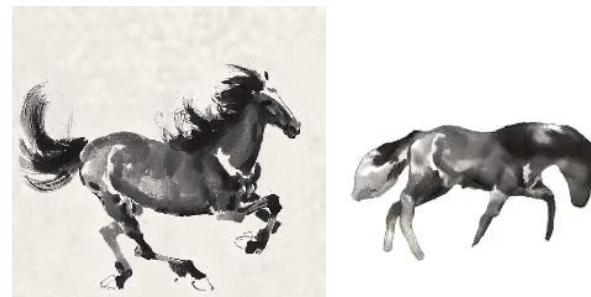


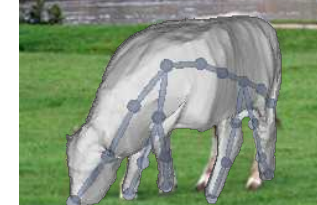
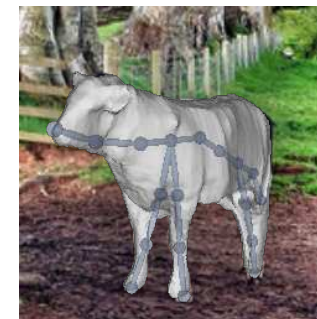
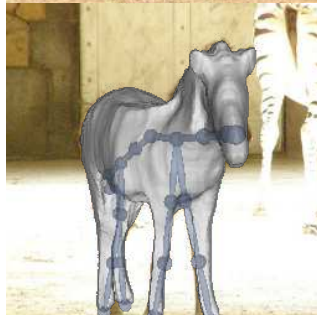
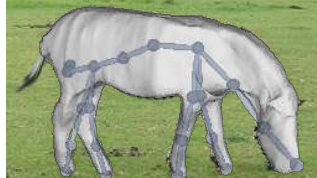
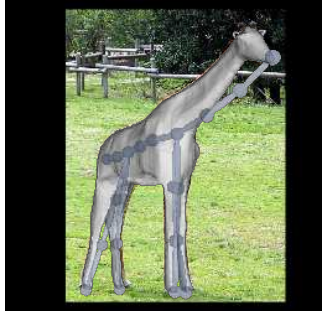


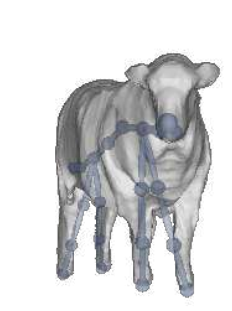
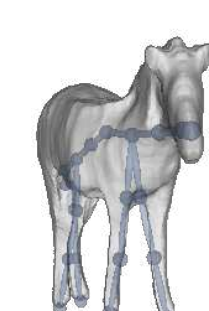
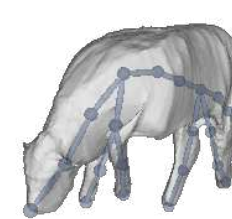
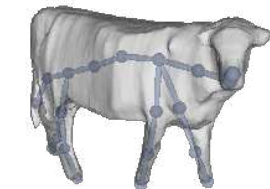
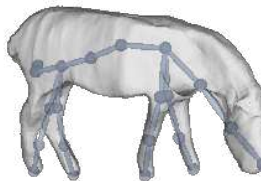
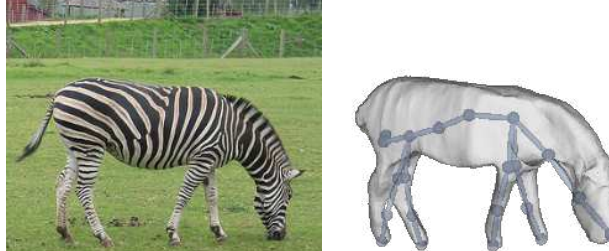
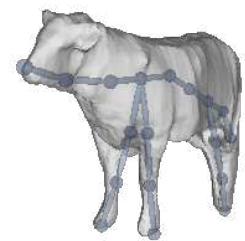
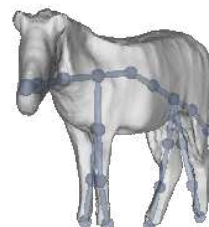
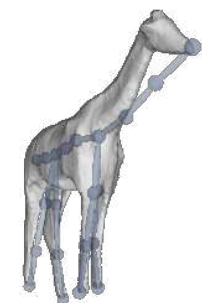


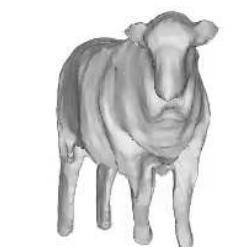
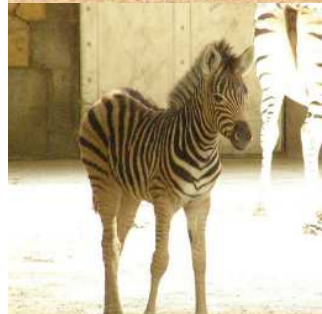
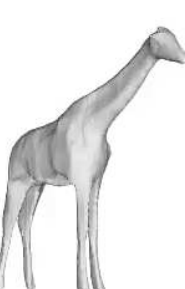
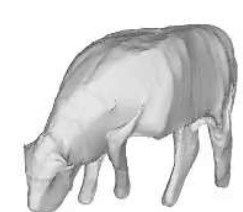
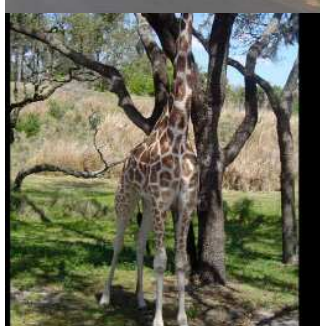
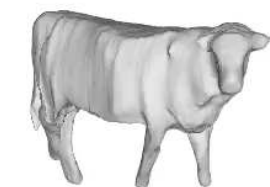
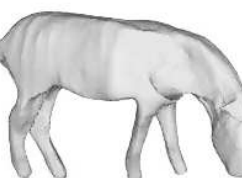
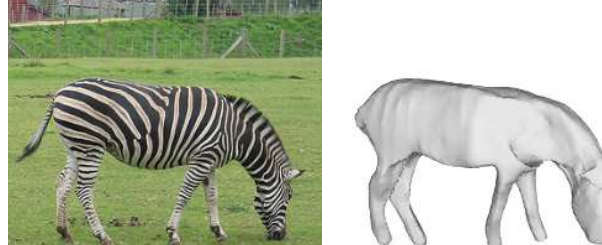
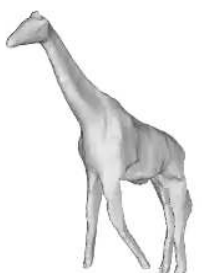
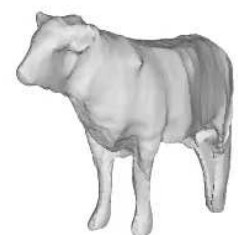
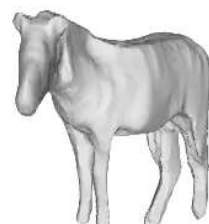
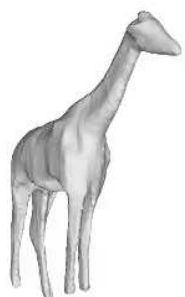




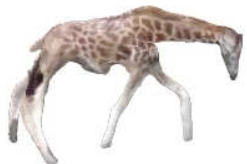








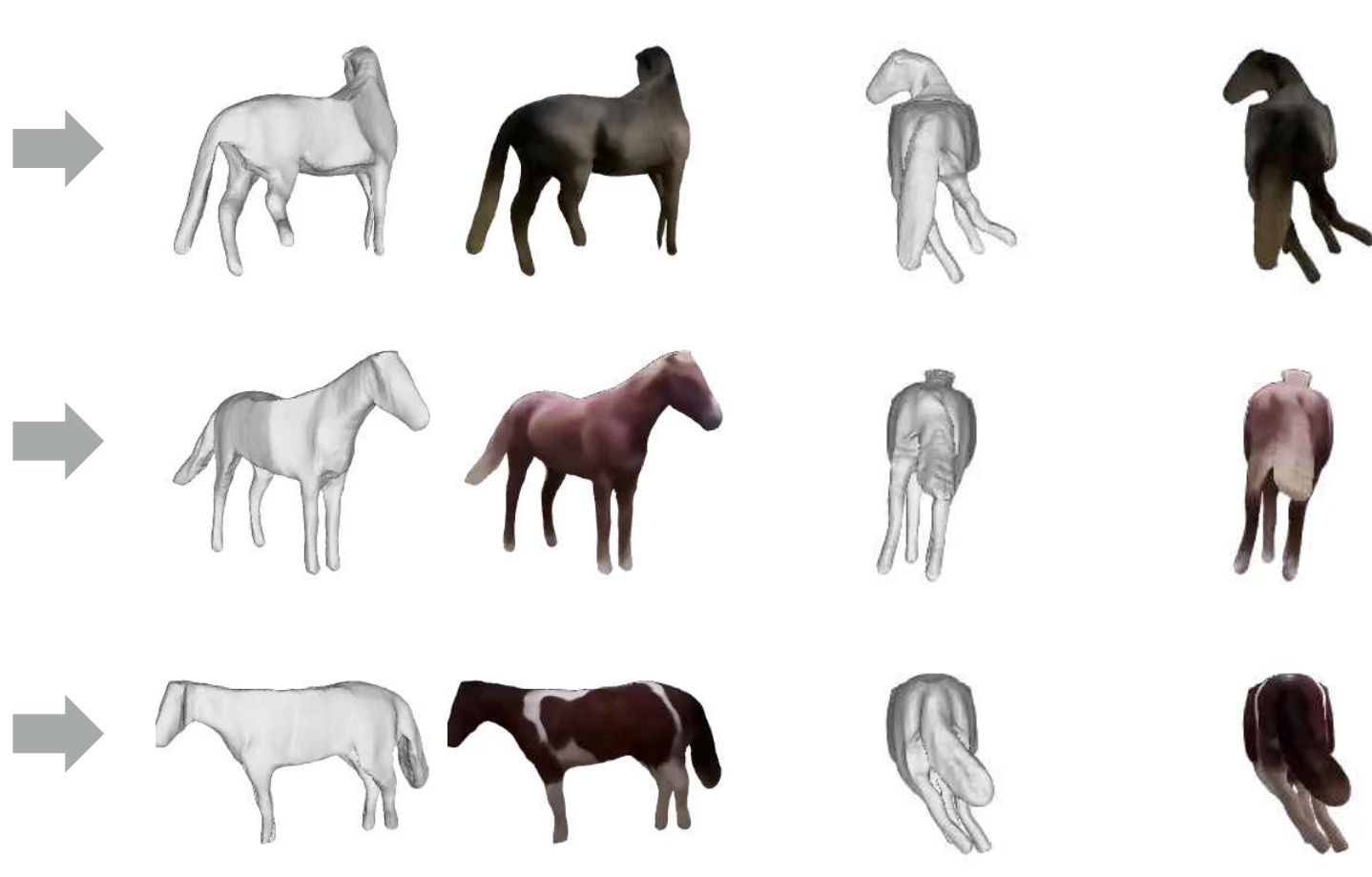




Frame-by-Frame Inference on Videos



Input Frames



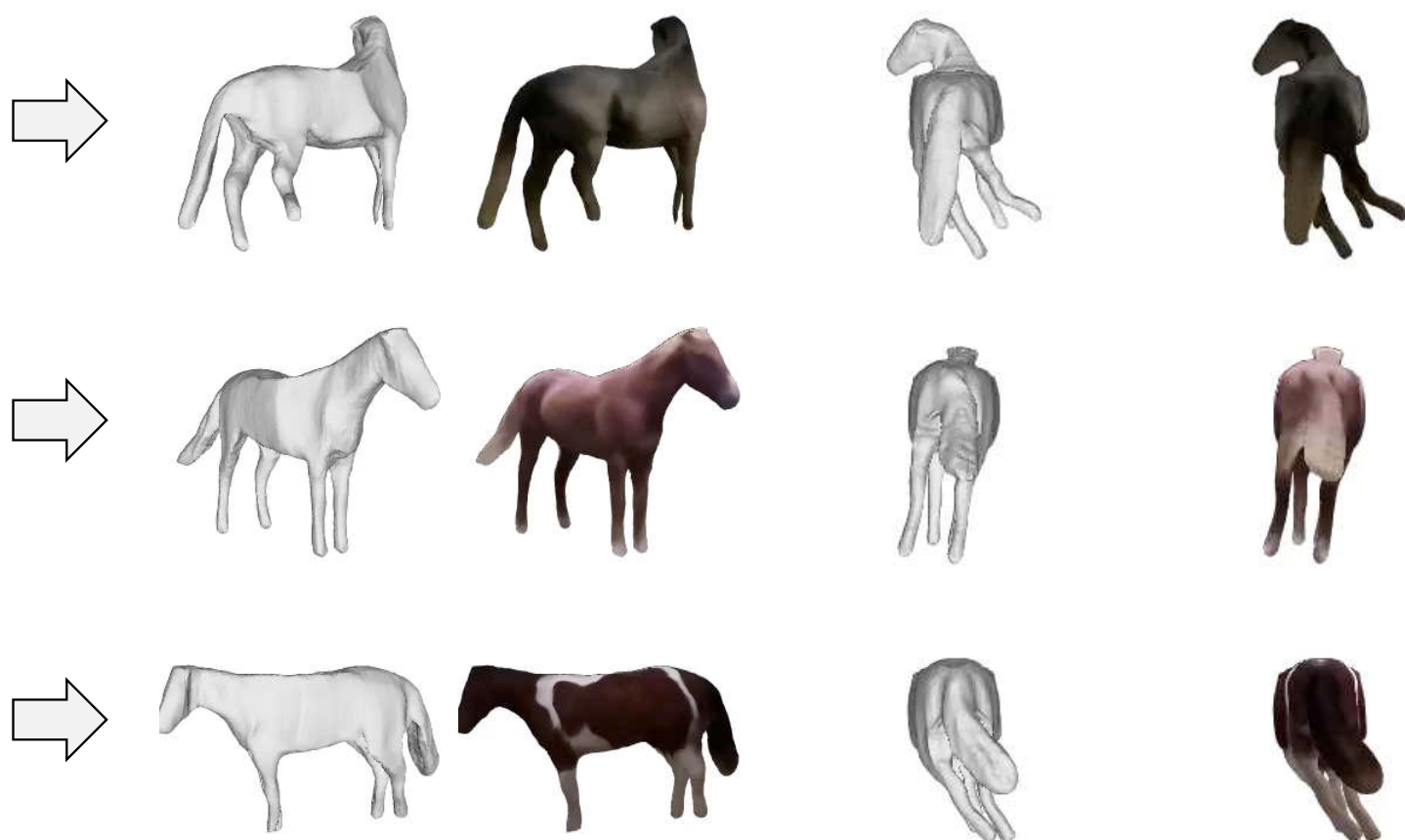
Input View

360° Rotations

Frame-by-Frame Inference on Videos

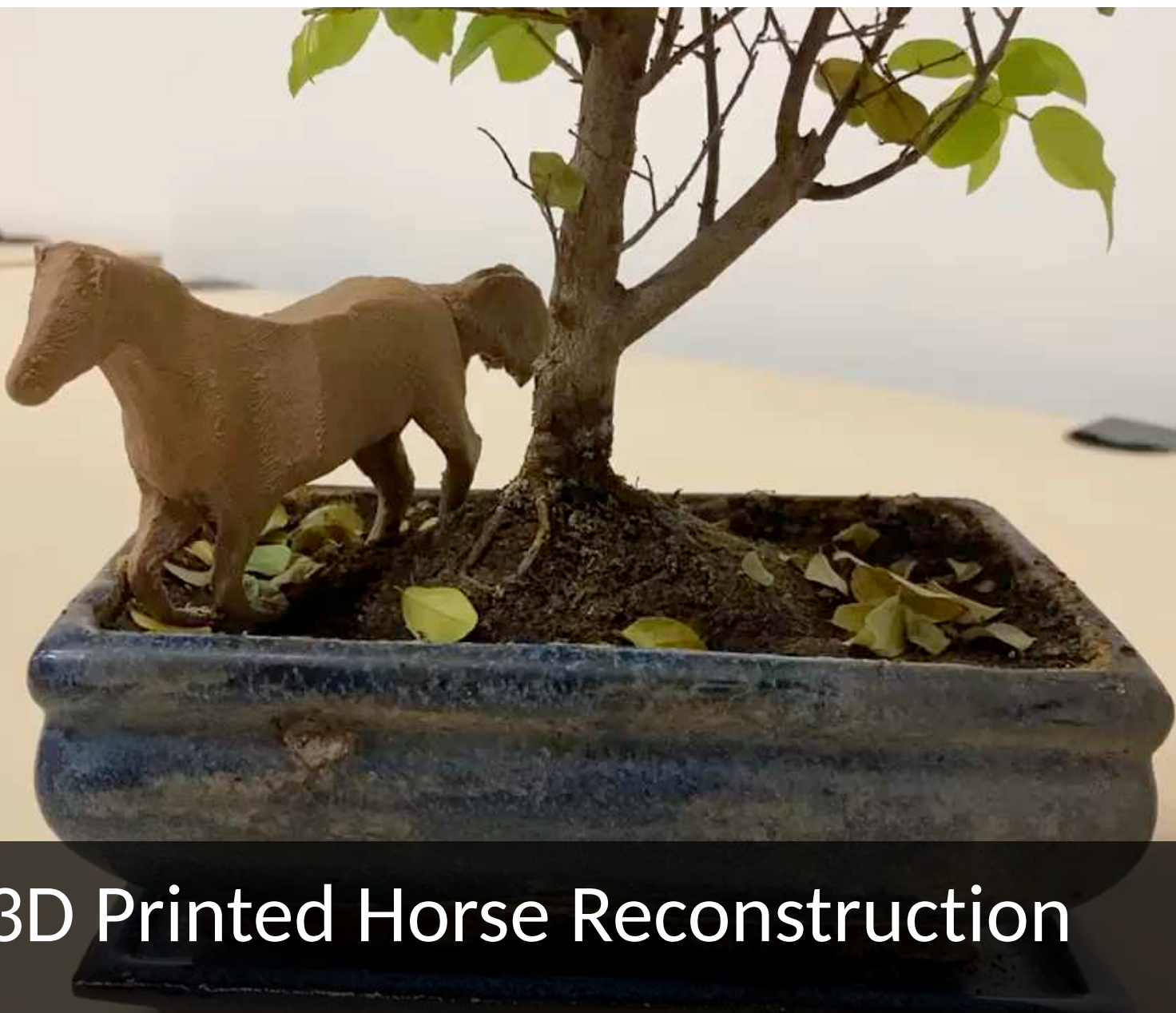


Input Frames



Input View

360° Rotations



3D Printed Horse Reconstruction

Conclusions

Neural Rendering



Scaling



Unsupervised 3D

